Theses and Dissertations

Summer 2015

Reaction of carbon nanotubes with chemical disinfectants: Byproduct formation and implications for nanotube environmental fate and transport

Edgard Manuel Verdugo
University of Iowa

Recommended Citation

REACTION OF CARBON NANOTUBES WITH CHEMICAL DISINFECTANTS:

BYPRODUCT FORMATION AND IMPLICATIONS FOR NANOTUBE

ENVIRONMENTAL FATE AND TRANSPORT

by

Edgard M. Verdugo

A thesis submitted in partial fulfillment
of the requirements for the Doctor of
Philosophy degree in Civil and Environmental Engineering
in the Graduate College of
The University of Iowa

August 2015

Thesis Supervisors: Associate Professor David M. Cwiertny
Professor Richard L. Valentine

Graduate College
The University of Iowa
Iowa City, Iowa

CERTIFICATE OF APPROVAL

_____

PH.D. THESIS

_____

This is to certify that the Ph.D. thesis of

Edgard M. Verdugo

has been approved by the Examining Committee
for the thesis requirement for the Doctor of Philosophy
degree in Civil and Environmental Engineering at the August 2015
graduation.

Thesis Committee: _____
                      David M. Cwiertny, Thesis Supervisor

                  _____
                      Richard L. Valentine, Thesis Supervisor

                  _____
                      Patrick T. O'Shaughnessy

                  _____
                      Tim Mattes

                  _____
                      Scott K. Shaw

To my parents for their encouragement and support.

ACKNOWLEDGMENTS

I would like to begin by thanking my advisor, David Cwiertny, whose influence started before I had even thought about pursuing an advanced academic degree. I cannot imagine being where I am today without his involvement as a teacher, advisor, and mentor. I sincerely thank you for taking me under your wing and allowing me to flourish in this demanding academic environment.

I would like to extend this to my co-advisor, Rich Valentine, who was always willing to share his vast knowledge and years of experience on any subject at hand. He welcomed me with open arms as a student and a researcher. Thank you for making me feel welcomed in this home away from home.

I cannot forget to thank my labmates Dr. Rebekah Oulton, Dr. Caylyn Lanzl, Dr. Yang Xie, Dr. Shen Qu, Kyle Nelson, Jason Haase, and Kathy Peter for their friendship and assistance. Also, I offer my genuine thanks to my undergrads, Kelly Genskow, Lydia Mensah, Isaac Yoder-Schrock, and Christian Bako, who assisted me greatly in getting this work done in a timely fashion.

I would also like to thank my friends and family, for expressing their support and cheering me on to the finish. I would especially like to thank to my parents for always believing in me and helping in every way they can without needing to be asked. I could not have done it without your love, support, and encouragement.

Last but not least, I would like to thank my coworker, best friend, and fiancée, Katie Greenstein, for supporting me in everything I did. You made every moment worthwhile.

ABSTRACT

Carbon nanotubes (CNTs) have exhibited great potential in water treatment due to their unique and tunable structural, physical, and chemical properties. Currently, they are used in environmental remediation as absorbents, catalysts or catalyst supports, membranes, and electrodes. However, a poorly understood determinant of the role of CNTs in water treatment is their interaction with chemical disinfectants (e.g., chlorine, chloramine, and ozone). For example, CNTs exhibit chemical properties similar to those of activated carbon (AC) and natural organic matter (NOM), especially when functionalized with surface groups (e.g., –COOH, –OH, –NH$_2$, and polymers) that are often critical to their performance during application, as well as their environmental fate. These reactive surface groups on CNTs may also influence the fate of oxidants by promoting surface reactions, potentially yielding byproducts that pose risks to ecosystems and human health.

To address these existing gaps in the environmental fate and reactivity of CNTs, this work establishes whether CNTs represent precursors for halogenated and nitrogenous disinfection byproducts (DBPs), and identifies the material properties of CNTs most influential on their reactivity toward disinfectants. In addition, we seek to understand how reaction with disinfectants alters CNT surface chemistry, and in turn impacts their environmental mobility and cytotoxicity. Finally, we determine how NOM and other aquatic variables known to impact DBP formation (e.g., Br$^-$, NOM, and pH) influence the rate and products of CNT reaction with disinfectants. Notably, results herein reveal that N-functionalized CNTs behave as precursors and sources of N-nitrosodimethylamine (NDMA), a probable human carcinogen, while chemical disinfection can produce N-

CNTs exhibiting surface chemistry and environmental behavior distinct from native (i.e., as-received) materials. Additionally, in order of increasing selected DBP formation, oxidized, chemically aged (via ozonation and chlorination), and polymer-functionalized CNTs behave as precursors of trihalomethanes (THMs) and haloacetic acids (HAAs). Finally, though the presence of NOM has no effect on the total formation of THMs, increasing solution pH and bromide ion concentration increases the THM formation potential during chlorination of CNTs. Outcomes of this work contribute to the current understanding of the role of carbon-based species as DBP precursors in disinfection and provide new context as to the environmental significance and implications of CNTs in natural and engineered aquatic systems.

PUBLIC ABSTRACT

Nanomaterials (materials which have at least one dimensional feature with length less than 100 nanometers), and carbon nanotubes (CNTs) specifically, have exhibited great potential in water treatment. CNTs are cylindrical structures comprising single or multiple concentric graphene sheets and have diameters from less than 1 nanometer (nm) up to 50 nm (one nm is one millionth of a millimeter). Due to their unique and tunable structural, physical, and chemical properties, CNTs are used in environmental remediation as absorbents, catalysts or catalyst supports, membranes, and electrodes. However, a poorly understood determinant of the role of CNTs in water treatment is their interaction with chemical disinfectants (e.g., chlorine, chloramine, and ozone). To address these existing gaps in the environmental fate and reactivity of CNTs, this work establishes whether CNTs represent precursors for halogen and nitrogen containing disinfection byproducts (DBPs), which are products that form during a reaction of a disinfectant with organic matter in the water. In addition, we seek to understand how reaction with disinfectants alters CNT surface chemistry, and in turn impacts their environmental mobility and cytotoxicity. Finally, we determine how NOM and other aquatic variables known to impact DBP formation (e.g., Br^-, NOM, and pH) influence the rate and products of CNT reaction with disinfectants. Outcomes of this work contribute to the current understanding of the role of carbon-based species as DBP precursors in disinfection and provide new context as to the environmental significance and implications of CNTs in natural and engineered aquatic systems.

TABLE OF CONTENTS

LIST OF TABLES

LIST OF FIGURES

CHAPTER 1: INTRODUCTION

1.1 Disinfection byproducts (DBPs): Formation and classification

To protect the public from disease causing organisms or pathogens, water providers add a disinfectant (i.e., chlorine, chloramine, or ozone) to drinking water. This practice, though effective at reducing infectious diseases, can alter the quality of finished water because it leads to formation of disinfection byproducts (DBPs). DBPs are unintended products of the reaction of these chemical disinfectants with naturally occurring organic matter (NOM) or other soluble organic substances during drinking water production and wastewater treatment that are an established threat to human and ecosystem health. DBPs are broadly classified as halogenated (i.e., containing Cl, Br, and/or I moieties) or non-halogenated, and can be further differentiated as carbonaceous (C-DBPs) or nitrogenous DBPs (N-DBPs).

Halogenated DBPs are commonly chlorinated, produced via reactions with chlorine containing disinfectants, especially the two most common, free chlorine (HOCl) and monochloramine (NH_2Cl; also known as chloramine, which is produced via reaction of free chlorine with added ammonia). Two important classes of halogenated DBPs are the EPA regulated trihalomethanes (THMs) and haloacetic acids (HAAs). THMs and HAAs are halogenated carbonaceous DBPs (C-DBPs) that form primarily due to chlorination of carbon rich organic matter (i.e., humic and fulvic acid).

While there are several non-halogenated classes of DBPs, perhaps the most significant are nitrosamines. Nitrosamines are formed primarily via reactions of monochloramine with organic nitrogen-containing substances [1]. Notably,

monochloramine is known to promote nitrosamine products via reaction with nitrogenous

precursors although it generally reacts more slowly than free chlorine and produces fewer

halogenated products.

Because iodide (I^-) and bromide (Br^-) are frequently present in water on average

near 20 µg/L [2] and 100 µg/L [3, 4], respectively, their oxidation to hypoiodous acid

(HOI) and hypobromous acid (HOBr) during disinfection can also yield iodinated and

brominated DBPs, as well as mixed halogen species (e.g. dichlorobromomethane) [3-5].

In addition, bromide can serve as a catalyst to generate unique formation pathways of

various DBPs. For example, the ozonation of N,N-dimethylsulfamide (DMS) generates

N-nitrosodimethylamine (NDMA) only when bromide, at concentrations as low as 15

µg/L, is present with a mechanism that begins with the formation of HOBr [6].

1.2 DBP regulation and toxicity

Currently nine organic DBPs are regulated in drinking water[7], although more

than 600 different DBPs have been identified to date [8]. Table 1-1 lists selected DBPs,

including the four regulated trihalomethanes (THM4), five regulated haloacetic acids

(HAA5), one unregulated halonitromethanes, trichloronitromethane (TCNM), and one

emerging non-halogenated N-DBP, NDMA.

DBPs, specifically THMs, were first identified in chlorinated water in 1974 [9]. In

the following years, a survey published by the U.S. EPA revealed that THMs were

pervasive in the nation's chlorinated drinking water [10], while a study published by the

National Cancer Institute (NCI) demonstrated chloroform (a fully-chlorinated THM) as a

carcinogen with laboratory animals [11]. In response to these findings, the U.S. EPA

began regulation of THMs in drinking water in 1979, setting a maximum contaminant

level (MCL) of 100 µg/L (ppb) [12]. Extensive study of the toxicity of DBPs has resulted in more stringent MCLs for drinking water over time – THMs and HAAs are linked to increased risk of cancer, and liver, kidney and central nervous system problems [13]. DBPs became more strictly regulated in 1998 under the Stage 1 Disinfectants and Disinfection Byproducts Rule (Stage 1 DBPR), with the total THMs (TTHM) MCL set at 80 ppb and HAA5 MCL set at 60 ppb [7]; these MCLs remain enforced today. The EPA has also developed the Stage 2 Disinfectants and Disinfection Byproducts Rule (Stage 2 DBPR), which requires compliance with the Stage 1 DBPR at individual monitoring sites (rather than over system-wide averages), to reduce the risk of high levels of DBPs in drinking water [7].

The emerging contaminant classes of DBPs typically occur at much lower concentrations than regulated DBPs, frequently from low µg/L (ppb) to ng/L (ppt) levels [14]. However, they are considered "high priority" by the EPA because toxicological studies have revealed high genotoxicity and cytotoxicity compared to regulated DBPs, which may drive future regulations [15-19]. For example, California has established a non-enforceable Public Health Goal of 3 ng/L for NDMA, reflecting the fact that it is a known carcinogen [20]. Notably, a shift from Cl-DBPs to Br- and I-DBPs is known to increase geno- and cytotoxicity many fold, in turn making these species likely subjects of equally stringent future regulations [15-19]. Iodoacetic acid is one such DBP of emerging concern [21]. Currently, the EPA develops priority lists (termed "Contaminant Candidate Lists") [22] of emerging contaminants, including unregulated DBPs, that may require regulation under the Safe Drinking Water Act (SDWA) pending further information about the pollutants (i.e., toxicity, documented occurrence in drinking water, availability

of methods of detection). These lists, published every five years, are the first step in developing enforceable federal MCLs. The EPA also requires monitoring of some unregulated emerging contaminants (such as nitrosamines, which include NDMA) via the Unregulated Contaminant Monitoring Regulation (UCMR) program [23].

1.3 Control of DBP formation: Importance of precursor control and disinfectant selection

Since the discovery of DBPs in treated water supplies [9, 24], a major thrust in water research is to identify best practices for providing protection from pathogens while simultaneously minimizing health risks from DBPs. Most research to date has centered on the EPA regulated trihalomethanes (THMs) and haloacetic acids (HAAs). THMs and HAAs are halogenated carbonaceous DBPs (C-DBPs) that form primarily due to chlorination of carbon rich organic matter (i.e., humic and fulvic acid). Over 185 model precursors for THM and HAA formation have been discovered [25]. There are generally two intertwined approaches that have been explored for minimizing DBP formation: identification and minimization of DBP precursors, and identification of alternative disinfectants for drinking water treatment.

DBP precursors are defined as those constituents in water or wastewater that form byproducts upon reaction with chemical disinfectants. They must be present in water supplies and also exhibit reactivity (or possess reactive functional groups) toward disinfectants (i.e., chlorine, ozone). If identified, pretreatment technologies to remove precursors prior to application of chemical disinfectants can be used to minimize the final concentration of DBPs in the finished water.

Generally, natural organic matter (NOM) is recognized as the primary precursor to DBPs [26-28]. NOM is the remnants of degraded plant and animal material associated with natural biochemical processes and materials derived from waste effluents [29, 30]. It contains many functional groups and potentially reactive moieties held together with a carbon matrix by both strong and weak bonds. It is a suite of substances having a distribution of components with apparent molecular weights ranging from a few hundred to thousands of Daltons [31]. An important fraction consists of "humic" substances that contain C, H, O, N, and S as major elements. NOM may also consist of discrete molecules such as amino acids and proteins (non-humic substances). However, the structure of NOM encompasses a wide range of organic structures and functional groups making it difficult to ascertain any accurate conclusions to the underlying chemistry (Figure 1-1). This has led to the development of more than 100 models that attempt to predict the formation of DBPs from NOM containing waters [32]. Researchers have used model precursors – smaller, organic molecules with key characteristics (functionalities, bonds) that are representative of those in NOM – as surrogates in reactions to develop fundamental mechanistic insight into DBP formation. Unfortunately, the use of model precursors had yielded inconclusive results [27, 33, 34]. Because of this, DBP formation chemistry continues to evolve.

Regarding types of disinfectants, chlorine is a strong oxidant and many DBPs are chlorinated, so some effort centers on identifying alternative oxidants. Chloramines are generally weaker oxidants and tend to yield less chlorinated DBP, but can potentially generate N-based byproducts [35-37]. Some have focused on other alternatives, including ozone, which yields other forms of DBPs (bromates, etc.) [6, 38]. UV light is a

nonchemical option for disinfection, and while halogenated DBPs are not generated, DBP precursors can form with photolysis [39, 40]. With the use of ozone and UV, chlorine or chloramines are often added before water enters a distribution system to provide a disinfectant residual as a protectant against pathogens in pipelines; these additions enable formation of DBPs. Inorganic constituents existing in the water, including iodide and bromide, can also result in the formation of iodinated and brominated DBPs, as well as more complex DBPs containing mixtures of halogenated species [3, 41-45]. All disinfectants utilize (photo)chemical reactions that will react with constituents found in water, resulting in formation of DBPs and/or DBP precursors.

1.4 Mechanistic considerations for DBP formation from known precursors

As noted above, a wide array of natural and anthropogenic forms of organic carbon are demonstrated precursors to DBP formation. However, despite more than 30 years of research, a detailed mechanism for DBP formation from NOM has largely been elusive due to its structural and chemical complexity. Instead, work with model precursors, some of which are shown in Figure 1-2, has provided the most useful insight into the various reaction mechanisms for DBP formation from organic matter. These models are believed to represent reactive moieties of NOM or are compounds actually found in drinking water. Several recent reviews [1, 25, 46, 47] and papers discuss the chemistry of the formation of many important DBPs and other halogenated species by reactions involving specific model precursor compounds (e.g., formation of THMs by chlorination of resorcinol [48], formation of NDMA from reaction of monochloramine with dimethylamine [36], and amine containing pharmaceuticals [49]). A large number of natural compounds can produce an array of DBPs from multiple DBP classes (e.g.,

THMs and HAAs) [50-53]. Even the aqueous chlorination of glucose produces THMs [54]. Specific moieties on model precursors are often believed responsible for DBP formation, including carboxylic acids, phenols, and amines [27]. As a specific example, chlorine can react with phenol by electrophilic substitution, in which THMs are formed by chlorination at the 2, 4, and 6 positions of phenol.

1.5 Engineered carbon nanomaterials as next-generation DBP precursors

Based on these prior studies, it is highly likely that carbon nanotubes (CNTs) are able to promote DBP formation via reaction with chlorine-based disinfectants. Most notably, functionalized CNTs, which are among the most valuable commercially, possess surface groups that resemble established DBP precursors (see Figure 1-2) and are likely to react with chemical disinfectants to generate a variety of known DBPs, among other possible reaction byproducts. For example, a reasonable bulk analogue for CNTs is activated carbon (AC), long used as a sorbent in water and wastewater treatment. Generated via pyrolysis and activation of an organic-rich base material (e.g., wood, coal) [55], the structure of AC is approximate to graphite, in which hexagonal arrangements of carbon atoms are stacked in layers of graphene [56]. AC is also rich in heteroatoms, namely oxygen and nitrogen, that attach at the edges of the graphite basal planes [57, 58] as functional moieties such as carboxylic acids, phenols, lactones, quinones and, in the case of nitrogen, amines, pyrrole- and pyridine-like species [59]. Based on these electron-rich surface moieties, it is not surprising that AC is readily oxidized during chemical disinfection with free chlorine and is, in fact, commonly used to dechlorinate water [55, 60]. Previous work has demonstrated the formation of halogenated byproducts including chlorophenols, hydroxylated PCBs, and various chlororesorcinols via reactions of

chlorine and chloramine on the surface of AC [61, 62]. Many times, these products were not generated in homogeneous systems free of AC. Hwang et al.[63] observed that free chlorine reacted with anilines adsorbed to AC to produce azobenzene, a potentially toxic substance. Noteworthy recent work with AC has also shown its ability to also promote formation of NDMA from surface associated amines [64, 65].

CNTs, which are widely utilized in industry and commerce as a result of their unique physical, chemical, and electronic properties [66, 67], share important material properties with AC from which reactivity toward free chlorine and chloramine should be expected. CNTs are one-dimensional nanostructures formed when a graphene sheet, the same planar carbon structure comprising bulk AC, is rolled into a cylinder of nanoscale diameter [68]. Via surface functionalization routes [69, 70], CNTs can be altered systematically to incorporate several of the surface moieties (e.g., $-OH$, $-COOH$, $-C=O$, $-NH_2$) commonly encountered on AC, as well as model DBP precursors (see Figure 1-2). More recently, advances in CNT fabrication and functionalization have allowed for the incorporation of larger macromolecules such as polymers, most commonly species like polyethylene glycol (PEG). We also cannot rule out, based on established recipes of CNT synthesis and functionalization that utilize chlorine- and nitrogen-containing reagents often under aggressive, oxidizing conditions, that in some instances commercially available CNTs may also represent direct sources of some DBPs upon dispersion in water, during which residual byproducts from their fabrication would be released into the aqueous phase.

While CNTs share many attributes with AC, unique differences owing to their nanoscale dimensions [71] should enhance their activity toward chlorine-based

disinfectants. For example, the near entirety of CNT surface area is external (with vendor-reported surface areas on the order of 1000 m^2/g), whereas most AC surface area (~600 m^2/g for granular carbon) is internal (in pores of the material). The electronic character of certain CNTs is also distinct. For CNTs made from a single graphene sheet (i.e., single-walled carbon nanotubes), the orientation of the rolled sheet has a profound impact on electronic properties, causing SWCNTs to range from metallic to semi-conducting in nature [68, 72]. As such, SWCNTs can exhibit redox activity [73, 74], which should in turn make them more prone to oxidation via chemical disinfectants. We contend, therefore, that CNTs represent a potential, as yet unrecognized, source of DBP formation during water and wastewater treatment.

1.6 Potential entry of CNTs in water supplies via their application and incidental release

While the surface chemistry of CNTs suggests their likely ability to function as DBP precursors, their importance in such a capacity depends upon the likelihood that CNTs or other functionalized carbonaceous nanomaterials encounter chemical disinfectants used during water and wastewater treatment. There are two probable routes of entry of CNTs into engineered treatment systems which may facilitate their exposure to and reaction with chemical disinfectants.

The first pathway is the release of CNTs into water supplies as a result of their extensive production and use. Thus, one important entry route may be waste discharge from production and manufacturing plants. With the increasing popularity of CNTs for commercial and industrial uses, production currently reaches several kilotons per year [67] and is expected to eclipse 10 kilotons per year by 2020 (Figure 1-3). Waste

discharge from CNT manufacture may be high in concentration (high μg/L level), and could impact receiving bodies from such waste. The majority of research on their environmental implications has shown that CNTs, particularly those with surface oxide groups, are very mobile in the environment [75, 76]. CNT mobility increases with metal content and the presence of organic matter as a co-solute [76]. Once in the water supply, they may ultimately make their way into drinking water sources.

CNTs can also be unintentionally released into the air, surface water, and wastewater through use (Figure 1-3). For example, products using CNTs (e.g., sensors, composite materials, or electronics) may be landfilled, after which CNTs can leach into groundwater. Researchers have been able to approximate the ultimate fate of CNTs incidentally released into the environment; the CNT concentration in exposed water systems is expected to be in the sub ng/L levels based on such modeling [77, 78]. Ultimately, the risk associated to human toxicity based on these estimations are not of concern [77].

The second route that we envision relates to the use of CNTs in water quality control applications, including treatment and sensing technologies for water. Indeed, CNT application in environmental remediation is being rapidly researched. A recent review by Mauter and Elemelech [68] presents a broad range of applications for CNTs, including sorbents, high-flux membranes, composite filters, antimicrobial agents, environmental sensors, renewable energy technologies, and pollution prevention. For example, water filters are currently being developed with mechanically and electrochemically robust networks of tangled CNT sheets to electrochemically oxidize organic viruses [79] and simple organic contaminants [80]. In our own research group,

Outlon et al. demonstrated the concept of applying CNTs as a reactive surface on a ceramic membrane that when combined with ozone produces hydroxyl radicals to serve as an advanced oxidation process [81].

Another water treatment application relies on the high surface area to volume ratio of CNTs, which makes them powerful sorbents. CNT-based sorbents typically exhibit rapid equilibrium times and high sorbent capacity. The most desirable attribute, however, is their tunable surface chemistry. The ability to tailor their physical and chemical adsorption forces via synthesis (i.e., size, shape, and number of walls) and functionalization (i.e., metals, ligands, or polymers) makes CNTs preferable over the conventional sorbents (i.e., activated carbon). Accordingly, the literature on the adsorption capabilities of CNTs is extensive, with their performance explored toward a diverse suite of pollutant targets including trihalomethanes [82, 83], fluoride [84], nickel [85, 86], strontium [86], lead [87, 88], copper [88, 89], cadmium [88], chromium [90, 91], americium [92], arsenate [93], perchlorate [94], tetracycline (antibiotic) [95], cyanobacterial toxins microcystins [96], aromatic compounds [97, 98], naphthalene [99], and NOM [100].

More recently, CNTs have been incorporated into impermeable support matrices that allow for tailored selectivity at increased fluxes during water filtration [68, 101]. The CNTs' nonpolar interior and tip-functionalized polar ends can provide strong affinity to polar water molecules and reject salt and other pollutants, making them strong contenders for desalination of sea and brackish water. A review by Das et al. [102] details the numerous advantages and potential of this application. As one example, fouling is a major problem limiting the application of membrane filtration. Because the majority of

fouling is due to hydrophobic particles, colloids, emulsion, and macromolecules depositing and accumulating on a membrane's hydrophobic regions, increasing the membrane hydrophilicity can reduce membrane fouling [103]. Accordingly, integration of CNTs into ultrafiltration membranes in combination with an applied electrical potential [104] or hydrophilic and/or bactericidal composite materials (i.e., silver) [105] has been shown to slow fouling.

In all of these water treatment applications, understanding of CNT reactivity toward chemical disinfectants is necessary. Not only will reactivity data provide insights into potentially adverse byproducts generated from such reactions, but it will also provide information related to the long-term stability of CNTs used in such applications and/or devices. Recently, much focus has been paid to the role of polymer membranes, a technology growing in prominence for water treatment, in generating and releasing DBPs and DBP precursors, respectively, into finished water supplies [106, 107]. Before CNT-enabled approaches gain their inevitable foothold in the treatment technology market, their potential for adverse, unintended DBP production must be established.

1.7 Study Rationale

To our knowledge, the extent of possible byproducts from the reactions between CNTs and chemical disinfectants has not been investigated under environmentally relevant conditions. Rather, focus is made on applying CNTs as sorbents for DBPs, a treatment technology fitting for post-chlorination [82, 83]. Chlorination of CNT surfaces has been demonstrated [69, 70, 108-110], but typically under conditions not representative of disinfection. Yuan et al. [111] utilized conditions closest to water treatment; $Cl_2(g)$ was bubbled into a suspension of multi-walled CNTs (MWCNTs)

prepared in distilled water at a flow rate of 2–3 mL/min for 4 h at 60 °C. This process purified the MWCNTs, removing residual catalyst and amorphous carbon, while introducing carboxyl groups and C-Cl bonds to the MWCNT surface, and the chlorinated MWCNTs were more easily dispersible in polar solvents. In another study, Gohier et al. [112] developed a resistive gas sensor using 2D mats of MWCNTs. The sensor detected $Cl_2(g)$ via a change in resistance induced by charge transfer between chlorine and the MWCNTs, producing C-Cl surface bonds as detected by X-ray photoelectron spectroscopy.

Predicting the rate and extent of DBP formation via CNT chlorination is challenging due to the range of material properties they exhibit. These variable properties are likely to influence their reactivity toward disinfectants. For example, CNT conductivity varies in response to the number of graphene sheets in their structure. SWCNTs can exhibit metallic or semi-metallic properties, whereas double-walled (DWCNTs; two graphene sheets) and multi-walled (MWCNTs; > two graphene sheets) CNTs behave as semiconducting materials [113], with the reduction potential of CNTs tending to increase with increasing band gap [74]. This in turn will influence the relative redox properties of these materials toward chlorine oxidants.

Variations in CNT purity and elemental composition may also influence reactivity during disinfection. Commercially available CNTs are loaded with residuals from catalysts used in synthesis, carbonaceous impurities (e.g., amorphous carbon), defects and physical heterogeneities [68], the extent of which can vary with synthesis method [114]. These impurities provide additional, potentially reactive sites on CNTs that may contribute to DBP formation. Because cost remains an important driver in CNT

application, the potential for unique activity in inexpensive, low purity CNTs must not be overlooked.

A final variable certain to influence CNT reactivity toward disinfectants is the nature of surface functional groups. Surface oxidation, which is necessary for increasing CNT polarity and water solubility, creates surface oxide groups including carboxyl (−COOH), carbonyl (−C=O) and hydroxyl (−OH) groups [115]. Based on the prevalence of these functionalities in common aromatic model compounds for C- and N-DBP precursors (see Figure 1-2), reaction of these surface moieties may promote DBP formation during chlorination and chloramination.

Interactions between CNTs and NOM are likely to alter trends in DBP formation relative to systems without CNTs. In addition to direct reaction with chlorine-based disinfectants, CNTs are likely to influence DBP production through their ability to concentrate NOM on their surfaces through sorption [116-120]. While it is well established that CNTs are sorbents for NOM, the resulting surface layer of NOM could exhibit any number of behaviors during disinfection. One scenario is that CNTs will limit DBP formation by limiting NOM availability in solution and lowering reactivity toward chlorine-based disinfectants. It is also possible that NOM adsorption on CNTs may promote DBP formation. CNT surfaces could concentrate NOM to levels not typically achievable in homogeneous solution. Further, uptake on CNTs could fractionate NOM, producing a surface-bound phase with unique and potentially elevated reactivity relative to the soluble NOM fraction. Potentially, CNT-bound NOM could exhibit rates and product yields distinct from DBP formation in the absence of CNTs. A scenario in which surface association of NOM alters DBP formation is not new; Hassan et al. [121] showed

that chlorine loss and the formation of HAAs in water with riverine NOM were significantly enhanced in the presence of goethite (α-FeOOH). They attributed this to possible changes in the conformation of adsorbed NOM that increased availability of reactive sites in the NOM toward chlorine.

1.8 Study Objectives and Hypothesis

To address these existing gaps in the environmental fate and reactivity of CNTs, this work explores the DBP formation potential of CNTs during various chemical oxidative processes. The content herein spans a range of concepts from basic chemical understanding of DBP formation to CNT chemical and physical characteristics. Specifically this work targets the formation of nitrosamines, trihalomethanes, and haloacetic acids in clean and natural well-controlled water matrices during chlorination, chloramination, and ozonation of suspended surface-modified CNTs. Collectively, it encompasses implications for the release or application of CNTs in engineered water matrices.

Specific objectives include:

- Establish whether CNTs represent precursors for halogenated and nitrogenous disinfection byproducts, and identify the material properties of CNTs most influential on their reactivity toward disinfectants.
- Assess how reaction with disinfectants alters CNT surface chemistry, and in turn impacts their environmental mobility and cytotoxicity.
- Determine how NOM and other aquatic variables known to impact DBP formation (e.g., Br^-, NOM, pH) influence the rate and products of CNT reaction with disinfectants.

These objectives are driven by the following hypotheses. First, because of the similar chemical characteristics between functionalized CNTs and NOM, CNTs will generate DBPs. Reaction rates, identities, and yields of DBPs will depend on CNT properties including sidewall configuration and surface chemistry. Second, conditions representative of water and wastewater disinfection will result in the addition of Cl on the CNT surface, and when Br^- is present, surface bound Br will also be incorporate into CNT surface due to their ability to halogenate organic carbon. Third, their oxidized surface after contact with chlorine (or other disinfectant) will influence the aqueous suspension stability and thus mobility, particularly non-functionalized CNTs will increase dispersivity, while CNTs with polar surface groups will lose stability on account of gaining oxidation and halogenation. Fourth, NOM uptake on CNT surfaces will result in rates and yields of DBP formation that are distinct from those that are observed in systems with either NOM or CNTs in isolation. Fifth, when bromide is present, CNTs will promote the formation of brominated DBPs during reaction with disinfectants.

1.9 Overview and thesis organization

This thesis contains three chapters of original research testing the hypothesis listed above. The first research chapter, Chapter 2, demonstrates that N-CNTs are not only a precursor but also a source for NDMA. Working with commercial N-CNTs possessing amine, amide and N-containing polymer functionalities, the extent of NDMA leaching upon dispersion of N-CNT powders in aqueous suspensions was determined. Chapter 2 also explores the chlorine demand and corresponding NDMA production for N-CNTs, while examining NDMA formation via N-CNT reaction with other common chemical disinfectants (e.g., monochloramine and ozone). A particular focus of these

studies was to establish how engineered N-CNTs compare to natural forms of organic matter as NDMA precursors. Changes in N-CNT surface chemistry arising from chlorination were identified with X-ray photoelectron spectroscopy (XPS), and the impact of these changes was then assessed in a series of suspension stability (i.e., sedimentation) studies and via a bioassay with *E. coli* to identify potential changes in N-CNT acute toxicity arising from chlorination.
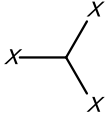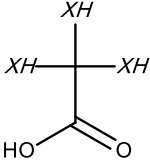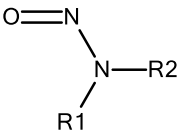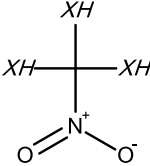
Chapter 3 explores the production of chloroform and mono-, di-, and trichloroacetic acid generated in response to the chlorine demand exerted by various types of CNTs. Both single-walled and multi-walled CNTs were explored, while also considering differences in DBP formation potential arising from the extent and method of chemical functionalization (e.g., oxidation via strong acid, ozone, free chlorine or UV light). Chapter 2 also explored DBP production during chlorination of polymers polyethylene glycol (PEG) and poly(m-aminobenzene sulfonic acid) (PABS) functionalized CNTs, specifically considering whether the polymer-CNT structure exhibited unique DBP formation potential relative to the polymer or CNT alone. Quantification of DBP was complemented by CNT analysis with XPS Raman spectroscopy, and suspension stability measurements to identify physicochemical properties of the CNT suspensions most critical to DBP formation.

Chapter 4 demonstrates the effect of bromide (Br^-) concentrations, pH, and NOM on the formation of DBPs during chlorination of CNTs exhibiting a range of surface chemistries. To address these questions, a selected suite of arc discharged synthesized SWCNTs from Carbon Solutions, Inc. (CS) with polymer (PABS and PEG), oxygen (primarily carboxylated), or no surface functional groups were reacted with free chlorine

in batch system with systematically varied water quality. First the effect of bromide ion concentration on DBP formation was investigated at dissolved bromide levels representative of natural waters. Then, in pH buffered systems, DBP formation was examined in CNT suspensions across a range of environmentally relevant pH values. Finally, using Suwannee River Humic Acid as a model of NOM, DBP formation in CNT/NOM mixtures was examined to determine whether formation is inhibited, additive, or synergistic in the presence of two known precursors.

Outcomes of this work are anticipated to contribute to the current understanding of the role of carbon-based species as DBP precursors in disinfection and to provide new context as to the environmental significance and implications of CNTs in natural and engineered aquatic systems. Results will not only establish whether CNTs serve as precursors to disinfection byproducts, but also identify the types, rates of formation, and total potential yields of selected DBPs.

Table 1-1: List of selected DBPs that are the focus of this project, including those regulated in drinking water and emerging classes not yet regulated but for which regulatory action is anticipated in the near future.

Category	General structure	Species analyzed
Trihalomethanes (THM)		Chloroform (CF) Bromoform (BF) Bromodichloromethane (BDCM) Dibromochloromethane (DBCM)
Haloacetic acid (HAA)		Monochloroacetic acid (MCAA) Monobromoacetic acid (MBAA) Dichloroacetic acid (DCAA) Dibromoacetic acid (DBAA) Bromochloroacetic acid (BCAA) Bromodichloroacetic acid (BDCAA) Chlorodibromoacetic acid (CDBAA) Trichloroacetic acid (TCAA) Tribromoacetic acid (TBAA)
Nitrosoamines		N-nitrosodimethylamine (NDMA)
Halonitromethanes (HNM)		Trichloronitromethane (TCNM)

X stands for any halogen, XH for any halogen or hydrogen, R any carbon group or hydrogen.
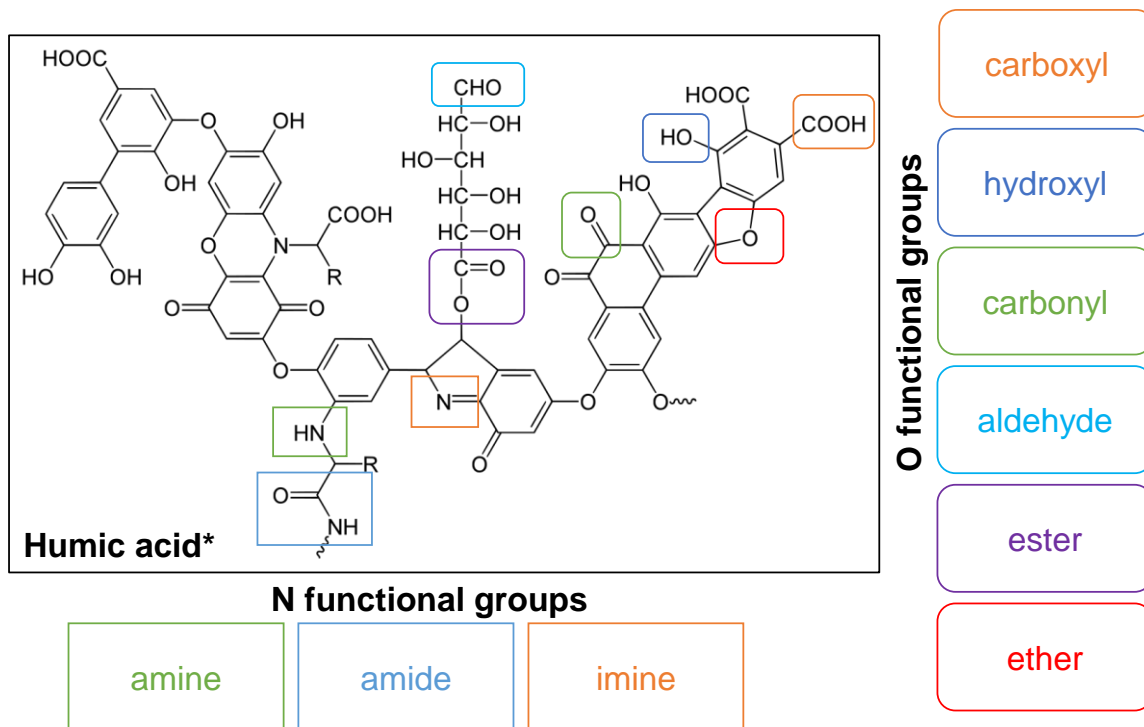
Figure 1-1: Representation of humic acid (*) as conceptualized in Stevenson 1994 [122]. Humic acid is a segment of NOM with various oxygen and nitrogen functional groups (highlighted with a box).
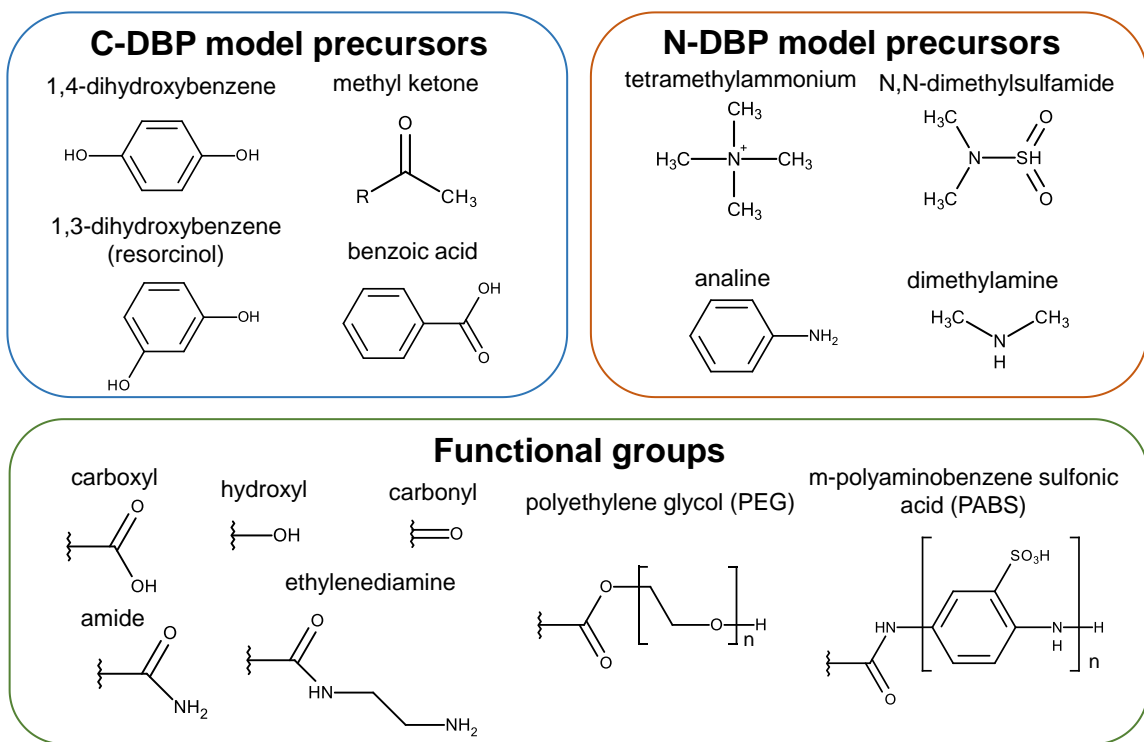
Figure 1-2: Array of C-DBP [27] and N-DBP [37, 63] model precursors and analogous functional groups that are available on commercial CNTs.
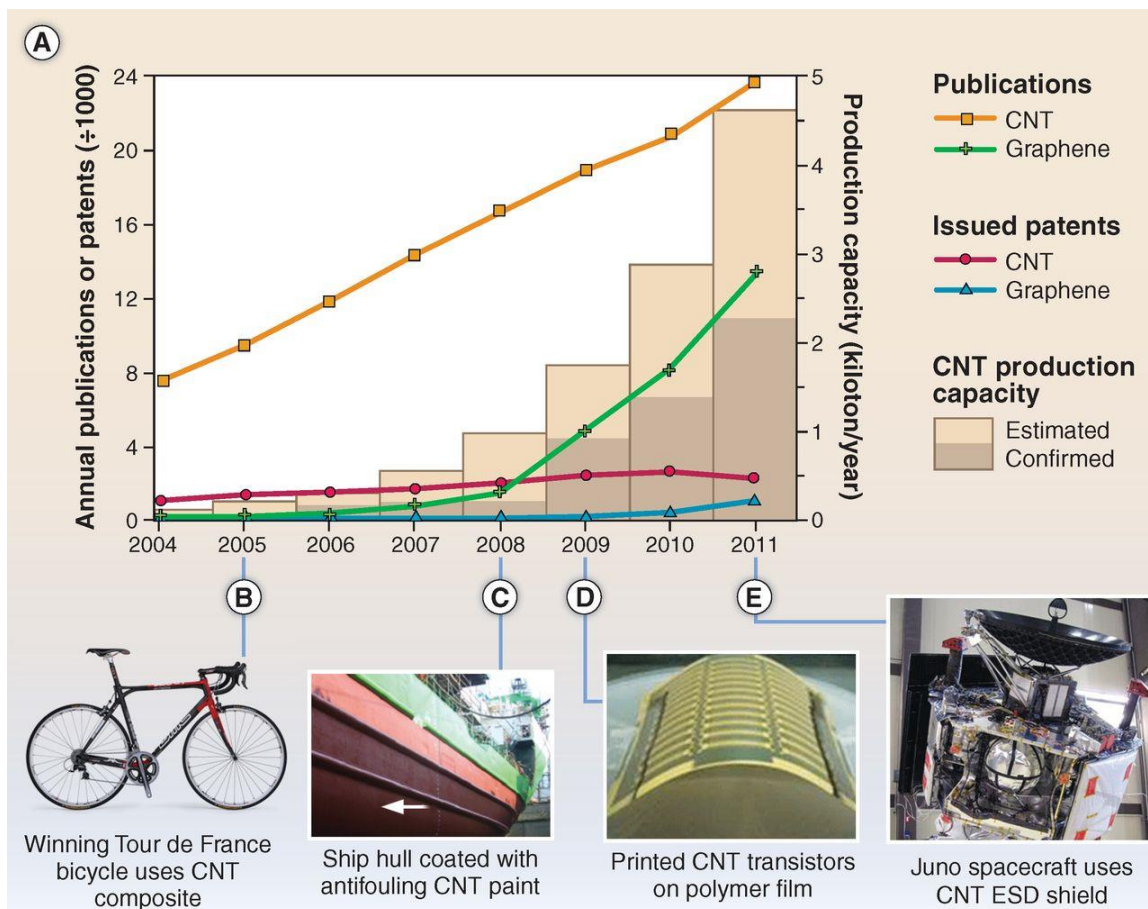
Figure 1-3: Trends in CNT research and commercialization. Used with permission [67].

CHAPTER 2: N-FUNCTIONALIZED CARBON NANOTUBES AS A SOURCE AND PRECURSOR OF N-NITROSODIMETHYLAMINE

2.1 Abstract[1]

Hazardous byproducts may be generated during the environmental processing of engineered nanomaterials. Here, we explore the ability of carbon nanotubes with nitrogen-containing surface groups (N-CNTs) to generate N-nitrosodimethylamine (NDMA) during chemical disinfection. Unexpectedly, we observed that commercial N-CNTs with amine, amide, or N-containing polymer (PABS) surface groups are a source of NDMA. As-received powders can leach up to 50 ng of NDMA per mg N-CNT in aqueous suspension; presumably NDMA originates as a residue from N-CNT manufacturing. Furthermore, reaction of N-CNTs with HOCl, monochloramine, and ozone generated byproduct NDMA at yields comparable to those reported for natural organic matter. Chlorination also altered N-CNT surface chemistry, with X-ray photoelectron spectroscopy indicating addition of Cl, loss of N, and an increase in surface O. Although these changes can increase N-CNT suspension stability, they do not enhance their acute toxicity in *E. coli* bioassays above that observed for as-received powders. Notably, however, dechlorination of reacted N-CNTs with sulfite completely suppresses N-CNT toxicity. Collectively, our work demonstrates that N-CNTs are both a source and precursor of NDMA, a probable human carcinogen, while chemical disinfection can produce CNTs exhibiting surface chemistry and environmental behavior distinct from native (i.e., as-received) materials.

---

[1] An abbreviated version of this work has been published: Verdugo, E.M., et al., *N-functionalized carbon nanotubes as a source and precursor of N-nitrosodimethylamine: Implications for environmental fate, transport, and toxicity*. Environ. Sci. Technol., 2014. **48**(16): p. 9279-9287.

2.2 Introduction

Nitrosamines, a non-halogenated class of disinfection byproducts (DBPs), are generated primarily via reaction of monochloramine with organic nitrogen-containing precursors, including natural organic matter (NOM) [1, 37]. Although nitrosamines typically occur at lower concentrations (e.g., low µg/L to ng/L levels [14, 123]) in drinking water than regulated DBPs (e.g., trihalomethanes), their high genotoxicity and cytotoxicity will likely drive future regulations [15, 17, 19, 124]. For example, while federal regulations for N-nitrosodimethylamine (NDMA) in drinking water are under development, California has established a non-enforceable Public Health Goal of 3 ng/L because it is a probable human carcinogen [20]. Given its potency, the identification and management of NDMA precursors is a priority for limiting its formation.

Based upon known precursors, carbon nanotubes (CNTs) are likely to generate DBPs during chemical disinfection. A reasonable bulk analogue for CNTs is activated carbon (AC), whose electron-rich surface moieties readily reduce chemical disinfectants (e.g., it can be used for dechlorination [55, 60]) to yield a variety of byproducts [61-63]. Recent studies have even shown that oxidation of secondary amines on the AC surface promotes NDMA formation [64, 65, 125]. By analogy, several commercial forms of CNTs have N-containing surface groups (N-CNTs; Table 2-1), materials gaining popularity for sensing [126] and biomedical [127] applications. These N-CNTs possess surface functionalities evocative of model NDMA precursors [125] including monomethylamine [50], aniline [128, 129], diethylamine [128], dimethylformamide (DMF) [130], and dimethylamine [128, 130, 131]. Moreover, a growing number of studies have observed that CNT surface functionalization imparts behavior reminiscent of

NOM. This includes a role for functionalized CNTs as sorbents for organic pollutants [132], complexation agents for metals [133, 134], sensitizers for reactive oxygen species (ROS) production upon light irradiation [135], and promoters of hydroxyl radical formation during ozonation [81]. Thus, it is reasonable to expect that these same surface functionalities may also react with chemical disinfectants to yield undesirable byproducts.

This study aims to better predict the adverse implications of nanomaterial entry into water and wastewater treatment facilities, where extreme chemical environments during disinfection are likely to facilitate nanomaterial transformation. We acknowledge that CNT concentrations in drinking water and domestic wastewater are not likely sufficient to contribute significantly to DBP production relative to traditional precursors (e.g., NOM). However, treatment of waste streams from nanomaterial production or manufacturing may produce scenarios where higher concentrations are available [78] to react with chemical disinfectants, potentially resulting in non-negligible NDMA levels given its potency. We also note the rapidly growing number of applications proposing to utilize CNTs in water treatment, particularly as components of water purification membranes [68]. Accordingly, details of their stability and reactivity in treatment systems may help to guide responsible CNT application. This includes evaluating whether commercial N-CNTs are a pollutant source; hazardous production byproducts could be subsequently released into water during their application. For example, because aggressive chemical conditions are necessary to link N-containing groups to CNT surfaces [136-139], byproducts including known NDMA precursors or even NDMA may be generated and retained on N-CNT surfaces as residues from their manufacturing.

Here, we demonstrate that N-CNTs are not only a precursor but also a source for NDMA. Working with commercial N-CNTs possessing amine, amide and N-containing polymer functionalities (Table 2-1), we explored the extent of NDMA leaching upon dispersion of N-CNT powders in aqueous suspensions. We also quantified the chlorine demand and corresponding NDMA production for N-CNTs, while examining NDMA formation via N-CNT reaction with other common chemical disinfectants (e.g., monochloramine and ozone). A particular focus of these studies was to establish how engineered N-CNTs compare to natural forms of organic matter as NDMA precursors. Changes in N-CNT surface chemistry arising from chlorination were identified with X-ray photoelectron spectroscopy (XPS), and the impact of these changes was then assessed in a series of suspension stability (i.e., sedimentation) studies and via a bioassay with E. coli to identify potential changes in N-CNT acute toxicity arising from chlorination. Collectively, our findings illustrate how engineered nanomaterials can adversely affect water quality via byproducts of their synthesis and environmental processing.

2.3 Experimental methods

2.3.1 Reagents

Chlorination experiments used sodium hypochlorite (NaOCl; Fisher; 5.65-6%) sodium sulfite (Na_2SO_3; Sigma Aldrich; $\geq$ 98.0%), anhydrous potassium phosphate monobasic (KH_2PO_4; RPI; ACS grade), and sodium hydroxide (NaOH; Acros Organics; ACS grade). Reagents used for chlorine analysis included anhydrous sodium phosphate dibasic (Na_2HPO_4; RPI; ACS grade), disodium ethylenediamine tetraacetic acid dehydrate (EDTA; Sigma; ACS grade), ferrous ammonium sulfate hexahydrate (FAS; J.T. Baker; ACS grade), and N,N-diethyl-p-phenylenediamine (DPD; Aldrich; 97%

purity). NDMA analysis used dichloromethane (DCM; Fisher; stabilized/certified ACS), 5000 µg/mL methanolic NDMA standard (Sigma-Aldrich; analytical standard), and deuterated NDMA internal standard in DCM (NDMA-D6; CIL; 98%). All solutions were prepared in deionized water (Thermo Scientific Barnstead TII).

2.3.2 Commercial N-CNTs

Four formulations of N-CNTs were acquired from NanoLab Inc. (NL) or Carbon Solutions, Inc. (CS) (Table 2-1). These contain amine (NL) and amide (CS) functionalities, as well as the N-containing polymer poly-m-aminobenzene sulfonic acid or PABS (CS). Both single-walled (CS, NL) and multi-walled (NL) CNTs were explored.

According to NL [139], their amine functionalized CNTs are prepared by reacting carboxylated carbon nanotubes with ethylenediamine in the presence of an unspecified coupling reagent. This produces a surface group with an amide linkage and a primary amine group (i.e., $CNT-CONH-CH_2CH_2-NH_2$). Both single-walled (NL $SWNH_2$) and multi-walled (NL $MWNH_2$) varieties of this amine-functionalized CNT were acquired to use experimentally. Single-walled CNTs functionalized with amide moieties (CNT-$CONH_2$) were acquired from CS. According to CS [138], reaction of carboxylated CNTs with oxalyl chloride in dimethylformamide (DMF) yields an acyl chloride surface group (CNT-COCl), which is then treated with gaseous ammonia bubbled though the DMF suspension to produce the desired amide functionality (CNT-$CONH_2$) [136]. SWCNTs functionalized with poly-m-aminobenzene sulfonic acid (PABS) were also acquired from CS. CS prepared PABS by mixing m-aminobenzene sulfonic acid (ABS) and aniline, a polymerization initiator, in 1 M HCl containing ammonium persulfate as an oxidizing

reagent. CS then prepared PABS-CNTs by mixing alkyl chloride functionalized CNTs (prepared as mentioned for amide functionalization) with a DMF solution of PABS [140].

To explore further the origins of NDMA leached from commercial N-CNT powders, we prepared our own N-CNTs according to a procedure by Ramanathan et al. [141]. Functionalization involved the reaction of carboxylated CNTs with ethylenediamine in the presence of N-[(dimethylamino)-1H-1,2,3-triazolo[4,5,6]pyridine-1-ylmethylene]-N-methylmethanaminium hexafluorophosphate N-oxide (with the common name of HATU), which is a frequently employed coupling reagent. Briefly, 20 mg of oxidized SWCNTs were suspended in 10 mL of ethylenediamine using sonication. After adding 1 mg of HATU to the suspension, the suspension was sonicated for an additional 4 h. The product was then diluted with 200 mL of methanol and filtered using 2 μm pore size polycarbonate filter. The filtrate was washed with DI water, which was collected for NDMA quantification.

2.3.3 NDMA release from as-received N-CNTs powders.

To determine the release of NDMA from as-received N-CNT powders, suspensions (1 g/L) of as-received N-CNTs were prepared in DI water in 20 mL vials crimp sealed with butyl rubber septa coated with PTFE. These suspensions were either sampled immediately (i.e., after 5 min of vigorous shaking by hand) to measure short-term release of highly labile NDMA or sonicated for 5 h prior to sampling to explore long-term release of any NDMA more tightly bound to the N-CNT surface. In both cases, a 1 mL sample was withdrawn, diluted to a final N-CNT concentration of 10 mg/L, and subsequently analyzed for NDMA as described below.

2.3.4 NDMA formation via reaction with chemical disinfectants.

To avoid the contribution of NDMA associated with as-received powders, all N-CNTs reacted with chemical disinfectants were first extensively washed via dialysis. Washing via dialysis was done by loading suspensions of N-CNTs into dialysis tubing (MWCO 3500) at approximately 1 g/L and dialyzed against DI water while sonicating the suspension every other day for 1 hour. Suspensions were dialyzed (5-7 d) until a dilution to 10 mg/L of N-CNT yielded an NDMA reading below our method detection limit (3 ng/L). Stock suspensions (1 g/L) of washed N-CNT suspensions were then prepared for use in experiments. Prior to use, stock suspensions were sonicated for 15 minutes (Bransonic Ultrasonics Corporation, 151OR-DTH, 42 kHz $\pm$ 6%) to disperse the N-CNTs. Suspensions of N-CNTs were reacted with free chlorine (HOCl), monochloramine and ozone in batch systems

2.3.4.1 Reaction with free chlorine.

Aqueous stock solutions of free chlorine (HOCl) were prepared by diluting concentrated sodium hypochlorite (Fisher; ~50 g/L as Cl_2) to ~500 mg/L in amber glass bottles sealed with Teflon-lined screw caps. Stock HOCl solutions were prepared daily, and their concentration was measured via titration prior to use. Chlorination experiments were conducted in either 5 mM phosphate or carbonate buffer at either pH 7 or 8. Chlorination experiments used an N-CNT loading between 5-20 mg/L and an initial HOCl concentration between 0.1-50 mg as Cl_2/L. The reaction was initiated by spiking in the desired volume of stock N-CNT suspension into a pH buffered solution of HOCl.

During reaction, reactor contents were well-suspended by mixing using a stir bar and a stir plate, while samples were periodically withdrawn to monitor NDMA and HOCl concentrations over time. For NDMA analysis, 50 mL of sample volume was extracted using a 50 mL sterilized polystyrene pipette and transferred into a 200 mL amber bottle containing 15 µL of 1 M sodium sulfite to quench residual HOCl. NDMA samples were stored in the fridge for no more than 5 days before analysis (see Section 2.3.7). For HOCl analysis, the sample volume was determined based on the initial HOCl concentration of the experiment. This helped ensure the mass of HOCl fell between our detection limits (2 µg – 0.5 mg as Cl_2). For example, a reaction with 15 mg-Cl_2/L of initial chlorine required about 10 mL of sample volume, whereas, no more than 5 mL was needed for 50 mg-Cl_2/L. All samples were diluted to 100 mL with DI water in a 250 mL Erlenmeyer flask and immediately analyzed via titration (see Section 2.3.7).

2.3.4.2 Reaction with monochloramine.

Aqueous stock solutions of monochloramine were prepared by adding a 7.14 mM HOCl solution to 10.7 mM ammonium chloride adjusted to pH 9 with NaOH. Stock solutions were prepared daily, and the monochloramine concentration was quantified via titration prior to experiments. Experiments with monochloramine were more limited, conducted in 5 mM phosphate buffer at pH 8 with 10 mg/L N-CNT and an initial monochloramine concentration of 15 mg as Cl_2/L. Reactions of N-CNTs with monochloramine were carried out in a manner identical to that described for free chlorine.

2.3.4.3 Reaction with ozone.

Ozonation experiments were conducted in 5 mM phosphate buffer at pH 7, 10 mg/L of N-CNTs, and an initial ozone concentration between 0.2-20 mg/L. Ozone stock solutions were prepared by bubbling an ozone/oxygen gas mixture generated via an LG-7 ozone generator into a flask of phosphate buffer solution chilled with an ice bath. Reactions were initiated by adding a volume of concentrated ozone stock solution to a 100 mL beaker containing a N-CNT suspension prepared in phosphate buffer. To minimize contributions from hydroxyl radical during ozonation, which can accelerate ozone decomposition and also degrade NDMA [142], suspensions also contained 320 μM of the radical scavenger tert-butanol. Ozone was measured via the Indigo Blue method [143]. Upon completion of the reaction, as indicated by the consumption of all available ozone, samples for NDMA analysis were collected as previously described and analyzed as shown below.

2.3.5 Influence of chlorination on N-CNT suspension stability and surface chemistry.

2.3.5.1 Suspension stability of N-CNTs

Stability of N-CNT suspensions was analyzed via sedimentation studies monitoring light transmittance at $\lambda = 700$ nm through a 1-cm path length cell. Sedimentation studies were conducted on N-CNT suspensions before chlorination, after chlorination, and after chlorination with subsequent sulfite dechlorination. Suspensions were prepared with 100 mg/L N-CNTs, which was necessary to produce measurable absorbance at 700 nm. To test the stability of N-CNTs after reaction with free chlorine,

the stoichiometry of reagents used in aforementioned chlorination studies (i.e., 10 mg/L

of CNTs and HOCl up to 50 mg as Cl_2/L) was preserved. Thus, 100 mg/L suspensions of

N-CNTs were reacted with up to 500 mg Cl_2/L HOCl for 1 d.

2.3.5.2 Morphology of N-CNTs

The morphology of suspended N-CNTs before and after chlorination was

evaluated using transmission electron microscopy (TEM). TEM images were collected on

a JEOL JEM 1230 transmission electron microscope operating in bright field mode at

120 kV. TEM samples were prepared by dip-coating a carbon-coated Cu grid in a sample

suspension.

2.3.5.3 Surface chemical composition of N-CNTs

The surface chemical composition of as-received, washed, and reacted N-CNTs

was investigated using a custom-designed Kratos Axis Ultra X-ray photoelectron

spectroscopy (XPS) system equipped with a monochromatic Al Kα X-ray source. An

extensive description of this system can be found elsewhere [144]. For XPS, N-CNTs

samples were collected from a 10 mg/L suspension after reaction (1 d) with 15-50 mg of

HOCl as Cl_2/L. Samples were immobilized on a 13 mm polyvinylidene difluoride

(PVDF) filter, and washed extensively with DI water (~40 mL) prior to analysis. A

similar procedure was used for control N-CNT samples, which were suspended but not

reacted with HOCl. For analysis, PVDF filters were mounted on Cu stubs. XPS analysis

was also conducted on bare PVDF filters to confirm that no background interference was

produced from the underlying substrate. Indeed, no evidence of the underlying filter was

visible in any scan based upon the well-defined graphitic carbon peak indicative of CNTs observed in the C 1s region.

XPS was used to collect full spectrum survey scans, as well as to examine O 1s, C 1s, N 1s, Cl 2p regions. The X-ray gun was operated using a 15 mA emission current at an accelerating voltage of 15 kV. Low-energy electrons were used for charge compensation to neutralize the sample. High-resolution spectra were acquired in the region of interest using the following experimental parameters: 20–40 eV energy window; pass energy of 20 eV; step size of 0.1 eV, and dwell time of 1000 ms. The absolute energy scale was calibrated to the Cu $2p_{2/3}$ peak binding energy of 932.6 eV using an etched copper plate. All spectra were calibrated using the C 1s peak at 285.0 eV. CasaXPS software was used to process the XPS data [145].

2.3.6 Influence of washing and chlorination on N-CNT toxicity.

Acute toxicity studies were performed using model organism *E. coli* strain K12 (MG1655; ATCC 47076). Initial experiments assessed membrane perforation, a suggested mechanism of CNT toxicity in microbes [146]. Fluorescent microscopy viability assays, conducted initially according to protocols in previous studies [146], provided poor reproducibility. As an alternative, we adopted a DNA efflux assay [146] to quantify decreases in membrane integrity. We also implemented an agar plate-based viability method [147] that provided a more comprehensive assessment of toxicity (i.e., mechanisms beyond membrane perforation).

2.3.6.1 Toxicity assay

E. coli strain K12 (MG1655; ATCC 47076) was used as a model organism in viability studies. In all experiments, an overnight culture of *E. coli* was inoculated into LB Base medium. Cells were collected by centrifugation for 5 minutes (1381 xg) at early exponential growth phase (OD_{600}= 0.3–0.4) and washed with 0.85% NaCl to remove residual growth media. For DNA efflux studies, pUC19 plasmid was electroporated into cells prior to experimentation, and growth media was supplemented with ampicillin (100 µg/ml). Bacto Agar was added (1.5%) to LB media to prepare culture plates for plating viability assays. Sterile saline solution (0.85%) was prepared with sodium chloride. Treatments were evaluated for statistical significance using a Student's paired t-Test with a two-tailed distribution.

2.3.6.2 DNA efflux assay.

After preparing *E. coli* as described previously, cells were resuspended in sterile saline solution (OD_{600} ~0.15). Aliquots (50 ml) of cell suspension were incubated with and without CNTs (10 µg/ml) for 1 hour (37 °C) with shaking at 200 rpm. After incubation, sample aliquots were passed through a 0.22 µm Millex low-binding PVDF (Millipore, Billerica, MA) membrane to remove CNTs and bacteria. A Qubit fluorometer High Sensitivity dsDNA assay kit (Invitrogen, Carlsbad, CA) was used to measure dissolved DNA concentrations in each sample. A new calibration was performed with each new DNA measurement using the manufacturer-provided dsDNA standards. All DNA efflux assays were performed in triplicate. Experiments were conducted to account for DNA not measured during fluorometric concentration determination due to sorption onto CNT mass. Aliquots (50 ml) of saline solution were supplemented with purified

pUC19 plasmid (~100 ng/ml) and incubated (37 °C) with and without CNTs (10 µg/ml) at 200 rpm. After 1 hour, sample aliquots were passed through PVDF membranes and dissolved DNA was quantified as described above.

2.3.6.3 Plating viability assay.

Appropriate cell dilutions for plating were determined previously based on spectrophotometric concentration estimates (OD_{600}). Aliquots (25 ml) of cell suspension were incubated (37 °C) with and without CNTs (200 µg/ml) with shaking at 200 rpm. After 1 and 3 hours, samples were removed and serially diluted. For each treatment, 100 µl dilution aliquots were applied to three LB agar plates and distributed with sterile plate spreaders. Plates were incubated overnight (37 °C) and colony forming units (CFUs) were counted the following day. Triplicate experiments were performed for each CNT type.

2.3.7 Analytical methods.

HOCl and monochloramine were measured via titration according to standard methods [148]. Ozone was measured via Indigo Blue [143]. NDMA was also analyzed according to standard methods [148], which relied upon quantification with GC/MS after solid phase extraction while using NDMA-D6 as an internal standard. Additional analytical details can be found below.

2.3.7.1 Titrations to determine HOCl and monochloramine

For titrations to determine HOCl and monochloramine concentrations, 5 mL of each buffer reagent and the DPD indicator solution were added to 100 mL of diluted sample, with the solution turning pink to red in hue in the presence of free chlorine. The

free chlorine concentration was then quantified by titration with ferrous ammonium sulfate (FAS) until the red color disappeared. Monochloramine was quantified by adding potassium iodide crystals to the titration flask after titrating for free chlorine to produce the same color hue which was again titrated to clear with FAS. The concentration was calculated by converting the titrant volume to chlorine mass (1 mL of FAS = 0.1 mg-Cl_2) and dividing by the original sample volume.

2.3.7.2 Sample processing and quantification of NDMA

For NDMA analysis, internal standard, NDMA-D6, was added to all samples (50 mL) to achieve a concentration of 800 ng/L. Carbon beads (200 mg) (Sigma-Aldrich; Lewatit AF 5) were added to the solution and allowed to mix for one hour prior to recovery. The contents of carbon-beads were extracted with dichloromethane and injected into an HP 6890 gas chromatograph coupled with HP 5973 mass-spectrometer (GC/MS). The GC was programmed with the following temperature ramping: initially 40 °C held for 2 min, and 10 °C/min to 60 °C held for 2 min. The sample was injected in pulsed split-less mode at 200 °C with a pressure of 4.2 psi using helium carrier gas. The pulse pressure at 30 psi initiated at 0.5 min for 1.4 min. A SLB-5ms capillary GC column (30 m length, 0.25 mm diameter, 0.25 mm film thickness) was operated under constant flow at 0.8 mL/min (calculated). The receiving MS operated in selective ion mode with the quadrupole mass analyzer temperatures set to 150 °C and chemical ion source temperature set to 250 °C, and was programmed to capture the abundance of the following characteristic mass to charge ratios (m/z): 75 m/z for NDMA and 81 m/z for NDMA-D6. A method detection limit of 3 ng/L was determined.

2.4 Results and discussion

2.4.1 NDMA release from as-received N-CNT powders.

Release of NDMA from freshly prepared suspensions of as-received N-CNTs powders is shown in Figure 2-1 (as ng of NDMA per mg CNT). All commercial N-CNTs leached NDMA, with considerable variability between formulations (e.g., compare NL SWNH$_2$ and CS SWNH$_2$) and batches from the same vendor (e.g., compare the three batches of CS PABS). Although NDMA concentrations in Figure 2-1 were quantified after 5 h of sonication, the majority of the NDMA was released nearly instantly upon addition of N-CNT powders to water (Figure 2-2).

This leached NDMA is likely a byproduct of CNT functionalization that then becomes associated with the nanotube surface during drying. Indeed, attempts to replicate N-functionalization routes utilized by commercial suppliers resulted in comparable concentrations (2 ng of NDMA per mg of CNT) of soluble NDMA. Independently, we also evaluated the tendency of NDMA (logK_{ow} of -0.57 [20]) to adsorb to N-CNTs, observing little to no uptake. Thus, consistent with its rapid release, we propose that NDMA is present on the N-CNT surface not as an adsorbed phase but rather as a dried residue of byproducts generated during functionalization.

The results in Figure 2-1 are reminiscent of recent work demonstrating that several commercial anion exchange resins are a significant source of nitrosamines, including NDMA, and nitrosamine precursors [149]. We note that the amount of NDMA released from select N-CNTs can be high relative to anticipated regulatory levels. For example, one batch of CS PABS leached 50 ng NDMA/mg CNT, suggesting that California's health goal (3 ng/L) would be exceeded at N-CNT concentrations above 60

µg/L. Our data also suggests that some N-CNT functionalization routes may be better than others for limiting NDMA production and subsequent release. Specifically, NL N-CNTs, with an amine surface group, generally leach less NDMA than the amide-functionalized CS N-CNTs, which utilize known NDMA precursor DMF [130] during functionalization. However, considering the batch-to-batch variability observed in Figure 2-1, a more extensive survey of commercially available materials and closer scrutiny of their synthesis routes is likely necessary to make such generalizations confidently.

2.4.2 NDMA formation via reaction with HOCl.

Chlorine decay and the corresponding NDMA production in N-CNT suspensions are shown in Figure 2-3. Results were essentially equivalent at pH 7 or 8 and independent of buffer composition (e.g., phosphate or carbonate). Thus, the majority of results presented herein were collected in phosphate buffer systems at pH 8. Note that chlorine decay and NDMA production were not observed in any controls (e.g., HOCl added to reactors without CNTs or CNT suspensions without free chlorine). Moreover, we reiterate that these reactions were conducted with N-CNTs that had been washed extensively via dialysis. Thus, we do not believe release of NDMA or NDMA precursors (e.g., as has been reported for polyDADMAC [150]) is responsible for the production we have observed. Rather, we contend that NDMA production in Figure 2-3b, which was observed for all N-CNT formulations, results from the reaction of HOCl on the N-CNT surface.

There are several noteworthy observations in Figure 2-3. First, rates of chlorine decay varied among different N-CNT formulations, with NL SWNH$_2$ and CS PABS exhibiting the most, statistically indifferent reactivity toward chlorine while NL MWNH$_2$

and CS SWNH$_2$ exhibited much more limited reactivity (Figure 2-3a). Variability

between the two NL formulations likely reflects differences in the available surface area

of SW (860 m^2/g) and MW (250 m^2/g) N-CNTs. Otherwise, variations in N-CNT

chlorine demand are consistent with established trends in chlorine reactivity toward

organic compounds [46]. Chlorine is known to react with both amines and amides

primarily via Cl transfer to induce chloramination, but amides (e.g., CS SWNH$_2$) are

generally less reactive toward chlorine because of their electron-withdrawing carbonyl

functionality [46]. The high reactivity of CS PABS presumably originates from the

secondary amine and aromatic moieties in the polymer, both of which are active toward

chlorination [46].

Generally, however, chlorine demand did not scale with NDMA production

(Figure 2-3); the relatively large chlorine loss in CS PABS systems produced only

modest NDMA and thus as yet unidentified byproducts are also likely being generated in

parallel. Though there is no statistical difference in the generation of NDMA from the

chlorination of CS PABS, NL MWNH$_2$, and CS SWNH$_2$ for the first 4 hours of the

reaction, a clear contrast of the formation potential of NDMA from N-CNTs can be found

in Figure 2-4. NDMA production also did not correlate with surface N concentrations

measured with XPS. Specifically, NL SWNH$_2$ (0.8% N from the relative area of the N 1s

region) yielded 5-fold more NDMA after 4 h than CS SWNH$_2$ (3.5% N from XPS). Thus,

as commonly reported for traditional, soluble NDMA precursors [50, 125, 151-153], the

chemical structure of the surface N moiety influences NDMA formation. More

practically, this creates an interesting juxtaposition to results in Figure 2-1, as NL CNTs

least prone to leaching NDMA generate the most during chlorination.

In subsequent experiments (Figure 2-4), we have found that the N-CNT concentration limits NDMA formation at high free chlorine concentrations (> 10 mg Cl_2/L; greater than would be expected for water treatment). Thus, in the presence of excess chlorine, the availability of reactive, presumably N-containing, surface sites limits NDMA formation. Conditions more representative of water treatment are shown in Figure 2-5, which examines the stoichiometry of NDMA production per unit chlorine consumed for NL $SWNH_2$ and CS $SWNH_2$. For NL $SWNH_2$, NDMA formation increased with increasing free chlorine demand, yielding roughly 10 ng/L of NDMA per mg/L of HOCl (as Cl_2) consumed. In contrast, NDMA formation was essentially independent of HOCl demand in CS $SWNH_2$ suspensions, implying they possess a fixed but limited number of surface groups available for NDMA formation (e.g., other N-containing sites present as surface impurities). We note that at these low HOCl concentrations, CS PABS did not generate measurable concentrations of NDMA (our method detection limit was 3 ng/L), although NDMA was obviously formed in CS PABS suspensions at higher HOCl concentrations (Figure 2-6)

From Figure 2-5, we can assess where N-CNTs rank among known precursors for NDMA formation. Chen and Valentine [154] explored NDMA formation via the reaction of monochloramine with natural organic matter (NOM) from the Iowa River, observing 30.5 ng of NDMA/mg of NH_2Cl as Cl_2. Thus, the yield of NDMA during chlorination of NL $SWNH_2$ (10 ng NDMA/mg HOCl as Cl_2) is of the same order of magnitude as that generated from a representative NOM sample.

2.4.3 NDMA formation via reaction with ozone and monochloramine.

In suspensions of either NL or CS $SWNH_2$, rapid ozone loss was accompanied with NDMA production (Figure 2-7). Interestingly, CS $SWNH_2$ resulted in greater rates of ozone decay even though ozone generally reacts very slowly with amides relative to primary amines [38, 155]. However, this reactivity trend toward ozone did not match NDMA production, with NL $SWNH_2$ suspensions producing more NDMA. Ozonation of NL $SWNH_2$ produced 1 ng/L of NDMA for every mg/L O_3 consumed, a yield that is 10-fold less than what we observed per mg of free chlorine (as Cl_2). For CS $SWNH_2$, NDMA production also increased with ozone demand, corresponding to a yield of 0.66 ± 0.064 ng/L NDMA per mg/L O_3. Recall that during chlorination, NDMA formation (4 ng/L) was essentially independent of free chlorine demand in CS $SWNH_2$ suspensions (see Figure 2-3). In contrast, the lowest concentration of ozone explored (1 mg/L) generated 4 ng/L of NDMA, with higher ozone concentrations enabling NDMA formation not attainable with free chlorine. During ozonation, therefore, a larger number of surface sites on CS $SWNH_2$ serve as NDMA precursors.

NDMA also formed during reaction of NL and CS $SWNH_2$ with monochloramine (Figure 2-8). Despite comparable monochloramine demand, CS $SWNH_2$ generated more NDMA (roughly 10 mg NDMA/mg NH_2Cl (as Cl_2)) than NL $SWNH_2$, relative reactivity that is distinct from that observed with free chlorine and ozone. While NDMA formation with CS $SWNH_2$ were on par with levels generated with HOCl under comparable conditions (compare Figure 2-5 and Figure 2-8), very little (< 5 ng/L) NDMA was generated in NL $SWNH_2$ suspensions. Once again, we believe these trends in NDMA formation are generally consistent with reports of NDMA formation from model,

dissolved precursors. Specifically, Mitch and Sedlak [50] observed rather limited NDMA formation for monomethylamine, a primary amine analogous to the ethyelenediamine functionality present on NL SWNH$_2$, whereas reasonable amide analogs of CS SWNH$_2$ (e.g., dimethylformamide) were found to produce several orders of magnitude more NDMA over identical timescales.

2.4.4 Influence of chlorination on N-CNT aqueous stability and surface chemistry.

Reaction with free chlorine affected the suspension stability of some, but not all, N-CNTs. For example, as received and washed NL N-CNTs (both SW and MW) were quite unstable in suspension (Figure 2-9 and Figure 2-10). After reaction with free chlorine, however, NL N-CNT suspensions were visibly more disperse (Figure 2-10b) and exhibited greater stability during sedimentation experiments (Figure 2-9). TEM analysis of these reacted N-CNTs generally showed that their morphology and structure was preserved, although some evidence consistent with oxidative damage was occasionally observed (Figure 2-10c, d). Ultimately, therefore, chlorination of NL N-CNTs yields a processed nanomaterial that will be far more mobile in aquatic environments than the "as received" or unreacted material.

Different behavior was observed for CS CNTs, for which as received and washed materials were essentially stable in suspension. These suspensions remained stable after reaction with free chlorine, a result observed both for amide- and PABS functionalized surfaces. Thus, as with reacted NL CNTs, chlorinated CS CNTs will also be mobile in aquatic systems.

Stability trends for N-CNT suspensions are complemented by results from XPS, which confirm that chlorination modifies their surface composition. Figure 2-11 shows XPS spectra for NL SWNH$_2$ and CS SWNH$_2$ samples before and after reaction with HOCl (i.e., 10 mg/L N-CNT suspensions reacted with 50 mg/L of HOCl as Cl$_2$). Generally, reaction with free chlorine increased the surface O concentration, likely contributing to the suspension stability observed after reaction. Chlorination also produced a decrease in surface N concentration (e.g., ~3-fold decrease in surface N on CS SWNH$_2$), which we propose is utilized for NDMA production. Reaction with free chlorine also produced higher binding energy features in C 1s spectra (e.g., near 289.5 eV for CS SWNH$_2$, attributable to surface COOH or O–C=O) [119], suggesting more oxidized forms of surface carbon.

Most intriguing, samples of both N-CNT formulations revealed a small amount of oxidized Cl on the CNT surface after reaction with HOCl. This increase in surface chlorine is most easily distinguished for NL SWNH$_2$, in part because as received CS SWNH$_2$ have a small amount of surface Cl as residual of the intermediate acyl chloride groups utilized during N-functionalization. For NL SWNH$_2$, we observed a broad signal in Cl 2p spectra roughly centered around 200 eV. The lower binding energy features could reflect either surface adsorbed chloride [112] or Cl addition to N (e.g., chloramines) [156], both of which have previously been assigned the same binding energy (197.8 eV). We believe the latter is most probable because of the known mechanism of chlorine addition to primary amines [151], prior spectroscopic observations of Cl addition to N in comparable polyamide membrane materials [157], our extensive sample washing prior to analysis, and the lack of a similar low binding feature

in CS SWNH$_2$. The higher binding energy feature in the Cl 2p region for NL SWNH$_2$, which was also observed for CS SWNH$_2$, is consistent with formation of C-Cl (201.0 eV) [112, 119, 158]. The presence of oxidized chlorine on the reacted CNT surface suggests these processed nanotubes may possess some residual disinfection (i.e. oxidizing) capacity after chlorination, a scenario we explored in subsequent bioassays with chlorinated N-CNTs.

2.4.5 Implications of NDMA leaching and N-CNT chlorination for toxicity.

The results presented thus far highlight that the surface chemical composition of N-CNTs will change as they make their way into a water supply (e.g., loss of surface-associated NDMA upon dispersion) and through a treatment plant (e.g., change in surface chemistry via chlorination). Accordingly, it is reasonable to suspect that such changes may influence the ecological and human health risks associated with exposure to N-CNTs. Accordingly, *E.coli* bioassays were conducted to compare the toxicity of washed and "as received" N-CNTs (and thus the effect of surface-associated residuals from synthesis including NDMA) and unreacted and chlorinated N-CNTs.

DNA efflux data (Figure 2-13) suggest that exposure to CS N-CNTs (both NH$_2$ and PABS) resulted in significant ($p < 0.05$) membrane disruption, whereas incubation with NL SWNH$_2$ did not produce an observable effect. Notably, as has been observed previously [159], DNA efflux tended to scale with N-CNT suspension stability (i.e., less aggregated and more disperse N-CNTs are most likely to puncture *E. coli* cell walls). As expected, there was no apparent influence of washing (i.e., removal of surface NDMA) on DNA efflux data for any N-CNT type because NDMA is not known to induce membrane disruption.

In contrast to results from DNA efflux experiments, plating assays revealed NL SWNH$_2$ induced the greatest colony forming unit (CFU) reduction (Figure 2-13), suggesting they exert toxicity by non-mechanical means. Moreover, although CS PABS and CS SWNH$_2$ were responsible for the greatest reduction in membrane integrity based on DNA efflux data, this cell damage did not significantly reduce *E. coli* viability as determined by CFU counts. Once again, however, there was generally no difference in the outcomes of the plating assay for washed and unwashed N-CNTs, suggesting that surface associated synthesis byproducts, including NDMA, do not pose an acute toxicity threat. Indeed, the levels of NDMA released via leaching (Figure 2-1) are less than expected for acute toxicity [160], and our assay results suggest no synergistic effects from tandem exposure to NDMA and N-CNTs.

Finally, plating assays assessed the influence of chlorination on the toxicity of NL SWNH$_2$ suspensions (Figure 2-12). Despite XPS evidence of surface Cl and increased dispersivity after chlorination (see Figure 2-9), no significant difference in CFU formation was found after *E. coli* exposure to NL SWNH$_2$ that had been reacted with 0.5 mg Cl$_2$/mg CNT for 3 days. Identical results were obtained with NL SWNH$_2$ reacted with 0.5 mg Cl$_2$/mg CNT for 22 d to ensure complete HOCl consumption so it would not influence CFU formation. Notably, dechlorination of reacted NL SWNH$_2$ with 0.3 mM sulfite eliminated toxicity, making suspensions even less of a risk to *E. coli* than unreacted NL SWNH$_2$. Additional sedimentation studies revealed that dechlorination with sulfite had no effect on suspension stability of reacted N-CNTs. Thus, we believe this inhibition of N-CNT toxicity is most likely linked to changes in surface chemistry

arising from the sulfite-mediated reduction of chlorinated NL SWNH$_2$, although additional investigation is warranted.

2.4.6 Implications of N-CNTs representing a source and precursor of NDMA.

Surprisingly, N-CNTs are a source of NDMA, exhibiting sufficient leaching capacity to exceed proposed NDMA health goals in suspensions of approximately 50-100 μg/L. NDMA likely exists on N-CNT surfaces as a dried residue of functionalization, which often utilizes nitrogenous compounds and redox conditions favorable to NDMA formation. Incidentally, it is highly likely that various uncharacterized byproducts including other nitrosamines and nitrosamine precursors (e.g., dimethylamine) exist on N-CNTs powders, and ongoing work could explore this possibility. Thus, this work reinforces an alternative scenario by which engineered nanomaterials can adversely affect water quality (i.e., pollutant source), beyond the direct consequences of N-CNTs suspended in the water column.

Our findings should motivate new research into sustainable routes for N-CNT preparation that minimize byproduct formation. Surface-associated NDMA must also be accounted for when developing N-CNT applications, especially those targeting water treatment and/or monitoring devices. Future studies exploring toxicological risks of N-CNTs need to consider the complex chemical mixture likely present on their surface. These residues, including NDMA, may not result in acute toxicity but will likely influence chronic exposure studies, where they could contribute to measurable toxicity endpoints. For both N-CNT applications and toxicity testing, we recommend integrating a washing step into all protocols, as we have done herein.

The role of N-CNTs as NDMA precursors, while not as surprising, is no less significant. Here, we show that NDMA formation is influenced not only by the nature of the N-containing functional group (e.g., amine, amide or polyaminobenezene) but also by the chemical oxidant (e.g., HOCl, O_3, or NH_2Cl). We are currently working to elucidate the mechanism of NDMA formation in N-CNT systems, particularly addressing whether the CNT surface promotes or catalyzes NDMA formation. Of note are our initial experiments with ethylenediamine (50–400 µg/L), a soluble analog of the N-group on NL $SWNH_2$, in which we do not observe any NDMA production via reaction with HOCl (15 mg/L) in the absence of CNTs. Thus, the ability of the ethylenediamine functionality on NL $SWNH_2$ to yield NDMA during chlorination appears unique to the heterogeneous N-CNT system, where NDMA formation mechanisms likely differ from those established for dissolved precursors [37]. For example, it may be possible that transient, reactive intermediates capable of promoting NDMA formation are generated via reaction of chlorine with π-bonds in the CNT sidewall or at non-nitrogen containing surface groups (e.g., oxides). We argue that developing such mechanistic insights of NDMA formation is critical to the sustainable design of N-CNTs, where the goal must be to identify functional groups that enable their promise in applications yet limit NDMA formation during manufacturing and environmental processing.

During N-CNT chlorination, various other species are likely generated in addition to NDMA, and the identity and consequences of these as yet unidentified DBPs merit closer scrutiny. We also reiterate that chlorination alters the surface chemical composition, suspension stability, and potentially the toxicity of N-CNTs. In essence, therefore, chlorinated N-CNTs represent another next-generation disinfection byproduct.

Finally, our work is another illustration of how functionalized CNTs can mimic the reactivity of NOM. Ultimately, with the extensive degree and range of surface groups added via functionalization, CNTs can be effectively transformed into an analog of organic carbon. As we continue to address the reactivity of carbon nanomaterials in natural and engineered aquatic systems, the extensive body of literature on NOM may provide a reasonable first approximation of the chemical processes in which functionalized CNTs will participate.

Table 2-1: N-CNTs utilized in NDMA leaching and formation experiments.

Manufacturer	Name	Dimensions[a]	Surface area $(m^2/g)^b$	Surface Group and Vendor's Functionalization Route
NanoLab	NL SWNH$_2$	D = 1.5 nm avg L = 1-5 µm	860	
	NL MWNH$_2$	OD = 15 nm avg L = 1-5 µm	250	
Carbon Solutions, Inc	CS SWNH$_2$	D = 1.5 nm avg L = 0.5-3 µm	100[c]	
	CS PABS	D = 1.5 nm avg L = 0.5-3 µm	6.5[c]	

[a]As reported by manufacturer; [b]measured herein; [c]values represent those measured on as-received powders, which were notably aggregated. Thus, values are lower than might otherwise be expected for SW-CNTs and may not accurately reflect available surface area in suspension given the superb dispersivity of these CNTs after sonication. Notably, breaking apart of aggregates with mortar and pestle prior to BET analysis resulted in smaller values (32 and 4 m^2/g for CS SWNH$_2$ and CS PABS, respectively). D is the diameter, OD is the outer diameter, and L is the length of an individual CNT.
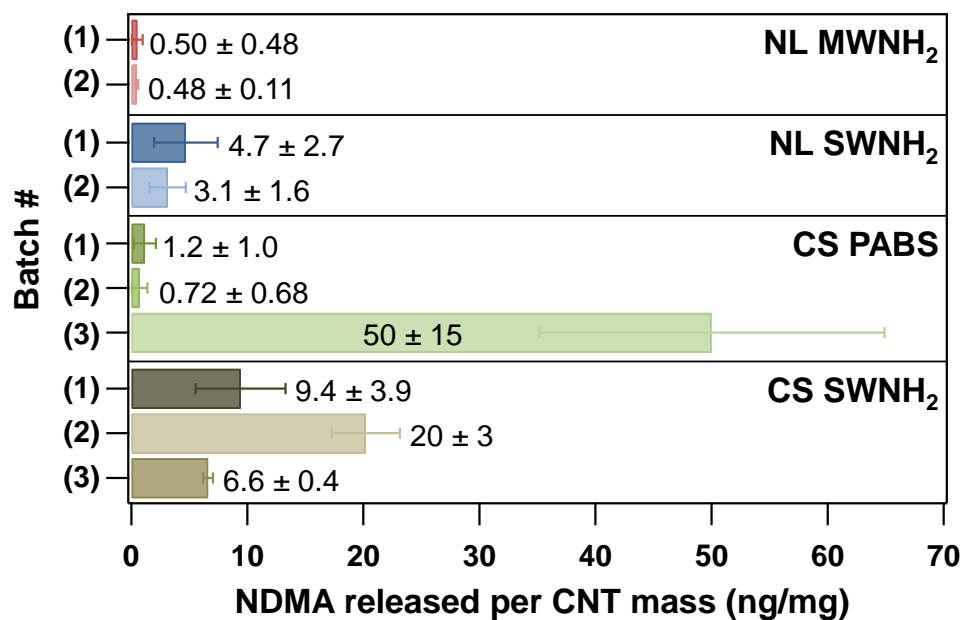
Figure 2-1: NDMA released (ng of NDMA/mg of CNT) from commercial N-CNT suspensions. Data are provided for all N-CNT formulations, where the numbers in parentheses indicate different batches for each type of material. Uncertainty represents one standard deviation for at least three separate leaching experiments with each batch. NDMA concentrations were measured for 1 g/L N-CNT aqueous suspensions after sonication for 5 hours.
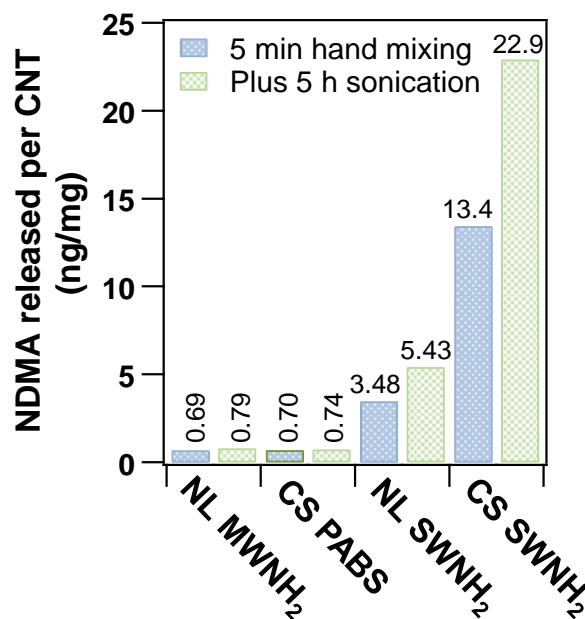
Figure 2-2: NDMA released per unit mass of as-received N-CNT powder (in ng NDMA/mg N-CNT) for each commercial formulation explored herein (see Table 2-1). Data is shown after suspending N-CNTs (1 g/L) in DI water and either shaking vigorously by hand for 5 min (blue checkered) or after sonicating for 5 h (blue holey). Generally, the majority, but not always all, of the NDMA was released near immediately upon dispersion of N-CNT powders in water, suggesting it is loosely bound to the N-CNT surface. The slightly higher results obtained after 5 h of sonication (which was the methodology used to generate data in Figure 2-1) likely indicate that a small fraction of the NDMA is more tightly bound to the N-CNT surface and only prone to leaching over extended periods of aggressive agitation (e.g., sonication).
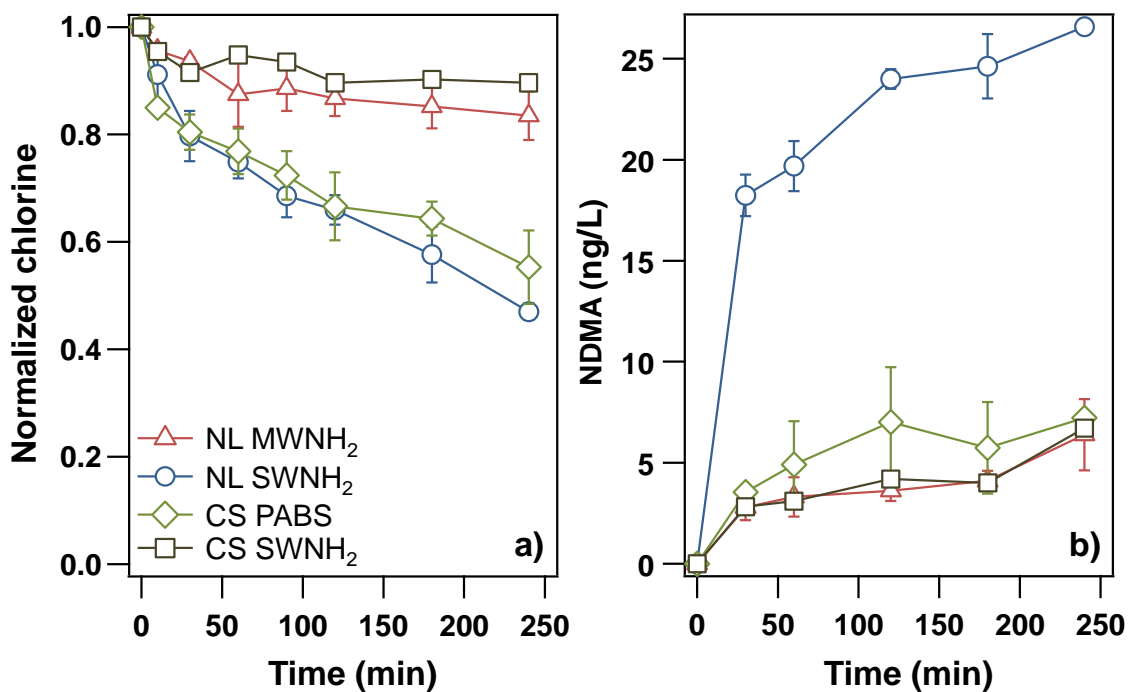
Figure 2-3: (a) Normalized chlorine consumption and (b) NDMA production during chlorination of N-CNT suspensions. Data points represent averages of at least duplicate analyses, where uncertainties indicate one standard deviation. Experiments were conducted at pH 8 in 5 mM phosphate buffer with 15 mg/L HOCl and 10 mg/L CNTs.
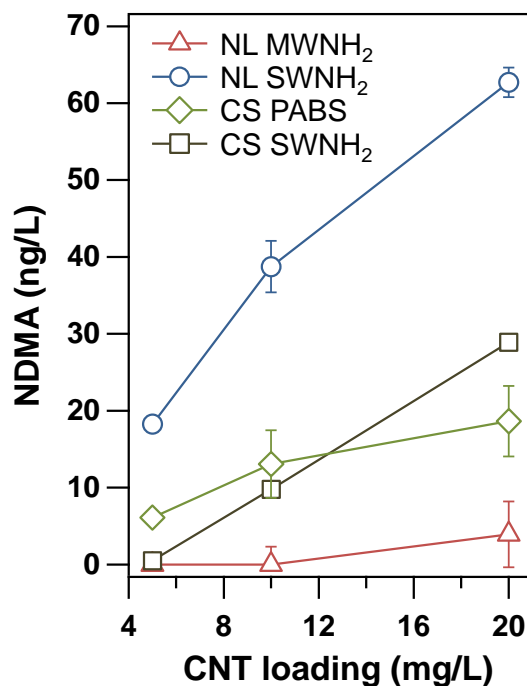
Figure 2-4: NDMA production (measured after 24 h) as a function of N-CNT loading (in mg/L) for the four types of commercial N-CNT formulations explored herein. Experimental conditions include 15 mg/L as Cl_2 of HOCl in pH 8 phosphate buffer and 5-20 mg/L of washed N-CNTs. Error bars represent one standard deviation from analysis of triplicate samples, thus representing analytical uncertainty. At high free chlorine concentrations (> 10 mg Cl_2/L; greater than would be expected for water or wastewater treatment), we generally found that the N-CNT mass concentration limits NDMA formation, consistent with our observation of a near-linear increase in NDMA production as a function of N-CNT loading. Thus, the availability of N-containing surface sites that function as an N source for NDMA production is limiting.
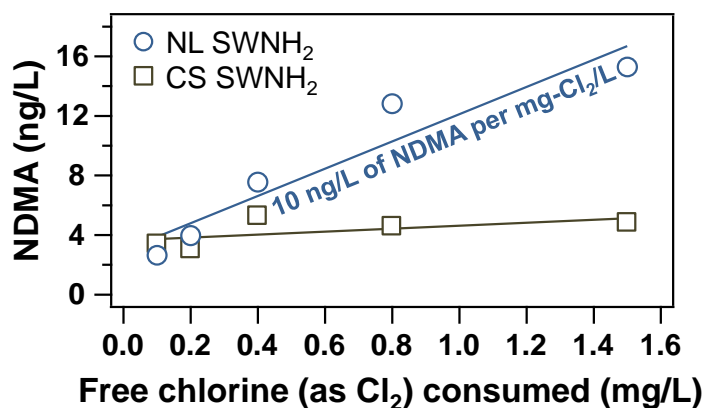
Figure 2-5: Representative data (from duplicate experiments) illustrating NDMA formation as a function of free chlorine demand at concentrations representative of water treatment. Assuming a linear dependence between NDMA production and free chlorine demand, results from best-fit linear regression analyses are shown (NL SWNH$_2$ R^2 = 0.904; CS SWNH$_2$ R^2 = 0.350). Results were obtained by reacting a fixed amount of N-CNTs (10 mg/L) with lower concentrations of HOCl (0.1-1.5 mg/L as Cl$_2$) for 1 day to allow the consumption of all available free chlorine. Reactions were conducted at pH 8 in 5 mM phosphate buffer.
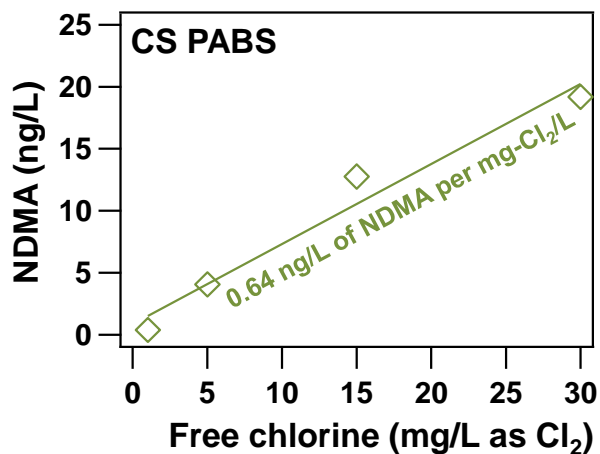
Figure 2-6: NDMA formation (after 24 h) as a function of initial HOCl concentration (as mg/L of Cl_2) for CS PABS suspensions. Experiments used an HOCl concentration between 0 and 30 mg/L as Cl_2 and were conducted in pH 8 phosphate buffer containing 10 mg/L of CS PABS. We observed a clear correlation between NDMA formation and available HOCl corresponding to a yield of 0.66 ± 0.064 ng/L of NDMA per mg/L HOCl (as Cl_2), which assumes complete consumption of free chlorine over 24 h in these suspensions. This yield is roughly 10-fold less than that observed for NL $SWNH_2$ (see Figure 2-5). We note that the HOCl concentrations explored in Figure 2-5 of the main text (from 0.1-1.5 mg/L) were not sufficiently high enough to generate measurable concentrations of NDMA from CS PABS (our detection limits was 3 ng/L).
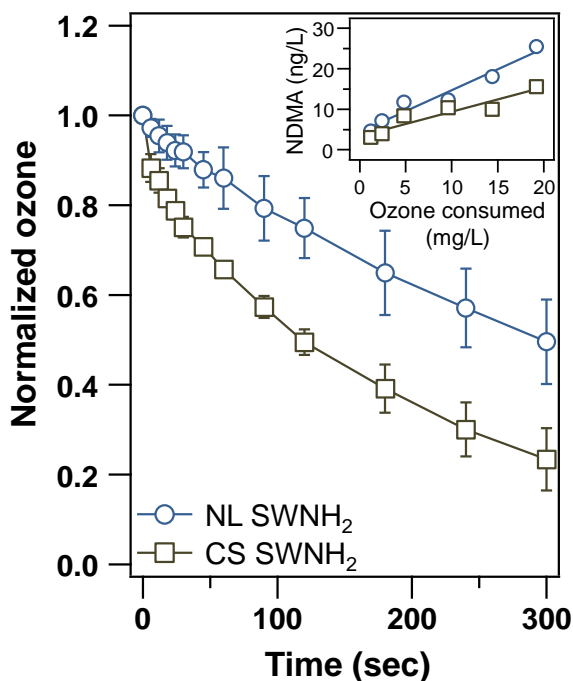
Figure 2-7: Normalized concentration of ozone ($[O_3]_t/[O_3]_0$) as a function of time in suspensions of NL and CS SWNH$_2$. Ozone decay data are shown for experimental systems conducted at pH 7 containing an initial O_3 concentration of 14.4 mg/L, 10 mg/L CNTs, and 128 µM tert-butyl alcohol as a radical scavenger. Data represent the mean and standard deviation (error bars) from at least duplicate experiments. The inset shows NDMA formation as a function of ozone consumption. Inset data was collected in complementary experiments conducted over a range of initial ozone concentrations (from 0-20 mg/L) and NDMA was measured at the conclusion of the reaction (i.e., after complete ozone consumption). Accordingly, the yield of NDMA during ozonation can be quantified from the slope of best-fit linear regressions (NL SWNH$_2$ $R^2 = 0.952$; CS SWNH$_2$ $R^2 = 0.882$) shown in the inset. Generally, while CS SWNH$_2$ exhibited greater reactivity toward ozone, more NDMA was produced in NL SWNH$_2$ suspensions. From our regression analyses, NL SWNH$_2$ suspensions yield 1 ng/L of NDMA per mg/L O_3 consumed, whereas CS SWNH$_2$ suspensions yield 0.6 ng/L NDMA per mg/L O_3 consumed.
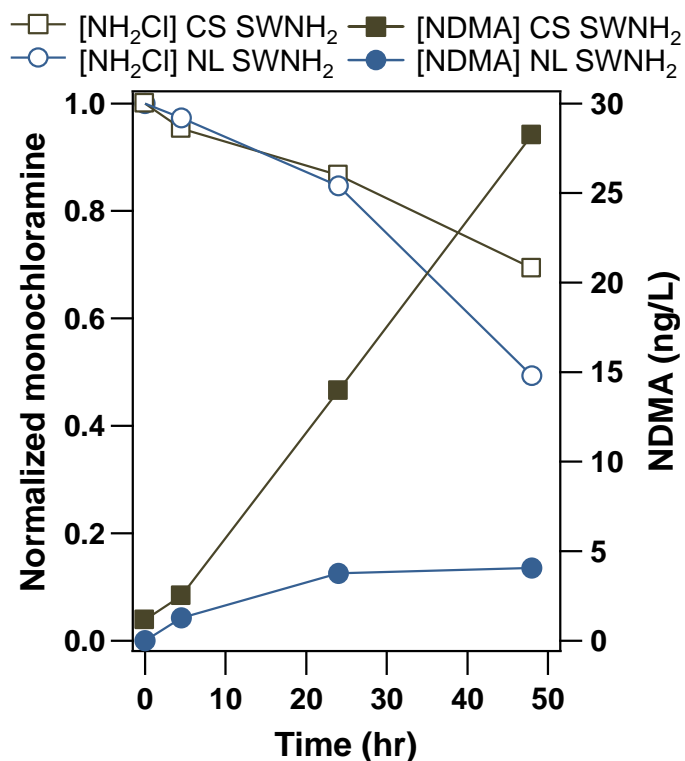
Figure 2-8: Normalized monochloramine (open symbols) and NDMA concentrations (solid symbols) as a function of time in suspensions of CS (brown squares) and NL (blue circles) SWNH2. Experiments were conducted at pH 8 in 5 mM phosphate buffer in suspensions containing 10 mg/L of N-CNT and an initial monochloramine concentration of 15 mg/L as Cl_2. This data is the only instance where CS N-CNTs generated more NDMA via reaction with a chemical disinfectant than NL N-CNTs. We note that from the concentrations of monochloramine and NDMA measured after 50 h, we estimate NDMA yields of approximately 10 mg of NDMA per mg of NH_2Cl (as Cl_2) for CS SWNH$_2$ and 1 mg of NDMA per mg of NH_2Cl (as Cl_2) for NL SWNH$_2$. For CS SWNH$_2$, this yield is of the same order of magnitude as that reported for organic matter (see discussion in main text).
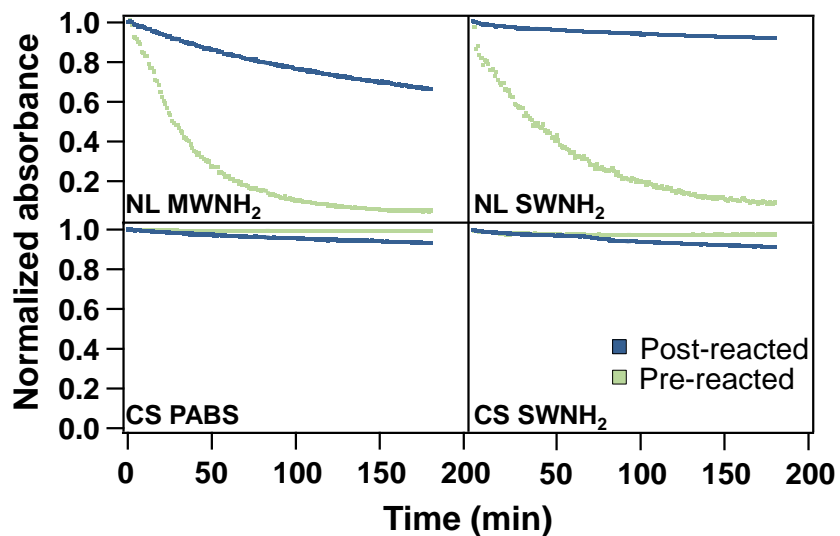
Figure 2-9: Results of sedimentation studies examining the suspension stability of N-CNTs before (pre-reacted; green) and after (post-reacted; blue) reaction with HOCl. N-CNT suspensions (100 mg/L) were reacted with 500 mg/L HOCl at pH 8 (5 mg Cl_2/mg N-CNT). Absorbance was measured at 700 nm through 1 cm path-length, quartz cuvette for 3 h. Generally, chlorination increases the stability of NL N-CNTs, whereas it has a minimal effect on the already stable CS N-CNT suspensions.
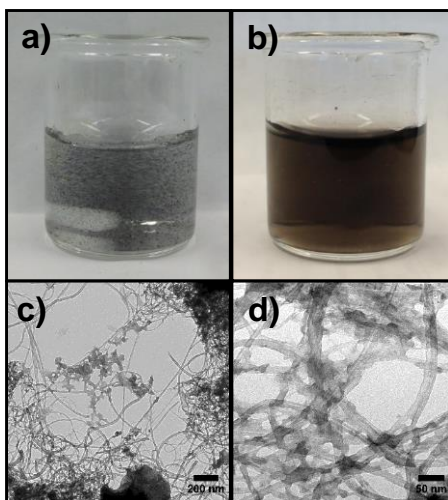
Figure 2-10: (a) Picture of a 100 mg/L suspension of washed NL SWNH$_2$ while mixing before reacting with HOCl. (b) Picture of the same suspension after 1 d of reacting with HOCl at 5 mg-Cl$_2$/mg-CNT. The reacted suspension of NL SWNH$_2$ is visibly more disperse, consistent with the greater suspension stability we observed during sedimentation experiments. TEM images of these reacted N-CNTs generally showed that their morphology and structure was maintained (c), although some evidence consistent with oxidative damage (e.g., damage to N-CNT sidewalls) was occasionally observed (d).
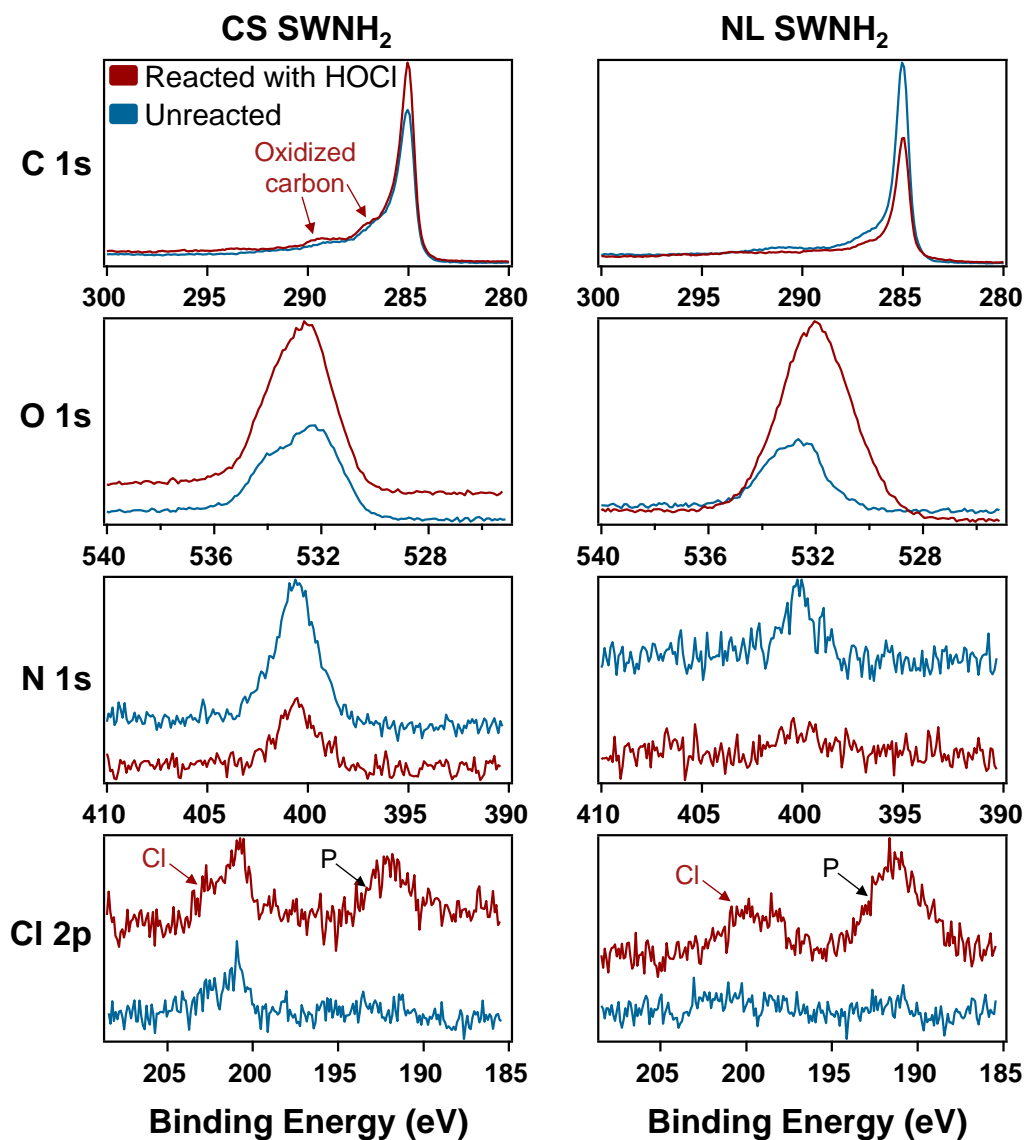
Figure 2-11: XPS spectra of NL SWNH$_2$ and CS SWNH$_2$ comparing C 1s, O 1s, N 1s, and Cl 2p regions before (blue) and after (red) reaction with HOCl. In the C 1s spectra, red arrows indicate features consistent with oxidized carbon. In the Cl 2p spectra, red arrows indicate the signal arising from surface Cl while black arrows indicate an increase in P in reacted samples, which we attribute as a residual of the phosphate buffer used in reactivity studies.
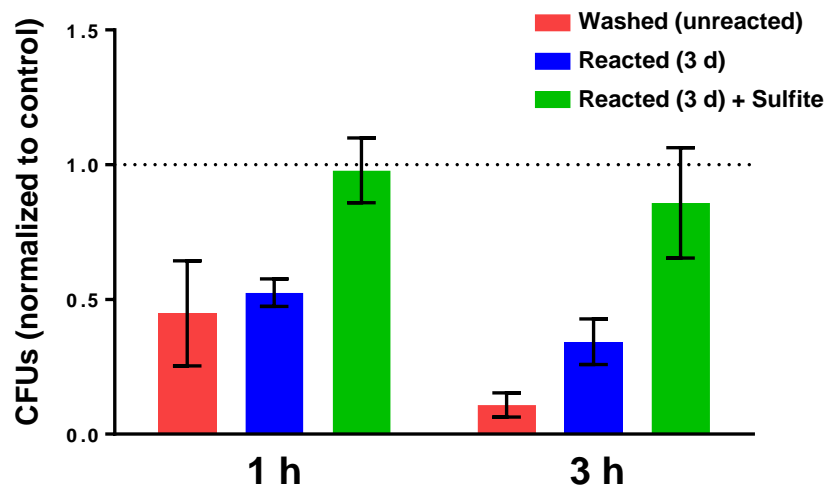
Figure 2-12: Comparison of CFU formation on LB agar (1.5%) plates resulting from *E. coli* suspensions (0.85% NaCl) exposed to washed (unreacted) NL SWNH$_2$ (10 mg/L) as well as NL SWNH$_2$ that had been reacted for 3 d with 0.25 mg of HOCl as Cl$_2$ per mg of CNT. For reacted samples, data are presented for NL SWNH$_2$ with (blue) and without (green) subsequent quenching with sulfite at 2:1 mol ratio. CFUs from plating assays are provided for *E. coli* suspensions incubated either 1 or 3 h with the various forms of NL SWNH$_2$. Values below 1.0 on the vertical axis indicate decreased CFU formation compared to a control. Experiments were conducted in triplicate for each treatment, and are represented as average values normalized to the control. Uncertainties represent one standard deviation of these triplicate results.
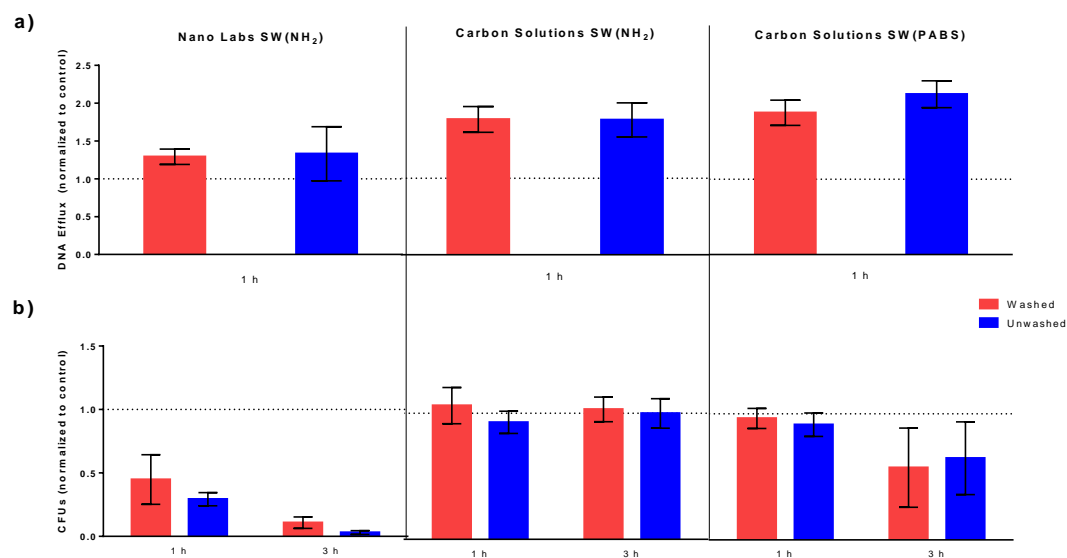
Figure 2-13: (a) Comparison of DNA efflux quantified in *E. coli* suspensions (0.85% NaCl) after 1 h incubation with CNTs (10 μg/ml). Values greater than 1.0 on the vertical axis indicate DNA efflux greater than a control. (b) Comparison of CFU formation on LB agar (1.5%) plates resulting from *E. coli* suspensions (0.85% NaCl) after 1 and 3 h incubation with CNTs (200 μg/ml). Values below 1.0 on the vertical axis indicate decreased CFU formation compared to controls. In both (a) and (b), independent experiments were conducted in triplicate for each treatment, and are represented as average values normalized to the control with error bars representing one standard deviation. Data are shown for as-received unwashed N-CNTs and N-CNTs after washing via dialysis as described in Section 2.3.4.

CHAPTER 3: FORMATION OF TRIHALOMETHANE AND HALOACETIC ACID BYPRODUCTS DURING CHLORINATION OF PRISTINE AND AGED CARBON NANOTUBES

3.1 Abstract

We know little about the reactivity of engineered nanomaterials in the environment, and their potential to yield hazardous byproducts. We have previously shown that nitrogen-functionalized carbon nanotubes (CNTs) represent both a precursor and source of nitrogenous disinfection byproducts (DBPs) including N-nitrosodimethylamine (NDMA). Here we explore the potential for pristine (i.e., as received), oxidized, polymer-functionalized, and chemically oxidized (via extended ozonation and sequential chlorination) CNTs to function as precursors for halogenated DBPs including trihalomethanes (THMs; e.g., chloroform) and haloacetic acids (HAAs; e.g., mono-, di- and trichloroacetic acid). During chlorination, formation of chloroform (CF) and HAAs was greatest for CNTs functionalized with the polymers PABS and PEG, producing as much as 3.5 µg/mg-CNT of CF and 10.2 µg/mg-CNT of HAAs at 4 h of chlorination (with larger yields observed over longer timescales). Further, while DBP formation in PABS-CNT systems was comparable to that generated from PABS in the absence of CNTs, DBP formation appeared unique for PEGylated CNTs as no DBPs were observed during chlorination of PEG alone. While non-functionalized and acid oxidized CNTs did not produce any measurable DPBs, the ability of CNTs to generate DBPs increased with their extent of oxidation via ozone and chlorine. In fact, we report a strong correlation between formation of CF and HAAs (primarily trichloroacetic acid) during chlorination with CNT surface oxygen content as quantified by X-ray

photoelectron spectroscopy for CNTs oxidized via ozonation or chlorination. Aside from THMs and HAAs, chloropicrin was identified as the primary DBP forming from chlorination of nitric acid functionalized CNTs, generating about 13 µg/mg-CNT in 4 h. Beyond these known DBPs, evidence suggests other as yet unidentified chlorinated byproducts are generated as a result of CNT chlorination, particularly for those oxidized by strong acids (e.g., nitric acid and sulfuric/nitric acid mixtures), and that their formation also scales with CNT surface oxygen concentration.

3.2 Introduction

We know little about the reactivity of engineered nanomaterials in the environment, and their potential to yield hazardous byproducts. The same chemical oxidants used in water disinfection (e.g., chlorine, ozone, peroxide, and/or ultraviolet light) but under harsher conditions (i.e., high oxidant concentration and high temperatures) have been used to purify carbon nanotubes (CNTs) and are even used to incorporate oxygen functional groups on the CNT surface [161-163]. If engineered nanomaterials make it to disinfection then the potential for reaction with chemical oxidants and potential formation of byproducts are possible. CNTs that are not removed in upstream separation processes, which may be true for highly stable species like oxidized or functionalized CNTs could be potentially problematic for disinfection and most popularly, chlorination, where organic carbon are well known to generate byproducts that are regulated by the United States Environmental Protection Agency (USEPA).

Halogenated disinfection byproducts (DBPs) are generated primarily via the reaction of chlorine, a common chemical disinfectant, with organic carbon precursors,

such as natural organic matter (NOM), found in drinking water sources [164]. These disinfection byproducts which include trihalomethanes (THMs) and haloacetic acids (HAAs), have been shown to cause cancer and reproductive effects in lab mice, while also representing suspected carcinogens and teratogens in humans [8]. Presently, the USEPA maximum concentration level (MCL) for total THM (TTHM, representing the sum of chloroform, bromodichloromethane, dibromochloromethane, and bromoform) is 80 µg/L, whereas the MCL for the sum of five chlorinated and brominated acetic acids (HAA5), three of which were detected here (monochloroacetic acid, dichloroacetic acid, and trichloroacetic acid), is 60 µg/L [7]. Because of their well-known hazard to human health, the identification and management of THM and HAA precursors is important for limiting their formation and minimizing exposure risk.

We have recently discovered that commercially available nitrogen functionalized carbon nanotubes (N-CNTs; those with amine and amide surface functional groups) that are used in sensors [165] and biological research [166] can serve as precursors for nitrogenous DBPs, specifically N-nitrosodimethylamine (NDMA). In many ways, this result is not surprising, as functional groups on the surface of CNTs impart character and reactivity evocative of NOM. Further, much prior work has been devoted to illustrating the production of DBPs during the chlorination or chloramination of precursors on activated carbon (AC) [61-65], which structurally represents a reasonable bulk analog for CNTs. These halogenated byproducts not only include traditional DBPs including THMs and HAAs, but also larger halogenated organics such as chlorophenols, hydroxylated polychlorinated biphenyl (PCBs), and various chlororesorcinols that can be generated via disintegration of the AC surface during reaction with chlorine [61, 62].

The current work builds upon our prior study (Chapter 2) with N-CNTs by considering the potential of other commercially available forms of CNTs to generate halogenated DBPs including THMs such as chloroform and HAAs including mono-, di- and trichloroacetic acid. While amine- and amide- functionalized CNTs remain somewhat limited in their practical application, non-functionalized CNTs, oxidized CNTs containing surface carbonyl, hydroxyl and carboxylic acid moieties, and polymer functionalized CNTs represent some formulations that are more widely used in commercial application (i.e., electronics [167], sensors [168, 169], composites [170], energy storage [171], and even water filters [67]). Most importantly, these functionalized CNTs contain surface groups (e.g., surface hydroxyl and carboxyl groups attached to the CNT sidewall of oxidized CNTs) that are comparable to the structures of many common reported "model" precursors used to elucidate the nature and DBP yield of NOM.

Accordingly, we quantify the production of chloroform, a common THM, and mono-, di-, and trichloroacetic acid, three common HAAs, generated in response to the chlorine demand exerted by various types of CNTs. We explore both single-walled and multi-walled CNTs, while also considering differences in DBP formation potential arising from the extent and method of chemical functionalization (e.g., oxidation via strong acid, ozone, free chlorine or UV light). We also considered DBP production during chlorination of polymers polyethylene glycol (PEG) and poly(3-aminobenzene sulfonic acid (PABS) functionalized CNTs, specifically considering whether the polymer-CNT structure exhibited unique DBP formation potential relative to the polymer or CNT alone. Quantification of DBP was complemented by CNT analysis with X-ray photoelectron spectroscopy (XPS), Raman spectroscopy, and suspension stability

measurements to identify physicochemical properties of the CNT suspensions most critical to DBP formation. Our findings help to illustrate how engineered nanomaterials can adversely affect water quality not only by their mere presence in solution but also by their ability to promote formation of regulated byproducts with recognized adverse health effects as result of their environmental processing.

3.3 Experimental methods

3.3.1 Reagents

All reagents were ACS grade or higher. Anhydrous sodium sulfite (Fisher Chemical; ACS grade) was used to quench chlorine during sample preparation. Anhydrous sodium phosphate dibasic (RPI; >99%) was used to buffer pH in aqueous solutions. Disodium ethylenediamine tetraacetic acid dehydrate (EDTA; Sigma; ACS reagent), ferrous ammonium sulfate hexahydrate (FAS; J.T. Baker; ACS grade), N,N-diethyl-p-phenylenediamine (DPD; Aldrich; 97% purity), and sulfuric acid (Fisher; ACS Plus) were used in the colorimetric titration method for analysis of chlorine. Pentane (n-pentane; Fisher; HPLC grade) was used for liquid-liquid extraction of THMs. 1,2-dibromopropane in methanol (Crescent Chemical Co., Inc.), and THM4 and HAA6 standard in methanol (Supelco; analytical standard) were used for GC standards for method calibration. Sodium sulfate anhydrous (Fisher; ACS grade), methanol (Fisher; Optima grade) were used for HAA extraction. Nitric acid (Sigma-Aldrich; ACS reagent) was used for functionalization of CNTs. m-Aminobenzenesulfonic acid (ABS; Aldrich; 97%), aniline (Sigma-Aldrich; ACS reagent), and ammonium persulfate (Sigma-Aldrich; ACS reagent) were used to synthesized PABS. All solutions were prepared in deionized water (Thermo Scientific Barnstead TII).

3.3.2 Carbon nanotubes

Eight formulations of CNTs were acquired from Carbon Solutions, Inc. (abbreviated hereafter as CS), NanoLab, Inc. (NL), or Cheap Tubes, Inc. (CH) (Table 3-1). These included single-walled (SW) and multi-walled (MW) CNTs with and without (NF) functional groups. Functionalized CNTs purchased from CS included those with carboxylic acid (COOH), PEG, and PABS surface groups.

3.3.3 CNT oxidation

In addition to working with commercially available carboxylated CNTs, we also used several routes of surface oxidation for non-functionalized CNTs from various commercial sources. This included more conventional oxidation routes using strong acids (e.g., nitric acid and sulfuric acid; [81]), as well as alternative approaches using extended and/or repeated exposure to ozone (O_3), UV light ($\lambda > 225$ nm), and free chlorine (HOCl). These alternative oxidative processes were chosen to mimic the oxidation of CNTs resulting from common approaches for disinfection during water treatment.

CNTs oxidized with HNO_3 (denoted by "-N" following the CNT name) were produced by suspending 100 mg of as-received CH MWNF or NL SWNF in 250 mL of concentrated HNO_3 [99, 172-174]. The suspension was sonicated (Bransonic Ultrasonics Corporation, 151OR-DTH, 42 kHz ± 6%) for 1 h prior to refluxing the mixture at 140 °C for 1.5 h while stirring vigorously. CNTs oxidized with a mixture of H_2SO_4 and HNO_3 (denoted by "-S/N") used a suspension of 100 mg of as-received CNTs in 8 mL of concentrated 3:1 $H_2SO_4:HNO_3$ [134, 175]. The suspension was then dispersed using sonication for 1 h, and the mixture was subsequently refluxed at 70 °C for 8 h without

stirring. For both methods, the oxidized CNTs were allowed to cool overnight before filtering the suspension with a 0.22 μm polycarbonate filter (EMD Millipore). The filtered solids were cleaned by repeated washing with DI water until the filtrate exhibited a pH greater than 5, at which point the oxidized CNTs were allowed to dry overnight at 100 °C. The resulting powder was then pulverized with a mortar and pestle before use.

Oxidation with HOCl (denoted by "-Cl$_2$") involved reacting a 1 g/L suspension of CH MWNF with NaOCl at 0.5, 1.0, 1.5, and 2.0 mg-Cl$_2$/mg-CNT for 30 d. After 30 d, the CNT suspension was stripped with oxygen to remove any volatile compounds (such as THMs) generated during the oxidation process (which would interfere with DBPs generated in subsequent chlorination studies). Oxidation with germicidal ultraviolet (UV) light (denoted by "-UV" following the CNT name) utilized wavelengths of light greater than 225 nm. Suspensions at 1 g/L were irradiated with these wavelengths of light from a 200 W Hg(Xe) lamp (Newport Corporation; Model 6290) equipped with a >225 cut-on filter (Newport Corporation; CGA-225). Oxidation with ozone (denoted by "-O$_3$") was accomplished by delivering a continuous 0.2 mL/min stream of an O$_3$/O$_2$ mixture generated using a Model SS-300 (Pillar Technologies) ozone generator into 50 mL of a 1 g/L suspension for up to 48 h. In the absence of CH MWNF, these conditions produced a steady-state ozone concentration in solution of 19.2 mg/L (0.4 mM). Prior to reaction with chlorine to measure THM and HAA formation, these ozonated suspensions were left open to air overnight to promote release of any residual ozone.

3.3.4 Synthesis of PABS

Experiments were conducted with PABS and PEG in the absence of CNTs so that the DBP formation of native polymers could be compared to that measured for polymer-

functionalized CNTs. PEG (600 Mn) was purchased from various manufacturers [Aldrich (1), Alfa Aesar (2), and Sigma, Bio Ultra (3)] and used as received. PABS was not commercially available, but instead was synthesized from established methods [140, 176]. PABS was prepared by mixing ABS and aniline (20 mol% of ABS) in 1 M HCl with ammonium persulfate (10:1 molar ratio to ABS). The mixture was allowed to react in an ice bath (~4 °C) for 6 h, after which the solution was filtered with a 0.22 µm polycarbonate filter. The precipitate was washed with acetone then suspended in water before finally precipitating it again in acetone. The precipitate product was collected via filtration and allowed to dry at room temperature. The product was confirmed as PABS via UV spectroscopy in 1 N NaOH solution, which yielded the expected absorbance bands at 290 nm and 510 nm diagnostic of PABS (see Figure 3-1) [176].

3.3.5 THM formation from chlorination of CNTs

Aqueous stock solutions of free chlorine (combination of HOCl and OCl$^-$) were prepared as mentioned above (see Section 2.3.4.1 above). Aqueous stock suspensions of CNTs (1 g/L) were prepared by adding a measured amount of dry CNT powder into a serum bottle, then adding the corresponding volume of water to achieve the desired solid loading. These suspensions were crimped sealed with grey butyl rubber stoppers and sonicated for 5 h to promote CNT dispersion. Immediately prior to use in chlorination experiments, CNT stock suspensions were sonicated for 5 min to re-disperse the CNTs and HOCl stock solutions were measured for free chlorine.

CNTs were reacted with free chlorine in batch systems contained in 20 mL vials. The reaction was initiated by adding the desired volume of stock CNT suspension into a pH buffered solution of HOCl. The vials were crimp sealed and mixed end-over-end at

60 rpm using a Model RT50 rotator (Cole-Parmer Instrument Company; Roto-Torque). Chlorination experiments were conducted in 5 mM (480 mg-PO$_4$/L) phosphate at pH 8. Experiments explored CNT loadings between 5-30 mg/L and used an initial HOCl concentration of 15 mg-Cl$_2$/L (0.2 mM).

After initiation of the reaction, vials were periodically collected over time to monitor THM and HOCl concentrations. For HOCl analysis, 5 mL of reactor volume was transferred into 250 mL Erlenmeyer flask with 100 mL of water and immediately analyzed via titration (see Section 3.3.7 below). The remaining 15 mL of reactor volume in a vial was quenched with 15 µL of freshly prepared 1 M sodium sulfite at excess and subsequently extracted for THM.

3.3.6 HAA formation from chlorination of CNTs

Stock HOCl solutions and CNT suspensions were prepare as described above. Chlorination experiments were conducted in 250 mL glass beakers sealed with Parafilm and covered with Al foil. Reactors contained at least 60 mL of 5 mM phosphate solution adjusted to pH 8. CNT loadings ranged between 5-20 mg/L, and initial HOCl concentration ranged between 5-30 mg-Cl$_2$/L. The contents of the reaction were well-suspended by mixing using a stir bar and stir plate. Samples (35 mL) were quenched with 40 µL of sodium sulfite and were stored in 50 mL amber bottles with PTFE-lined screw caps in the refrigerator for no more than 5 d before analysis.

3.3.7 Analytical methods

HOCl was measured via titration with FAS (see Section 2.3.7.1 above for details). THMs were analyzed according to EPA Method 551.1, which relied upon quantification

with gas chromatography (GC) coupled with an electron capture detector (ECD) after liquid-liquid extraction while using 1,2-dibromopropane as an internal standard. Briefly, pentane (2 mL) containing 30 µg/L of 1,2-dibromopropane internal standard was added to 15 mL of sulfite quenched sample and vigorously mixed for 10 s. The pentane layer was collected after the phases separated (~1 min). The contents of pentane were injected (3 µL; in split-less mode) into an HP 6890N gas chromatograph (GC; Agilent Technologies, Inc.) housing a DB-5 column (J&W 122-5033) leading into an electron capture detector (ECD; Agilent Technologies, Inc.; G2397A). The temperature rampings were as follow: 40 °C for 5 min, 40–70 °C at 10 °C/min, 70–260 °C at 20 °C/min. The injector temperature was 200 °C. Helium was used as the carrier gas at 1 mL/minute (constant flow). The ECD was set at 250 °C. A method detection limit of 1 µg/L was determined.

Haloacetic acid samples were analyzed according to EPA Method 552.3, which uses GC-ECD after derivatization and liquid-liquid microextraction. Briefly, 1.75 mL of concentrated sulfuric acid was added to 35 mL of sample volume to bring the pH of the sample down to less than 0.5. Next, 14 grams of sodium sulfate anhydrous (Na_2SO_4) and 1.75 grams of copper II sulfate pentahydrate ($CuSO_4 \cdot 5H_2O$) was added to the sample and shaken until dissolved. Then 4 mL of methyl tert-butyl ether (MtBE) and 20 µL of 5 µg/L internal standard, 1,2-dibromopropane, were added to the solution. Solutions were vigorously mixed for 1 min. Next, the solutions were methylated by transferring 3 mL of the upper MtBE layer into a 15 mL amber vial with PTFE-lined screw caps, adding 2 mL of 10% sulfuric acid in methanol, and reacting them for 2 hours in a 50 °C water bath. Vials were removed from the water bath and allowed to cool. Then 5 mL of 10% sodium

sulfate solution was added to each vial and shaken by hand for 2 min. The mixture was allowed to settle (~ 1 min) and 1 mL of the upper MtBE layer was collected for GC-ECD analysis. The sample was injected into the GC in split-less mode and separated on a DB-5 column. Temperature ramps were as follows: 35 °C for 10 min, 35–75 °C at 5 °C/minute, 75 °C for 15 min, 75–100 °C at 5 °C/minute, 100 °C for 5 min, 100–135 °C at 5 °C/minute, and 135 °C for 5 min. The injector temperature was set at 250 °C. Helium was used as the carrier gas at 1 mL/minute (constant flow). The ECD was set at 250 °C. A method detection limit of 3 μg/L for MCAA, 1 μg/L for DCAA, 1 μg/L for TCAA was determined.

3.3.8 CNT physical and chemical characterization

CNTs were characterized before and after chlorination to examine for possible changes in their physicochemical properties resulting from the reaction. Pre- and post-reacted CNTs were imaged via transmission electron microscopy (TEM) to examine for changes in morphology or damage to the CNT sidewalls. Samples for TEM were prepared and analyzed as described in Section 2.3.5.2. Surface chemical speciation was obtained using X-ray photoelectron spectroscopy, quantifying (at %) the surface species (C, O, Br, and Cl) of CNTs before and after reaction. Additional details about sample preparation and instrumentation for XPS analysis can be found in Section 2.3.5.3. Finally, the suspension stability of CNTs was determined via sedimentation studies, which monitor the transmission of light (700 nm wavelength) through a suspension as a function of time. Sedimentation experiments were conducted as described earlier in Section 2.3.5.1.

3.4 Results and discussion

3.4.1 Trends in THM and HAA production of during CNT chlorination

Figure 3-2 shows normalized chlorine demand (Figure 3-2a), as well as the corresponding production of chloroform (Figure 3-2b) and HAAs (Figure 3-2c) as a function of CT, which represents the product of free chlorine in mg-Cl$_2$/L and contact time in hours. Data are shown for non-functionalized CNT (CSSWNF), oxidized CNT (CS SWCOOH), and two polymer functionalized CNTs (CS SWPABS and SC SWPEG). All data in Figure 3-2 have been corrected for any chlorine demand (<5% demand after 48 h) and adventitious DBP formation (<3 µg/L CF and <5 µg/L HAAs formed after 48 h) observed in CNT-free controls. As expected, chlorinated DBPs (e.g., chloroform and chloro-acetic acids) were the only type detected as other halogens (e.g., bromide and iodide) were not present in these experimental systems (the formation of such brominated and iodinated DBPs will be assessed in Chapter 3). We note that in Figure 3-2, we only report values of dichloro- and trichloroacetic acid. In many CNT suspensions, while monochloroacetic acid production was observed, it could not be accurately quantified due to the formation of an unknown reaction byproduct (discussed in greater detail in Section 3.4.5 below) that not only co-eluted with MCAA but also produced a much larger GC-ECD response, thereby obscuring our ability to integrate the much smaller MCAA peak. We would estimate typical production of MCAA on the order of < 3 µg/L.

Of the CNTs investigated, polymer-functionalized CS SWPABS was the most reactive towards chlorine (Figure 3-2a) while also generating the most chloroform (CF) and chlorinated HAAs. The greater reactivity of CS SWPABS in Figure 3-2 also holds across all CNT types considered (see Table 3-2). On the other hand, CS SWNF did not

produce any CF or HAAs after 48 h of chlorination, behavior that was also exhibited by all other commercial, non-functionalized CNTs (Table 1-1). Smaller, but quantifiable and reproducible, levels of chlorinated DBPs were observed for the oxidized CNTs shown in Figure 3-2, which were oxidized by the vendor (Carbon Solutions, Inc.) using nitric acid. As summarized in Table 3-2, which compares CF and chlorinated HAA formation after 4 h of chlorination (selected as a representative retention time of a chlorine contactor [55]) for the entire suite of CNTs investigated herein, the relative trend in DBP formation potential in Figure 3-2 is generalizable as follows: polymer-functionalized CNTs >> oxidized CNTs > non-functionalized CNTs ≈ 0. We note that N-functionalized CNTs are not included in this relationship because some varieties (amide-functionalized from CS) generated CF and HAAs, while other forms (aminated CNTs from NL) only generated small quantities of DCAA. Specific details about the CF and HAA formation potential for each of these CNT families are further detailed in the following sections.

3.4.2 CF and HAA formation during polymer functionalized CNT chlorination

Because some polymers represent precursors to DBPs [106, 107], the origin of DBP production in CS SWPABS and CS SWPEG suspensions was further investigated. Specifically, we wanted to determine if the amount of DBPs generated on polymer functionalized CNTs was entirely attributable to the polymer or, alternatively, the binding of the polymer to the CNT surface resulted in DBP formation distinct from that of the polymer alone. As listed in Table 3-2, CS CNTs without a polymer coating (or any other functional group) did not generate any detectable DBP (THMs or HAAs) during chlorination.

Figure 3-3 illustrates the relationship between CF formation and chlorine exposure (as the log of contact time, or log CT), during chlorination of CS SWPABS and CS SWPEG. For comparison we also provide these data for chlorination of each polymer in isolation, in which experiments with free PABS and PEG (i.e., not associated with CNT) were conducted. As seen in Figure 3-3, while free PABS yielded appreciable CF formation across the CT values, no CF formation was observed during chlorination of free PEG. Thus, no data for CF formation in free PEG systems is provided. For the rest of the CF-producing systems, CF formation generally increased with increasing CT values, as is expected for DBP formation. The same behavior was found for HAA production (Figure 3-4) where free PABS generated more HAAs than CS SWPABS. Meanwhile, no formation of HAAs were seen for free PEG, while CS PEG generated appreciable HAAs

At the mass loading investigated, free PABS produced more chloroform at all CT values relative to its CNT-bound analog, CS SWPABS. However, we believe our data suggest that CF formation from CS SWPABS is as expected from the CF formation potential of free PABS. Specifically, the slope of the log-log plots in Figure 3-3 represent an effective yield for chloroform in these polymer systems, where free PABS and CS SWPABS exhibit slopes (0.36 ± 0.12 and 0.46 ± 0.07, respectively) that are statistically equivalent. This likely implies similar mechanisms of CF formation in both systems, and therefore, a minimal influence of the CNT surface on CF formation in the CS SWPABS suspensions. TEM micrographs comparing the CNT surface of CS SWPABS with the surface of an oxidized CNT (see Figure 3-12) show that PABS mostly coats the CNT surface. Thus, chlorine will most likely react on the PABS functional group rather than directly on the CNT sidewall. The slightly greater net production of CF by free PABS

(shown in Figure 3-3) is likely due to minor differences in the total mass of PABS available in each system (i.e., uncertainly in the estimate of PABS mass associated with the CNT surface). Alternatively, it is also possible that a smaller number of reactive sites responsible for CF formation exist on PABS when bound to the CNT surface (i.e., sterics induced by the linkage of PABS to the CNT surface may limit the number of sites for HOCl reaction).

A more interesting result is observed with CS SWPEG relative to free PEG. While free PEG generated no CF, as previously noted, CS SWPEG generated appreciable CF (albeit less than in either PABS-containing system). Incidentally, physical mixtures of free PEG and various CS CNTs (either as received or oxidized) also failed to produce any CF when chlorinated. Thus, it appears the chemical binding of PEG to the CNT surface generates new sites that are not only reactive toward HOCl (or reactive byproducts of HOCl decomposition) but also capable of generating CF. Notably, the functionalization procedure for the generation of CS SWPEG first involves nucleophilic acyl substitution of carboxylated CNTs, yielding a chlorinated surface group to which PEG is added. In the event that PEGylation does not completely saturate these surface sites, we cannot rule out their possible contribution to CF formation.

While Figure 3-3 explores the relative formation of CF by free and CNT-bound polymers, Figure 3-4 considers HAA production in these same systems. Trends in HAA formation match those observed for CF. Specifically, free and CNT-bound PABS represent precursors to HAAs, and the amount generated roughly scaled with available PABS mass in each suspension. In contrast, chlorination of free PEG did not yield HAAs, but a small but reproducible amount of HAAs were produced in PEGylated CNT

suspensions. Although these data deviate from linearity on a log-log scale, we calculated their slopes to facilitate comparison to other CNTs and our earlier results for CF formation. Once again, data suggest that PEG coated CNTs exhibit DBP formation potential that is unique and not predictable from the reactivity exhibited by the individual components from which they are fabricated.

3.4.3 CF and HAA formation during chlorination of N-functionalized CNTs

A notable result with N-functionalized CNTs is that only CS N-CNTs, which rely on an amide functionality, generate CF in addition to DCAA and TCAA, whereas the aminated NL N-CNTs only yield small amounts of DCAA HAAs (Table 3-2). This suggests that the chemical structure of the surface N group likely influences DBP formation potential, which is consistent with results from model N-containing organic precursors for THMs and HAAs. For example, one might expect a preference for HAA formation from N-functionalized CNTs based on the known reactivity of tyrosine. Tyrosine, with its aromatic moiety [177], has been shown to generate more HAAs than other non-aromatic amino acids. We acknowledge, however, that the formation of CF in the amide but not amine functionalized CNT systems is not entirely understood.

For completeness, we have included in

Table 3-2 the NDMA yields for N-functionalized CNTs measured in Chapter 2. The values for NDMA in

Table 3-2 encompass both the release of surface bound NDMA resulting from the synthesis and functionalization of commercial N-CNTs and the amount of NDMA produced during chlorination under our standard experimental conditions (15 mg-Cl_2/L

initial HOCl, 10 mg/L CNT, pH 8, 4 h reaction). When assessing the DBP formation potential from N-containing CNTs, both chlorinated and nitrogenous DBPs will need to be accounted for.

3.4.4 CF and HAA formation during chlorination of oxidized CNTs

Figure 3-5a shows the formation of chloroform as a function of the surface oxygen concentration on CNTs as quantified by the O 1s region of the XPS spectra for each CNT type. Data are shown for CNTs that are non-functionalized (NF), oxidized with either concentrated nitric acid (N) or mixtures of nitric and sulfuric acid (S/N), commercially available N-CNTs, a carboxylated CS SWCNT processed with extended exposure to germicidal UV, and CH MWCNTs that were processed via extended exposure to aqueous ozone (O_3) or extended chlorination (Cl_2).

Several observations are notable, including non-functionalized (as-received) CNTs, with relatively little surface oxygen, consistently reacting with chlorine but not generating any appreciable chloroform. In fact, most surface oxidized CNTs, including those acquired commercially, those oxidized with strong acids in our laboratory, and CS SWCOOH treated by extended UV irradiation, also yielded little to no chloroform. The noteworthy exception were CH MWNF that were oxidized via extended ozonation and chlorination. In these cases, surface oxygen increased with ozonation and chlorination, as expected, and this in turn produced a near linear increase in chloroform production. In fact, CNTs with similar amounts of surface oxygen but prepared either via oxidation with strong acids or via extended exposure to germicidal UV did not produce similar amounts of chloroform upon chlorination. Thus, there appears to be something unique to the

nature of CNT surface generated via ozonation and chlorination that promotes chloroform production.

Figure 3-5b considers HAA formation as a function of CNT surface oxygen. As with CF formation, production of HAAs is largely independent of surface oxygen concentration. The exception, once again, is for CNTs aged via extended ozonation (we note that HAA production was not quantified for CNTs oxidized via reaction with free chlorine. For the correlation in Figure 3-5b, the speciation of HAAs generated by ozone-processed CNTs is dominated by TCAA. Collectively, therefore, linear correlations observed in Figure 3-5 may suggest a shared intermediate in the production of CF and TCAA during chlorination of ozonated CNTs.

It is difficult to rationalize the trends in CF and HAA formation in Figure 3-5 based upon established behavior for conventional NOM model precursors often used to study DBP formation. For example, several model precursors possess functionalities analogous to those encountered on oxidized CNT surface. Aromatic model precursors such as 3-hydroxybenzoic acid, phloroglucinol, and 4-hydroxybenzoic acid [51] possess hydroxyl groups, whereas ferulic acid and sinapic acid [33] possess carboxyl functionalities, and can be viewed as reasonable solution phase analogs of oxidized CNTs. Nevertheless, while all of these lower-molecular weight organics have been shown to generate significant amounts of THMs and HAAs, most oxidized CNTs do not.

It has also been suggested that soluble forms of hydrophobic carbon, which has a high content of aromatic rings, phenolic hydroxyl groups, and conjugated double bonds, are generally the largest source of THMs and HAAs [178]. While CNT sidewalls can be conceptualized as containing aromatic rings throughout their entire structure, we are left

to conclude that their mechanical strength and rigidity makes formation of soluble DBPs via reaction with chlorine difficult, even for CNTs that have been extensively oxidized via aggressive mixtures of strong acids. Because ozone (and chlorine) are commonly viewed as more milder oxidants than strong acid mixtures, it seems that increases in CF and TCAA formation in response to extended ozonation and chlorination are most probably attributable to specific surface sites generated via these oxidation processes than considerations (e.g., defect density) more generally related to integrity of the aged CNT sidewall.

The linear regression analysis elucidates near identical slopes (0.15 ± 0.009 for O_3 and 0.18 ± 0.026 for Cl_2 aging) for the functional relationship between CF production and surface oxygen concentration for ozone and chlorine aged CH MWNF. The similarity in these slopes suggests similar mechanisms of chloroform formation on each type of processed CNT, which may also imply comparable surface oxides generated on CNT surfaces via ozonation and chlorination.

Insights into the nature of the surface sites responsible for CF and TCAA formation in ozone processed CNTs may be derived from the model precursor literature, as well as from the growing body of work related to the characterization of CNT surfaces after ozonation. Ozonation of aqueous suspended CNTs is considered an effective treatment for removing impurities while simultaneously oxidizing the surface with hydroxyl (C-OH), carbonyl (C=O), and carboxyl (COOH) functional groups [115, 179, 180] to promote suspension stability. In fact, from the existing body of literature on CF and HAA formation from model precursors, we propose that the surface of these ozonated and chlorinated CNTs contains functionalities similar to that of resorcinol. The mechanism

for HAA and CF formation via the chlorination of resorcinol is shown in Figure 3-7 [26], in which it undergoes a series of enolization and haloform reactions. Specifically, the reaction is initiated by the rapid chlorination of the carbon atoms activated by ortho OH-substituents (or phenoxide ions) in an alkaline environment. Next, the haloform reaction yields an intermediate carbanion, which subsequently is protonated to produce Species A or alternatively halogenated further to generate Species B (as shown in Figure 3-7). Both Species A and Species B undergo further hydrolytical or oxidative fissions (red dotted lines in Figure 3-7) to form CF, TCAA, or halogenated acetone.

The ability for CNTs to generate CF and TCAA via this mechanism depends on the density of surface hydroxyl groups resulting from oxidation. Through XPS (in Figure 3-6a) we are able to qualitatively differentiate the O functionalities generated by the various oxidation processes (Cl_2, O_3, and S/N). Here, the peak in the O 1s region dictates favorability of C-O (533.5 eV) by CH MW-O_3 and of C=O (532.0 eV) by CH MW-Cl_2 [115]. Additionally, the inset in Figure 3-6b speaks more to the ozone oxidation of CNTs were the speciation of ozone is again showing unique favorable O functional groups (denoted by the component at 286.4 eV indicative of C-O [180]) compared to chlorine oxidation. This finding, supports our original hypothesis of ozone favoring the formation of resorcinol type structures. We would therefore expect two adjacent OH sites to be generated on the CN surface by ozone at lower total surface oxygen concentrations due to its ability to incorporate more O into the CNT sidewall than chlorine, which may explain why we see an increase in CF and HAA formation at lower total surface oxygen concentrations on ozone treated CNTs relative to chlorine treated CNTs.

Finally, the rate of CF and HAA production is also dictated by the type of structures available on the CNT surface. For example, resorcinol-type structures are fast acting compared to phenolic compounds, with chlorine rate constants of $\sim 4 \times 10^3 \text{ M}^{-1} \text{ s}^{-1}$ and $0.36 \text{ M}^{-1} \text{ s}^{-1}$ for resorcinol and phenol respectively [181, 182]. This means that ozone oxidized and chlorine oxidized CNTs would not only produce a greater yield of CF and HAAs relative to other oxidized CNTs but also produce these species at faster rates.

3.4.5 Alternative DBPs generated during CNT chlorination

In addition to CF and HAAs, other as yet unidentified compound were also observed to be generated during the chlorination of CNTs. Through comparison of peaks in our GC-ECD chromatograms to retention times of commercially available, known DBP standards (Figure 3-9), we were able to identify chloropicrin (trichloronitromethane; TCNM) as a chlorination byproduct in some CNT suspensions. Chloropicrin is considered highly toxic to mammals. For example, the lethal concentration to cause death to half of the tested population (LC_{50}) of fish and aquatic invertebrates are 5.15 ppb and 71 ppb, respectively. In particular, TCNM was most often produced during chlorination of nitric acid oxidized CNTs (i.e., CS SWCOOH, NL SW-N, and CH MW-N) and the PABS functionalized CNTs (CS SWPABS). In fact, TCNM was the major product during chlorination of commercially oxidized CS SWCOOH (see Figure 3-8) generating at about 13 µg/mg-CNT in 4 h. The concentrations of TCNM produced (>300 µg/L) under our experimental conditions (15 mg-Cl$_2$/L and 24 h of contact time) can reach the LC_{50} with as little as 200 µg/L of CS SWOOH for a population of fish.

Our observation of chloropicrin is somewhat puzzling because it contains nitrogen, the source of which is unclear in our CNT suspensions. Traditionally,

chloropicrin production has been reported from the chlorination of nitro compounds, like nitro-2 phenol, found in nitrogen rich organic matter or from the presence of nitrite and a THM model precursor [183]. Because nitric acid is used under refluxing conditions to oxidize CNTs, nitric ions could be captured by the CNT surface via sorption or bonding. Hence providing a source for nitrite that then chlorinated with CNTs form chloropicrin. Because the literature has not identified the presence of nitro functional groups on the surface of nitric acid oxidized CNTs, it is perhaps possible that fixation of atmospheric nitrogen (N_2) on the oxidized CNTs is occurring, as has been proposed for formation of nitrogenous DBPs during chlorination of activated carbon [64, 65, 184].

Several other unknowns were observed during analysis of samples for HAAs. Figure 3-10 shows a portion of a GC-ECD chromatogram for a sample taken from a chlorinated CS PABS suspensions. Also provided for comparison is the chromatogram for a DBP standard, showing the location and relative responses of MCAA and DCAA via our analytical method. Multiple, ECD-responsive products that are as of yet unidentified can be seen, with retention times similar to but distinct from known, regulated HAAs.

Most notable among these unknowns is the product that elutes at 17 minutes just prior to MCAA. Similar to correlations reported in Figure 3-11 for chloroform and HAAs, we have observed the formation of this unidentified product to scale linearly with surface oxygen concentration on the CNTs. However, unlike CF and HAAs, the formation for this unidentified DBP scaled with surface oxygen concentration regardless of the method used to oxidize CNTs (i.e., the correlation exists across acid oxidized, but less for ozone aged). Additional work is necessary to identify this unknown, which based

on ECD response alone, would be characterized as one of, if not the, major byproduct of CNT chlorination.

3.4.6 Implications of CNTs representing precursors of halogenated DBPs.

The role of CNTs as THM and HAA precursors is influenced by the nature of the functional group (e.g., carboxylated, PABS, or PEG) and also by the chemical oxidant. Our results showed that polymer functionalized CNTs exhibited the highest CF and HAA formation potential of all the CNTs tested here. Meanwhile, extensive oxidation with ozone or chlorine of NF CNTs led to an increase in DBP formation potential. However, to reach regulatory MCL, polymer functionalized and oxidized CNTs must be present at high loadings (>20 mg/L CNTs). Though these concentrations are unattainable in typical engineered water systems were the expected concentration is in the sub to low ng/L levels [77, 78], their implementation as materials during or post chlorination could yield DBPs at levels of concern, and hence could have negative implications to the quality of treated water.

We are currently working to elucidate the mechanism of DBP formation in PEG containing systems, particularly addressing whether the CNT surface promotes or catalyzes CF and HAA formation. Of note are our initial experiments with PEG in which we do not observe any CF or HAA formation via reaction with HOCl (15 mg/L) in the absence of CNTs. Like we suspect in Chapter 1, it may be possible that transient, reactive intermediates capable of promoting formation of THMs and HAAs are generated via reaction of chlorine with π-bonds in the CNT sidewall or at non-nitrogen containing surface groups. We argue that developing such mechanistic insights of DBP formation is critical to the sustainable design of CNTs, where the goal must be to identify functional

groups that enable their promise in applications yet limit DBP formation during environmental processing.

During CNT chlorination, various other species are likely generated in addition to CF and HAAs, and the identity and consequences of these as yet unidentified DBPs merit closer scrutiny. We also reiterate that chlorination alters the surface chemical composition, suspension stability, and potentially the toxicity of CNTs. In essence, therefore, chlorinated CNTs represent another next-generation disinfection byproduct.

Results herein also have implications for the transport and mobility of CNTs in the environment. CNTs oxidized with ozone or chlorine, besides exhibiting greater DBP formation potential, also have enhanced stability in aqueous suspensions. Rates of settling in CNT suspensions are shown as a function of their extent of oxidation for ozone- and chlorine-treated CNTs in Figure 3-13. The suspension stability of these oxidized CNTs increased with extent of ozone and chlorine treatment when compared to their non-functionalized form. This has implications for environmental release through leaching as well as mobility and transport through the environment. In addition, CNTs that are highly stable in solution are considered more toxic to bacteria and animals [76], and will also be more difficult to remove via traditional drinking water treatment technologies (e.g., coagulation, flocculation and sedimentation or media filtration).

Finally, our work is another illustration of how functionalized CNTs can mimic the reactivity of NOM. Ultimately, with the extensive degree and range of surface groups added via functionalization, CNTs can be effectively transformed into an analog of organic carbon. As we continue to address the reactivity of carbon nanomaterials in natural and engineered aquatic systems, the extensive body of literature on NOM may

provide a reasonable first approximation of the chemical processes in which

functionalized CNTs will participate.

Table 3-1: List of CNTs purchased from selected vendors. Vendor specified CNT type, synthesis route, and functional groups are reported.

Manufacturer	Name	Surface group	Type	Synthesis
Carbon Solutions, Inc. (CS)	CS SWNF	NF	SW	Arc discharge
	CS SWCOOH	Carboxylic acid		
	CS SWPEG	PEG		
	CS SWPABS	PABS		
	CS SWNH$_2$	Amide		
NanoLab, Inc. (NL)	NL SWNF	NF	SW	CVD
	NL SWNH$_2$	Amine		
Cheap Tubes, Inc. (CH)	CH MWNF	NF	MW	CVD

SW = single-walled, MW = multi-walled, NF = non-functionalized, CVD = chemical vapor deposition, PEG = polyethylene glycol, and PABS = poly(m-aminobenzene sulfonic acid)

Table 3-2: THM, HAA, NDMA and TCNM formed during chlorination of CNTs normalized to CNT loading. Chlorination reaction conditions: 15 mg/L initial HOCl, 5-20 mg/L CNT, 5 mM potassium phosphate at pH 8, and 4 h reaction. Values shown are averages plus or minus the standard deviation of 3 or more samples.

CNT type	Fraction of chlorine consumed	CF (µg/mg)	DCAA (µg/mg)	TCAA (µg/mg)	THAA (µg/mg)	NDMA (ng/mg)[a]
CS SWPABS	0.32	3.46 ± 0.810	3.9 ± 1.31	6.3 ± 2.09	10.2 ± 2.47	0.7 ± 0.25
CS SWPEG	0.19	0.75 ± 0.086	0.8 ± 0.34	0.8 ± 0.20	1.6 ± 0.39	ND
CS SWCOOH	0.15	ND	0.4 ± 0.29	0.3 ± 0.20	0.7 ± 0.35	ND
CH MW-N	0.07	ND	ND	ND	ND	NA
NL SW-N	0.2	ND	ND	0.3 ± 0.06	0.3 ± 0.06	NA
CH MW-S/N	0.07	ND	0.5 ± 0.26	0.6 ± 0.11	1.1 ± 0.28	NA
NL SW-S/N	0.15	ND	0.4 ± 0.06	0.7 ± 0.09	1.1 ± 0.11	NA
CS SWNH$_2$	0.20	0.10 ± 0.032	0.3 ± 0.25	0.1 ± 0.05	0.4 ± 0.25	0.7[b]
NL SWNH$_2$	0.23	ND	0.2 ± 0.12	ND	0.2 ± 0.12	2.4 ± 0.16
CS SWNF	0.16	ND	ND	ND	ND	NA
CH MWNF	0.09	ND	ND	ND	ND	NA
NL SWNF	0.36	ND	ND	ND	ND	ND

[a]NDMA values do not include leaching concentrations due to batch-to-batch variability. [b]Value was not reproduced at these experimental conditions. [c]Estimated from Figure 3-8. ND = not detected, NA = not analyzed.
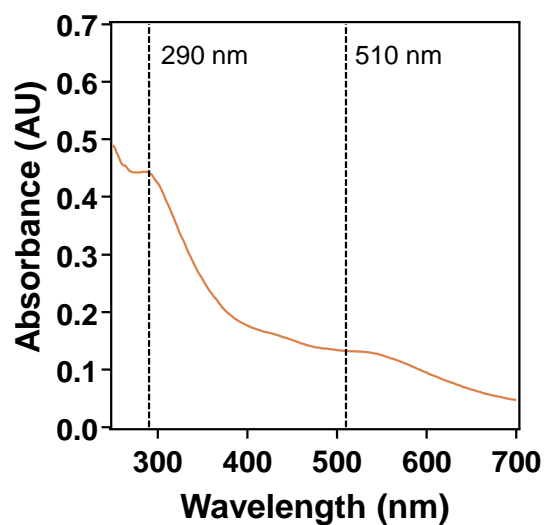
Figure 3-1: UV spectrophotometry scan of PABS in 1 N NaOH solution in a 1 cm path length quartz cuvette. Dashed lines represent expected diagnostic absorbance bands at 290 nm and 510 nm.
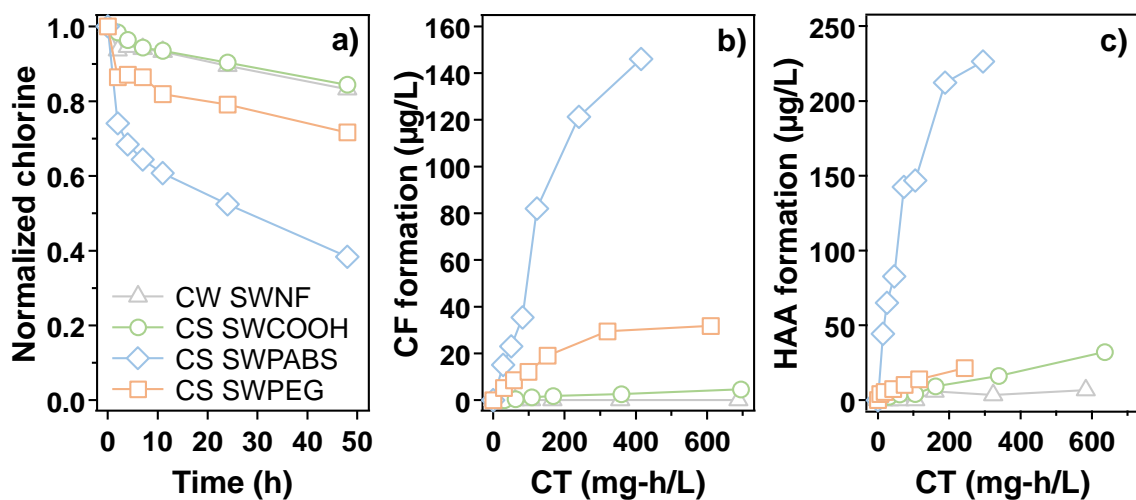
Figure 3-2: (a) Representative chlorine decay as a function of time and (b) chloroform formation and (c) HAA formation as a function of CT in mg-h/L for CS SWNF, CS SWCOOH, CS SWPABS, and CS SW PEG. Experimental conditions: 15 mg-Cl$_2$/L initial HOCl, 10 mg/L CNTs, and pH 8. Results were corrected by subtracting out the chlorine demand and DBP formation of chlorine reaction controls with no CNTs.
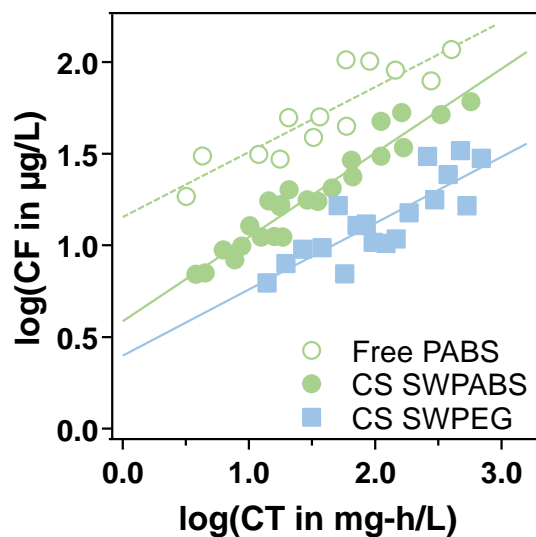
Figure 3-3: Formation of CF versus CT on a log-log scale during the chlorination of polymer functionalized CNTs and polymer only (except for PEG which did not generate any considerable chloroform). Best fit linear regressions are shown. R^2 values are 0.790, 0.929, and 0.705 for free PABS, CS SWPABS, and CS SWPEG, respectively. Reaction conditions: 15 mg/L initial HOCl, 10 mg/L solids loading, and pH 8.
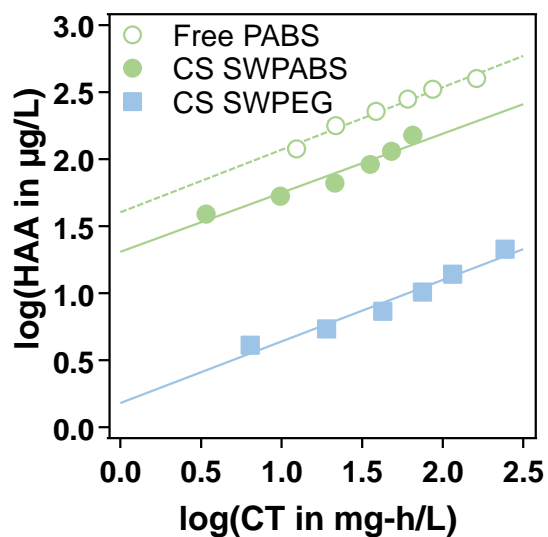
Figure 3-4: Formation of HAA versus CT on a log-log scale during the chlorination of polymer functionalized CNTs and polymer only (except for PEG which did not generate any considerable chloroform). Best fit linear regressions are shown. Slopes (and R^2 values) are 0.46 ± 0.03 (0.981), 0.44 ± 0.06 (0.941), and 0.46 ± 0.05 (0.963) for free PABS, CS SWPABS, and CS SWPEG, respectively. Reaction conditions: 15 mg/L initial HOCl, 10 mg/L solids loading, and pH 8.
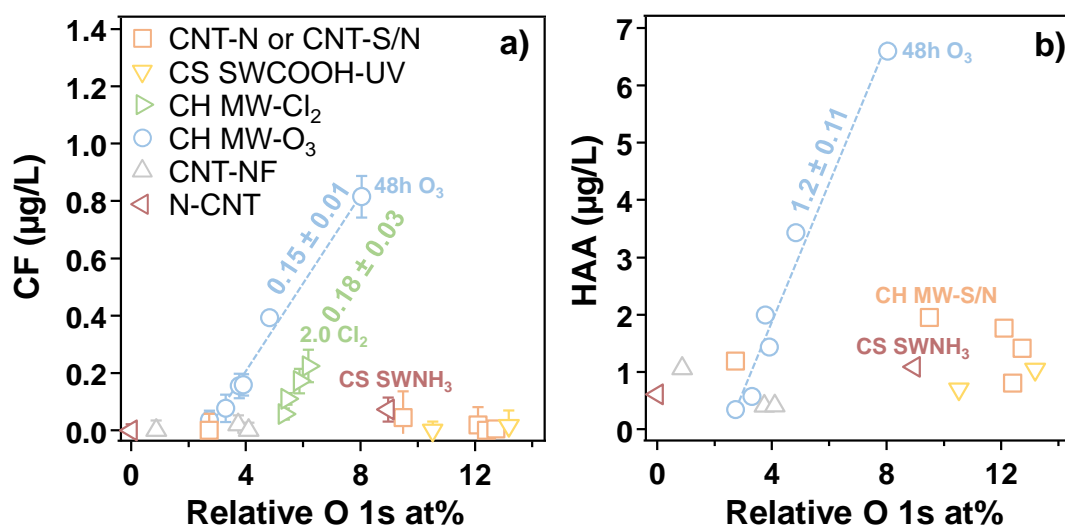
Figure 3-5: (a) Chloroform and (b) HAA formation during chlorination of CNTs versus the O 1s concentration measured by XPS. The relative oxygen content is the difference between the CNT sample and the polymeric substrate O 1s concentrations. Experimental conditions: 10 mg/L CNTs, 15 mg/L initial HOCl, pH 8, and 4 h reaction. Markers represent averages with error bars of standard deviation of 3 or more observations.
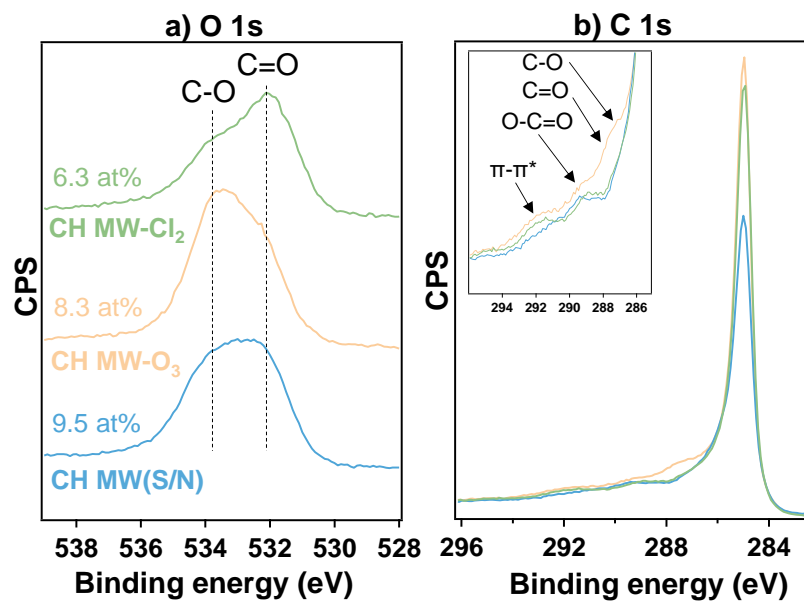
Figure 3-6: XPS spectra of CH MW oxidized with chlorine (-Cl$_2$), ozone (-O$_3$), or a sulfuric/nitric acid mixture (S/N) comparing (a) O 1s and (b) C 1s, regions. In the C 1s spectra, an inset focuses on oxidized carbon.
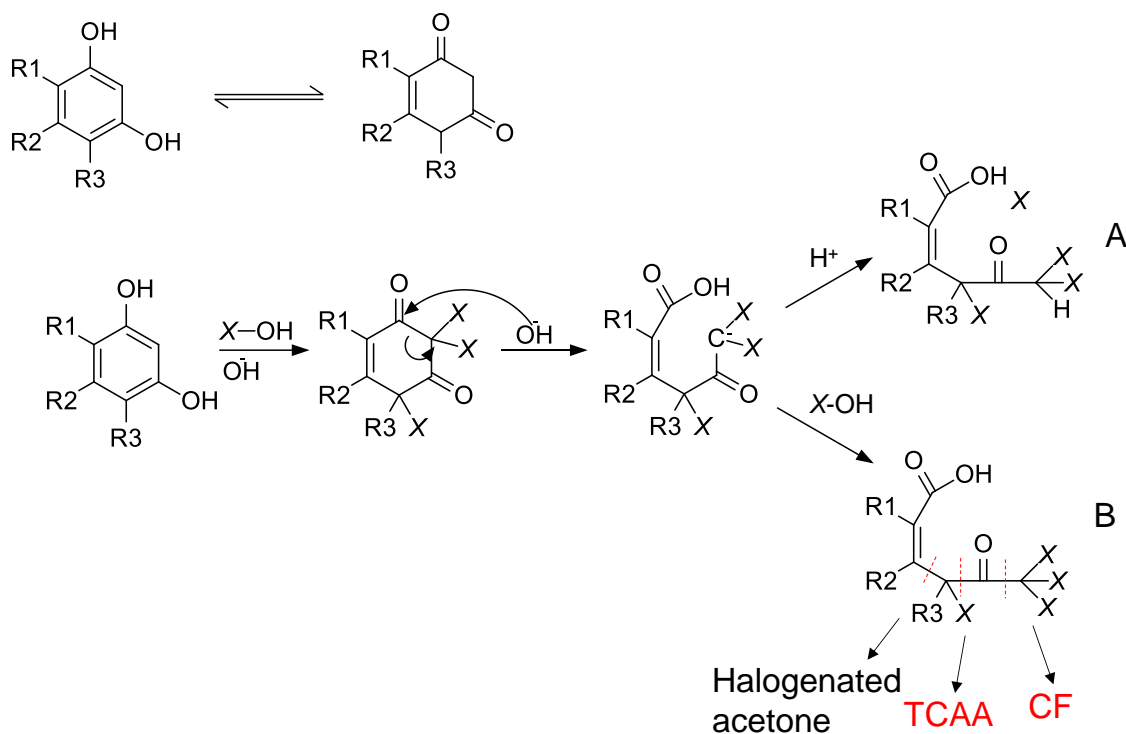
Figure 3-7: Mechanism of chloroform and TCAA formation via the chlorination of resorcinol [26]. (1): Fast chlorination of the carbon atoms that are activated by ortho OH-substituents (or phenoxide ions) in an alkaline environment. (2): The haloform reaction yields an intermediate carbanion. (3): The carbanion is rapidly protonated to produce Species A or alternatively halogenated further to produce Species B. Both Species A and Species B undergo further hydrolytical or oxidative fissions (red dotted lines) to form CF, TCAA, or halogenated acetone.
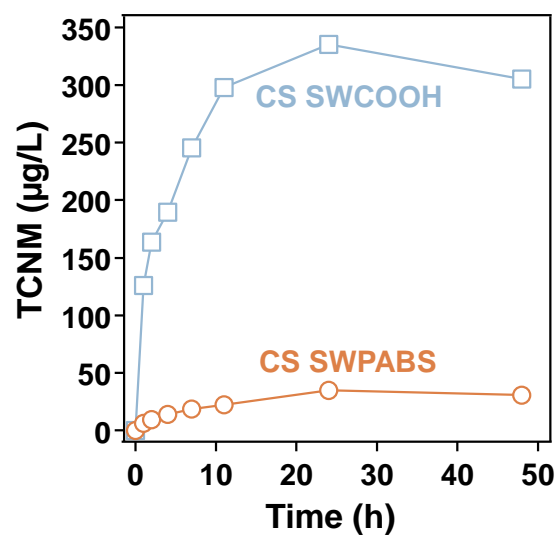
Figure 3-8: Formation of chloropicrin (TCNM) versus time during chlorination of CS SWCOOH and CS SWPABS. Experimental conditions: 13 mg/L CNT, 15 mg-Cl_2/L, pH 8, and 0-24h reaction time.
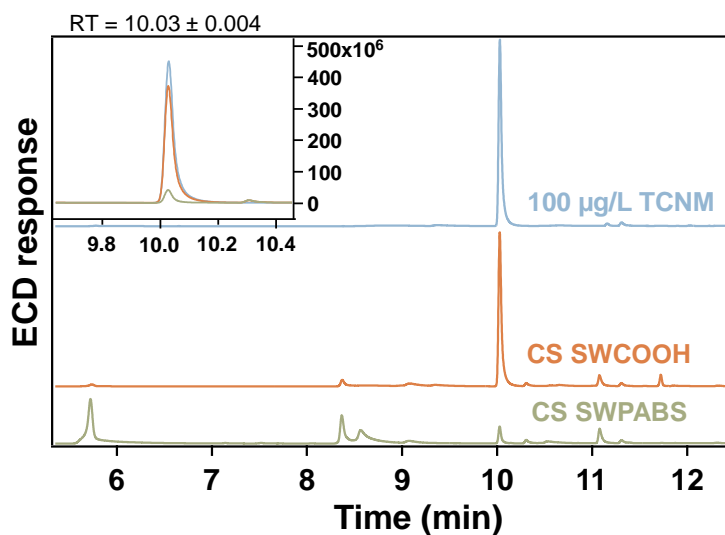
Figure 3-9: GC-ECD chromatograms of TCNM (blue) and of samples from the chlorination of CS SWCOOH (orange) and CS SWPABS (green). The peaks were matched by comparing retention times (change ± 0.004). Samples from chlorination experiments were ran under the following experimental conditions: 15 mg-Cl$_2$/L HOCl, 10 mg/L CNT, pH 8, 4 h reaction.
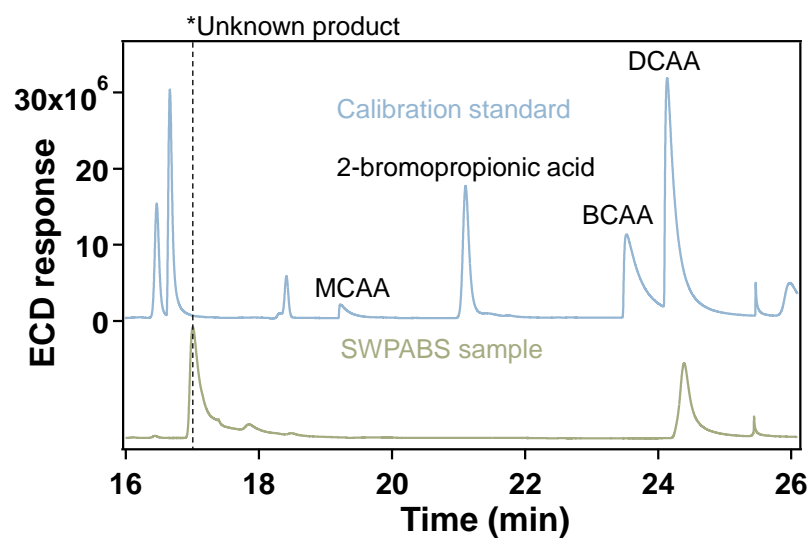
Figure 3-10: GC-ECD chromatogram of a chlorination sample of CS SWPABS (brown) compared with MCAA and DCAA (blue). Peak at 17 min is an unidentified product.
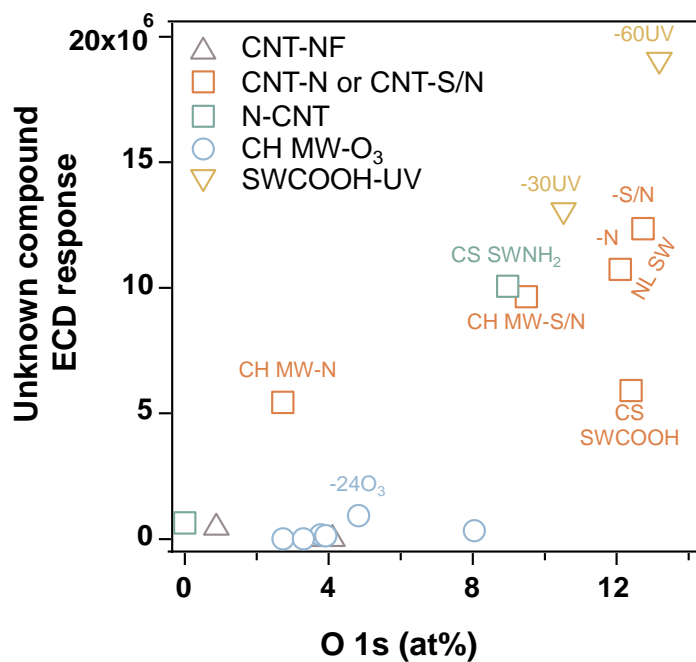
Figure 3-11: ECD response of the unknown compound observed at 25 min. Experimental conditions: 15 mg-Cl$_2$/L HOCl, 10 mg/L CNT, 4 h reaction time, and pH 8 water.
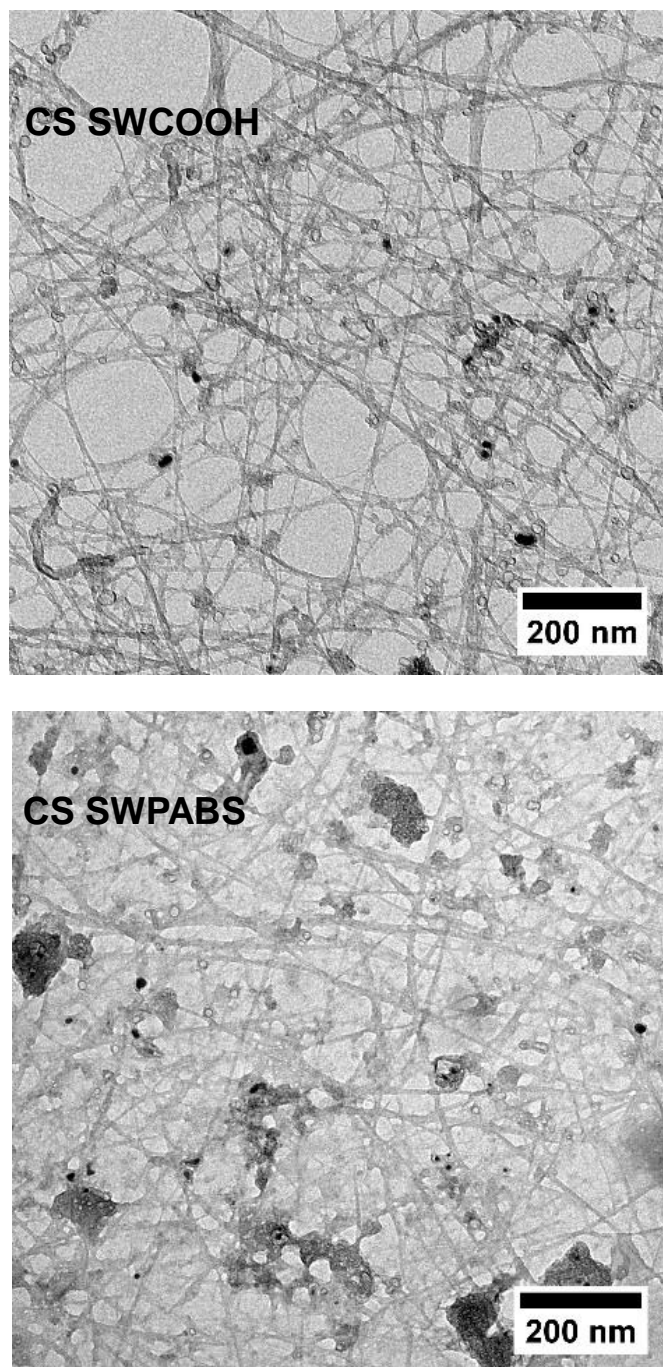
Figure 3-12: TEM micrographs of CS SWCOOH and CS SWPABS comparing CNT surface. The surface of CS SWPABS is largely coated by the PABS functional group and hence less CNT surface is available for chlorine attacks.
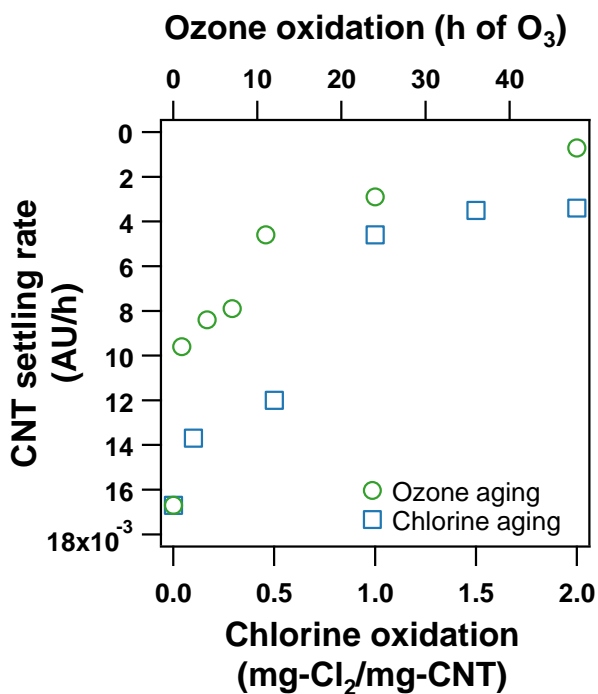
Figure 3-13: Settling rates of CNTs in water (no ionic strength) versus oxidation with ozone (green circles) or chlorine (blue squares). Settling rates, in absorbance units (AU) per hour (h), were calculated by doing a linear regression through the 5-20 min linear region of a rate scan. Rate scans were done on a 1 cm path length cuvette using a spectrophotometer set at 700 nm wavelength. A smaller setting rate indicates better suspension stability. Reaction conditions: 1 g/L CH MWNF in DI, 30 d chlorination or continuous ozonation (19.2 mg/L steady-state concentration).

CHAPTER 4: EFFECT OF WATER QUALITY ON TRIHALOMETHANE FORMATION DURING CHLORINATION OF CARBON NANOTUBES

4.1 Abstract

We have shown that CNTs form trihalomethanes (THMs), haloacetic acids (HAAs), and N-nitrosodimethylamine (NDMA) during chemical disinfection (i.e., chlorine, chloramine or ozone) and that DBP yields and speciation depends on the surface chemistry of the CNT. Here we demonstrate the effect of natural aquatic conditions on the formation of disinfection byproducts during chlorination of CNTs. In particular, we focused on the effect of pH, concentration of natural organic matter (NOM) as humic acid, and bromide ion concentration on the formation potential of THMs. With a large selection of CNT types available in the market, we focused on single-walled CNTs with the following functional groups and in increasing DBPs formation potential: (1) purified via heat treatment but with little to no surface functional oxides; (2) oxidized using nitric acid (containing R-COOH, R−OH, R=O functional groups); (3) functionalized with polyethyleneglycol (PEG); and (4) functionalized with m-polyaminobenzene sulfonic acid (PABS). With increasing pH, chlorination of functionalized CNTs yielded more THMs. With increasing bromide, the yield of THMs increased while also trending toward favoring brominated analogs (e.g., mono, di, and tribrominated THMs). In the presence of humic acid, all CNTs exhibited a simple additive effect for THM formation (i.e., total THM = THM from CNTs + THM from humic acid) except for non-functionalized CNTs, which had an inhibitory effect presumably due to the sorption of humic acid on the CNT surface. Generally, the influence of each aquatic variable in CNT suspensions mirror

those established in the literature for THM formation during chlorination of natural waters (waters that contain NOM and bromide). Collectively our work demonstrates CNTs behaving as classic precursors to THMs under representative engineered water matrices.

4.2 Introduction

Public health concern over disinfection byproducts (DBPs) was first raised over 40 years ago with the identification of chloroform in drinking water [9]. Since that time, extensive investigations have been conducted on the formation of DBPs, with emphasis on their two most prevalent classes, trihalomethanes (THMs) and haloacetic acids (HAAs). These studies have also helped to identify important water quality parameters that influence the formation of these DBP families. Aside from the nature and concentration of organic precursor materials (e.g., natural organic matter or NOM), two important variables are pH, which influences free chlorine speciation, as well as the presence of co-solutes such as bromide that can lead to mixed halide byproducts. Collectively, therefore, effective management of DBP formation requires an appreciation for the interplay between precursor materials, aquatic chemical conditions, and the nature of the chemical disinfectant.

In our earlier work (see Chapter 2 and 3), we were the first to show that certain types of CNTs function as precursors to DBPs. In particular, polymer-functionalized CNTs result in formation of chloroform (CF), N-nitrosodimethylamine (NDMA), and di- and trichloroacetic acid (DCAA and TCAA, respectively) during chlorination at levels of concern relative to traditional DBP precursors. In contrast, most other forms of CNTs

(e.g., non-functionalized and oxidized) exhibited more limited or no formation of CF or HAAs under the same conditions, although as yet unidentified byproducts were observed. However, all prior work has been conducted in highly idealized, model aquatic systems. To most completely characterize the role of CNTs as an emerging precursor for DBPs, we must also explore their DBP formation potential across a range of the aforementioned aquatic variables known to influence DBP production from more traditional precursors.

Brominated DBPs are generated when naturally occurring bromide in source water (ranging from 7 to 400 µg/L [3, 4]) is rapidly oxidized by chlorine to hypobromous acid (HOBr) as shown by the reaction:

$$HOCl_{aq} + Br^- \rightleftharpoons HOBr_{aq} + Cl^- \qquad \text{Equation 4-1}$$
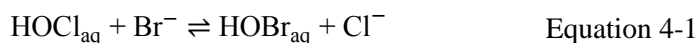
This active oxidant can react with natural organic matter (NOM) or other carbonaceous precursors to form brominated DBPs in a manner analogous to hypochlorous acid (HOCl) [5, 9, 185]. In fact, HOBr reacts faster with model organic compounds and acts as a more efficient substitution agent than HOCl, although HOCl is a more powerful oxidant [185-188]. Hence, bromide incorporation into THMs and HAAs is favored over chlorine. Accordingly, increasing bromide ion concentration shifts the speciation of THMs and HAAs from chlorinated species in the absence of bromide to mixed halide species and ultimately to fully brominated forms at high bromide levels [44, 185-187]. Four THMs, chloroform (CF), bromodichloromethane (BDCM), dibromochloromethane (DBCM) and bromoform (BF), and nine HAAs, chloro- (MCAA), dichloro- (DCAA), trichloro- (TCAA), bromo- (MBAA), bromochloro- (BCAA), bromodichloro- (BDCAA), dibromo- (DBAA), dibromochloro- (DBCAA), and tribromo-acetic acid (TBAA), can be produced

from chlorination of water in the presence of bromide. Notably, brominated DBPs are more genotoxic, cytotoxic, and carcinogenic than their chlorinated analogues [21].

Solution pH is a critical variable in DBP formation because it controls both the speciation of free chlorine and potential reactive sites in organic DBP precursors. For example, the speciation of free chlorine as either hypochlorous acid (HOCl) or hypochlorite (OCl^-) depends on pH, with a reported acid dissociation constant (pK_a value) for HOCl of 7.58 at 20 °C [189]. Relative to hypochlorite, HOCl is a stronger oxidant and thus preferred for disinfection. In addition to free chlorine speciation, solution pH can also influence DBP formation by altering the protonation state of functional groups on organic matter precursors. Some potential reactive functionalities (e.g., phenols and amines) are likely to have pK_a values within the typical pH range for drinking water and wastewater, and can be expected to exhibit different reactivity toward free chlorine if they are in the protonated or deprotonated states. Taking both of these factors into consideration, studies of DBP formation as a function of pH have generally found that increasing pH tends to increase THM formation while HAA formation trends depend on the type of precursor [178, 190, 191].

In fact, the formation of THMs at different pH values is determined by the formation mechanisms of the precursor species and subclasses (i.e., trihalopropanones, trihaloacetonitriles, and trihaloacetaldehydes), which hydrolyze in alkaline conditions to form THMs. Based on a mechanism by Boyce and Hornig [192] the relative formation of THM species from the common precursor structure ($R-CO-CX_3$) is determined by the nature of the R group and pH. It is here that under alkaline conditions, base catalyzed

hydrolysis prevails, yielding more THMs, while in acidic environments HAAs will be formed if the R groups is a readily oxidizable functional group capable of donating an electron pair to the rest of the molecule.

Finally, a wealth of studies have shown that the chemical composition of organic matter strongly influences the extent and distribution of DBPs generated during chlorination [8]. Most relevant to our work herein with CNTs, however, are prior observations that association of NOM with various surfaces during chlorination can alter DBP formation. For example, Hassan et al [121] showed that chlorine loss and the formation of HAAs in water with riverine NOM were significantly enhanced in the presence of goethite (α-FeOOH). They attributed this to possible changes in the conformation of adsorbed NOM that increased availability of reactive sites in the NOM toward chlorine. Similarly in work with activated carbon (AC), a reasonable bulk analog for CNTs, showed additional products forming from the reaction between free chlorine with adsorbed organic phenolic compounds on activated carbon that did not form in bulk water [61]. It was recognized that activated carbon exposed to chlorine promotes unique reactions different from bulk solution chlorination, such as hydroxylation of the aromatic ring, oxidation to quinones, chlorine substitution, carboxylation and oxidation coupling [62].

In this chapter, we explore the effect of bromide (Br^-) concentrations, pH, and NOM on the formation of DBPs during chlorination of CNTs exhibiting a range of surface chemistries. While no such studies have been conducted before, there is evidence in the literature that these variables will be critical to DBP formation in CNT

suspensions. For example, CNTs are powerful adsorbents of organic material [100].

Thus, it is possible that association of NOM with CNTs will inhibit DBP formation by

decreasing the amount of dissolved NOM available for chlorination and adsorbed NOM

blocking possible reactive sites on the CNTs. Alternatively, DBP formation may be

enhanced in mixtures of NOM and CNTs if reactive functionalities on NOM become

more accessible through conformational changes in the adsorbed organic layer. The net

effect on DBP production is difficult to predict a priori as NOM-CNT interactions will

not only depend on the surface chemistry of the CNTs, but also solution pH. Indeed,

adsorption of NOM to MWCNTs tends to increase with decreasing pH, which in turn

increases CNT dispersion [100]. Furthermore, the type of NOM (i.e., humic acid or fulvic

acid) dictated adsorption on non-functionalized MWCNTs, were less soluble, higher

molecular weight humic acids had generally higher adsorption capacity than fulvic acids

due to their high content of aromatic carbon [100]. We note that relative to NOM and pH

effects, far less is known about how bromide will affect DBP formation in CNT

suspensions, However, it has been shown, albeit under far more aggressive conditions,

that CNTs can undergo bromination, producing surface Br sites without otherwise

damaging the structural integrity of the CNT surface [193].

To address these questions, a selected suite of arc discharged synthesized

SWCNTs from Carbon Solutions, Inc. (CS) with polymer (PABS and PEG), oxygen

(primarily carboxylated), or no surface functional groups (see Table 3-1 for CNT details)

were reacted with free chlorine in batch system with systematically varied water quality.

First the effect of bromide ion concentration on DBP formation was investigated at

dissolved bromide levels representative of natural waters. Then, in pH buffered systems,

DBP formation was examined in CNT suspensions across a range of environmentally relevant pH values. Finally, using Suwannee River Humic Acid as a model NOM, DBP formation in CNT-NOM mixtures was examined to determine whether formation is inhibited, additive, or synergistic in the presence of two known precursors. In all systems, we determined DBP speciation and yields, suspension chlorine demand, and, for Br^- containing systems, the bromine incorporation factor. Results herein will allow us to conclude whether results from model systems in prior Chapters can be reasonably extended to more complex aquatic matrices representative of water and wastewater treatment systems.

4.3 Experimental Methods

4.3.1 Reagents

Suwannee River Humic Acid (SRHA) was purchased from the International Humic Substances Society (IHSS; St. Paul MN) and used as received. Generally batches of SRHA are composed of 53% C(w/w), 9.13 meq/g-C of carboxylic groups, and 3.72 meq/g-C charge density of phenolic groups [194, 195]. Potassium bromide (Fisher Chemical; ACS grade) was used to set the concentration of bromide ion in chlorination experiments. Phosphate buffer adjusted with o-phosphoric acid (Fisher Chemical; 85%; ACS grade) was used to control pH in all experiments. All other reagents, including the CNTs used in this work and chemicals used in DBP formation experiments, have been described previously (see Section 2.3.1 and 3.3.1). All aqueous solutions and suspensions were prepared in deionized (DI) water using a Thermo Scientific Barnstead TII.

4.3.2 Chlorination experiments

Aqueous stock solutions of free chlorine (combination of HOCl and OCl⁻) and CNT suspensions were prepared as mentioned above (see Section 3.3.5). Immediately prior to use in chlorination experiments, CNT stock suspensions were sonicated for 5 min to re-disperse the CNTs and HOCl stock solutions were measured for free chlorine. Aqueous stock solutions of SRHA were prepared by dissolving as received standards of SRHA at 250 mg/L loading in a glass bottle covered with Al foil to omit light.

Chlorination experiments were conducted as described in Section 3.3.5, with the exception of added SRHA (2.5 mg/L) or bromide (up to 2.1 μM, which is equivalent to 167.8 μg-Br/L). For pH-dependent experiments, reactors were constructed with pH values ranging from 5–10 (± 0.02 pH units for the initial pH value) in a 5 mM phosphate buffer. At the end of each experiment, the system pH was once again measured, and we observed the pH to be stable within 0.1 pH units of pH 8 experiments. In chlorination experiments where we varied pH we noticed a change up to 0.5 units above and 0.4 units below the selected pH due to buffering limitation from phosphate.

4.3.3 Analytical methods

Samples from chlorination experiments were analyzed for concentrations of chlorine and THMs. No HAAs were looked at in this work due to complications with our analytical methods where some peaks corresponding to Br-HAA were unresolved. A sample (5 mL) for measurement of free chlorine was collected, transferred to a 250 mL volumetric flask and analyzed immediately using the colorimetric method described previously in Chapter 3. A sample (15 mL) for THM analysis was collected from the

remaining reactor volume and dechlorinated with sodium sulfite for all THMs.

Dechlorinated samples were then extracted immediately with pentane (see Section 3.3.5).

Prepared samples were stored at 0–1 °C for no more than two nights before being

analyzed on a gas chromatogram with an electron capture detector (GC-ECD). More

details on THMs analysis and sample preparation see Section 3.3.7.

4.3.4 CNT physical and chemical characterization

In systems with bromide, CNTs were characterized before and after chlorination

to examine for their physicochemical alteration. Surface chemical information was

obtained using X-ray photoelectron spectroscopy, quantifying (atomic %) the surface

species (C 1s, O 1s, N 1s, Br 3p, and Cl 2p) of CNTs before and after reaction.

Additional details about sample preparation and instrumentation for XPS analysis are

available in Section 2.3.5.3.

4.4 Results and Discussion

4.4.1 Effect of bromide on THM formation

Figure 4-1 illustrates THM speciation as a function of bromide (Br^-)

concentration during chlorination of different CNT suspensions. These plots are

complimented with Table 4-1 were the concentrations of THMs at selected Br^-

concentrations are provided for CNTs or SRHA. Generally, for CNT suspensions that

generated THMs, increasing the concentration of Br^- (at a fixed CNT loading) produced

a corresponding increase in total THM (TTHM; sum of the four THM concentrations for

CF, BDCM, DBCM and BF). This was observed for all CNT types considered except

non-functionalized CNTs (SWNF; Table 4-1 and Figure 4-1a), which generated very

little CF and no observable brominated THMs. Increases in total THM as a function of

Br$^-$ concentration have been reported for various model NOM precursors [196, 197], and

we also observed such behavior when chlorinating solutions of SRHA in the presence of

Br$^-$ (see Figure 4-1e).

TTHM concentration increased with increasing bromide ion concentration with

molar increases of TTHM ranging by a factor of 1.3 to 60.8. Figure 4-2 shows TTHM

versus Br$^-$ on a log-log scale. Included are slopes obtained from linear regression analysis

(where uncertainties represent one standard deviation). On a log-log scale, the slopes of

these lines represent the functional dependence of TTHM formation on Br$^-$ concentration

(see Equations 4-2 and 4-3) where a slope of unity would indicate a first-order

relationship (i.e., the case where a two-fold increase in Br$^-$ would result in a

corresponding two-fold increase in TTHM production).

$$[TTHM] \propto [Br^-]^x \qquad \text{Equation 4-2}$$

$$\log[TTHM] \propto x\log[Br^-] \qquad \text{Equation 4-3}$$

As previously noted, there is no dependence of TTHM on Br$^-$ for SWNF,

consistent with its slope statistically equivalent to zero. Accordingly, SWNF reactivity

with bromine will not be discussed in subsequent sections. For Br-THM producing

CNTs, SWCOOH showed the greatest dependency to Br$^-$ concentration. Conversely,

SWPEG showed the least dependency to Br$^-$ concentration. Moreover, the slope of

SWPABS was equivalent to that observed for SRHA. We propose that the similar

relationships for SWPABS and SRHA are indicative of a shared mechanisms for Br$^-$

incorporation into THMs in all systems. In contrast, the much greater dependence on Br$^-$

for TTHM production on SWCOOH systems suggests a different incorporation pathway. Perhaps this should be expected, as the polymer layer of SWPABS presents a wider variety of potential reactive centers for HOBr relative to an oxidized CNT surface.

Another noteworthy observation in Figure 4-1 is that as the concentration of Br^- increases, the yield of CF decreases. Concomitantly, the speciation of TTHM gradually shifted to favor mixed chlorobromo species and even fully brominated species (e.g., BF) in some instances at the highest Br^- concentrations explored. This shift in TTHM speciation is seen most clearly for SWPEG (Figure 4-1c), in which all four regulated THMs are observed at the highest Br^- concentration. In fact, unlike the behavior of other THM-generating CNTs (SWCOOH and SWPABS) and SRHA, formation of Cl-THMs decreased at high Br^- concentrations in CS PEG suspensions, presumably as these species further reacted to generate more brominated THMs.

Typically, the presence of bromide increases a system's chlorine demand, and this demand should scale with bromide concentration. For example, the chlorine demand of humic acid in the presence of bromide exhibits a positive relationship [187]. This is because Br^- can consume free chlorine through the reaction depicted in Equation 4-1, and subsequently the generated HOBr is more reactive towards organic compounds than HOCl [185-188, 198]. Also, Br^- can get used in oxidation reactions that do not involve incorporation of Br^- into organics [199].

Unexpectedly, the chlorine demand (Figure 4-3) did not scale with Br^- concentration for CNT suspensions, but rather remained constant across all Br^- concentrations considered. In some cases, this may be due to an excess of free chlorine,

where in the least reactive CNT suspensions (e.g., SWNF and SWCOOH) as little as 1%

of the initially available 15 mg-CL$_2$/L chlorine concentration was consumed over 4 hours.

However, SWPABS consumed more than 30% of the initial chlorine concentration yet

still exhibited chlorine demand that was independent of bromide concentration ($0.5 \times$

10^{-3} mg-Cl$_2$/μg-Br$^-$). For SWPABS formation of known and identifiable Br-THMs

accounts for only ~10% of the Br$^-$ available in the system, perhaps suggesting that the

difference in reactivity between HOBr and HOCl in this system is not significant.

4.4.2 Factors influencing bromine incorporation into THMs in CNT suspensions.

It is well known that the ratio of bromide-to-chlorine plays an important role in

bromine substitution during THM formation [5]. Because bromide is present at less than

1% the molar concentration of HOCl in our systems (as well as natural waters), bromide

gets oxidized quickly and completely during chlorination. It has been well documented

that free bromine (combination of HOBr and OBr$^-$) is primarily responsible for the

formation of Br-THMs [200] though other brominated oxidants, BrCl, Br$_2$, BrOCl, Br$_2$O,

could be forming during the chlorination of bromide [198, 201]. Therefore, the ratio of

initial bromide to chlorine consumed should give a reasonable approximation for the ratio

of bromide to chloride substitution. Gould et al. [202] proposed a dimensionless bromine

incorporation factor (BIF):

$$BIF = \frac{C_{BDCM} + 2C_{DBCM} + 3C_{BF}}{C_{TTHM}} \qquad \text{Equation 4-4}$$

where C is the concentration in molarity of each Br-THM (in the numerator) and total

THMs (in the denominator). This factor has been adopted by other researchers [185, 197,

203] to assess bromine substitution in THM speciation. A theoretical maximum value for BIF is 3 for the case where the only THM present in the system is BF.

Figure 4-4 shows that the BIF as a function of Br^- concentration for THMs produced from four different CNT types. Data for chlorination of SRHA is provided for comparison. Because the initial chlorine dose was the same in all systems, the results in Figure 4-4 can be interpreted to represent bromide-to-chlorine ratios as well as bromide to carbon precursor ratios. For all CNTs except SWNF (which did not produce any Br-THMs) BIF increased nearly linearly with increasing Br^- concentration. Such relationships are consistent with results for more traditional DBP precursors including organic matter from natural waters (from Manitoba and Oklahoma with measured TOCs of 8.5 and 5.3 mg/L, respectively) or commercially available humic acid [5, 197, 200], for which it is commonly observed that bromine incorporation into THM increases at higher bromide concentration.

Notably, the relative trend in BIF for Br-THM producing CNTs (i.e., SWCOOH > SWPEG > SWPABS = SRHA at a given bromide concentration) is inverse to the trend in TTHM production reported in Figure 4-2. Thus, SWCOOH and SWPEG, despite their low chlorine demand, are most efficient at integrating bromide into their byproducts relative to SWPABS (or SRHA). Accordingly, this may imply a unique role for the CNT surface, and reactive sites thereon, in helping to promote bromine incorporation into THM. In contrast, the lower BIF on SWPABS could be related to the presence of labile N-containing functionalities on its surface because such species may react with HOBr (or other brominated oxidants) rather than allow them to react at other sites that may yield Br-THMs.

There is the potential for several system variables to influence BIF in CNT suspensions. For example, Figure 4-5 illustrates the influence of CNT mass loading (at a fixed initial chlorine concentration of 15 mg/L) on the BIF for THM-producing CNTs. Data are shown as a function of bromide concentration. We note that results for SWNF are not provided as they did not generate any measureable Br-THMs across the CNT mass loadings investigated (5–20 mg/L).

Different behavior was observed across CNT types. For SWPABS (Figure 4-5c), BIF decreased with increasing CNT loading. This trend has been reported before for natural riverine NOM [203]. This decrease in BIF for SWPABS is most likely attributable to the presence of N-containing functionalities on its surface, which will be highly reactive toward HOBr (and any other brominated oxidants). As SWPABS loading is increased at a fixed HOCl concentration, there is greater probability for these N-containing surface sites to react with and consume HOBr. However, this reaction would be unlikely to yield Br-THM because their production requires a carbon-based reaction center. Consequently, this preferential consumption of HOBr at surface sites unable to yield Br-THMs lowers the BIF for the SWPABS system at higher mass loadings.

Unlike SWPABS, BIF values for SWCOOH and SWPEG exhibited a much weaker dependence on CNT concentration, with at most a slight decrease between the lowest (5 mg/L) and highest (30 mg/L) suspension loadings. This behavior suggests that THM speciation for SWCOOH and SWPEG is essentially independent of chlorine demand in these systems (which will increase at higher CNT solid loadings). We believe this is consistent with a CNT surface consisting of relatively uniform reactive sites with respect to their reactivity toward free chlorine and bromine, as might be expected for

SWCOOH and SWPEG surfaces consisting primarily of carbon and oxygen centers. We note that none of the CNT systems exhibited trends in BIF diagnostic of surface site limitation. In this scenario, which has been reported previously for other THM precursors (i.e., humic acid) [197], the BIF increases with precursor loading due to limited but highly reactive sites toward free bromine.

Given the more complex reactivity of the SWPABS surface, additional work attempted to identify the conditions most favorable for Br-THM formation. Figure 4-6 reveals how BIF values change as a function of CNT loading, initial HOCl concentration, and reaction time in SWPABS suspensions. Data essentially represent a composite BIF across a range of Br^- concentrations, obtained from the slope of BIF versus Br^- concentration plots (like those in Figure 4-5). In all cases slopes which were determined via linear regression analysis (lowest $R^2 = 0.997$; $p < 0.001$), and uncertainty represents one standard deviation for the regression analysis.

Figure 4-6 shows the decreasing trend between BIF and SWPABS loading observed in Figure 4-5. Furthermore, similar decreasing trends in BIF are also observed with increasing initial HOCl concentration (Figure 4-6b) and with overall reaction time (Figure 4-6c; note all BIF values presented thus far were calculated after 4 h). The decline in BIF with increasing initial HOCl is attributable to a smaller fraction of available oxidant in the system being present as HOBr. As expected, therefore, Cl-THM predominate under conditions where HOCl, rather than HOBr, is the primary oxidant due to its greater abundance. The decrease in BIF over longer reaction times is consistent with reports with natural waters [197]. In this case, the slow acting HOCl will have more

time to react meanwhile the limited HOBr is exhausting, hence chlorinated products will increase with increasing time.

4.4.3 Influence of bromination on CNT physical and chemical properties.

CNTs exposed to chlorine and Br⁻ under our environmentally relevant experimental conditions may influence the composition of the CNT surface, as well as the stability of CNTs in suspension. Through the use of XPS, we examined the surface chemistry of SWNF and SWCOOH both with and without chlorination. For those CNTs reacted with free chlorine, experiments were conducted both in the presence and absence of 168 µg/L of Br⁻. This is similar to the XPS analysis conducted in Chapter 2 with N-CNTs.

For reacted samples, chlorine was detected at trace levels (~0.1 at%) on the surface of SWNF and SWCOOH after reaction. However, in no instance was surface bromine ever detected on the surface of reacted CNTs. Other changes to the surface chemistry were observed as a result of Br⁻. For example, chlorination experiments conducted in the presence of Br⁻ resulted in a greater increase (by 1.1 at%) in the surface oxygen content on SWNF than was observed for reactions conducted without Br⁻. This is consistent with HOBr being a more reactive oxidant than HOCl.

4.4.4 Effect of pH

Thus far we have reported DBP formation from chlorination of CNTs at pH 8, but we expect CNT reactivity toward free chlorine to vary as a function of pH value due to the speciation of HOCl ($pK_a = 7.58$ at 20 °C). Figure 4-7 illustrates CF formation as

function of pH for all THM-producing CNTs. We note that SWNF was unable to produce detectable CF concentrations (>0.5 µg/L) across all pH values considered.

Increasing the pH from 6 to 10 enhanced the CF yields by nearly 9-fold for SWCOOH, 3-fold for SWPABS, and 1.5-fold for SWPEG. We believe that all increases in CF formation observed across this pH range are attributable to pH-dependent steps in the mechanism of CF production, rather than changes in the surface chemistry or suspension stability of the CNTs. For example, it is well known that SWCOOH is susceptible to changes in its surface charge, suspension stability [204, 205] and optical properties [204] due to protonation or deprotonation at low and high pH respectively. However, at pH values above 5 all surface sites should be deprotonated based upon reported values for the point zero charge (pH_{pzc}) for SWCOOH [89, 92]. Likewise, there should be no changes in the nature of ionizable groups on SWPABs from pH 6-10; the predicted pK_a for aminobenzene sulfonic acid (using ChemAxom [206]) are consistent with fully deprotonated sulfonate ($pK_a = -2$) and amino groups ($pK_a = 3.27$) across this range. Finally, we emphasize that this pH-dependent trend of increasing THM formation with increasing pH is analogous to findings with NOM [178, 190, 191].

Figure 4-7b shows the chlorine demand of CNTs across the pH range from 6 to 10, with a slight maximum in all cases at circumneutral pH (between 7 and 8). For the most part, however, the chlorine demand for THM producing CNTs was relatively constant across the pH range. The consistency of the chlorine demand across pH, contrasted by the increase in CF formation with rising pH, suggest other chlorinated byproducts are likely produced at lower pH values that have yet to be identified, particularly for SWPABs.

We observed the dispersion of SWCOOH in bromide containing water decrease with increasing pH after the reaction with chlorine took place. Typically carboxylated CNTs at pH higher than 4 (above the pH_{pzc}) would increase in suspension stability. However due to reactions with halogenated oxidants, this trend was reversed, which could signify a change in its pH_{pzc} and a concomitant change in surface chemistry.

4.4.5 Effect of NOM on THM formation

As a final consideration, Figure 4-8a and 4-8b show the formation of CF and change in chlorine concentration, respectively, as a function of time for mixtures of various CNTs and 2.5 mg/L of SRHA (CNT/SRHA). Data for a system of 2.5 mg/L SRHA in the absence of CNT are provided for comparison. The most active system with respect to chlorine demand and CF formation was the mixture of SWPABS and SRHA, which after 48 h resulted in nearly 300 μg/L of CF production and almost complete consumption of HOCl. For CF formation, most other CNT and SRHA mixtures clustered around 100 μg/L over this same timescale. Perhaps most notably from Figure 4-8 is the efficiency with which CF is generated during chlorination of SRHA, which exhibited a relatively small free chlorine demand relative to the CNT/SRHA mixtures.

A goal of these experiments with SRHA mixtures was to observe if any synergies in CF production occurred in the presence of functionalized CNTs. Figure 4-9 shows plots of CF formation as a function of the product of chlorine concentration and contact time (CT), which was calculated by taking the area under the chlorine kinetics curve, for all for CNT types considered herein. In Figure 4-9, data are presented for CF production in CNT suspensions (without SRHA), SRHA solutions (without CNTs) and mixtures of

CNTs and SRHA. In addition, curves in Figure 4-9 represent anticipated CF formation calculated from the sum of CF formation measured in CNTs and SRHA alone.

Many types of CNTs represent sorbents for NOM, and these interactions could exhibit a range of influence on CF formation during chlorination. One scenario is that CNTs will limit DBP formation by limiting NOM availability in solution and lowering reactivity toward chlorine. This inhibitory scenario appears to be at play for non-functionalized CNTs (Figure 4-9a), where CF formation in the SWNF and SRHA mixtures is less than the sum anticipated from experiments with each mixture component in isolation. However, for all other CNTs, CF formation in SRHA mixtures appears to be additive, without any synergistic or inhibitory effects.

Figure 4-10 helps to further highlight the inhibitory effect on CF production in SRHA mixtures for SWNF suspensions. Figure 4-10 presents log-log plots for CF formation as a function of CT for SWCOOH (Figure 4-10a) and SWNF (Figure 4-10b) systems. CF formation data are presented for CNT and SRHA mixtures (CNT/SRHA), SRHA solutions, and the calculated additive results anticipated from formation in isolated CNT and SRHA (CNT + SRHA) experiments. Figure 4-10a, no distinction of CF formation was made between SWCOOH/SRHA systems and the additive results based upon CF formation for each of the mixtures components. This additive behavior for SWCOOH suggests it interacts minimally with SRHA, presumably due to the repulsive forces from the negatively charged carboxylate groups on the CNT surface and deprotonated functional groups on the SRHA at this pH.

In contrast, data in Figure 4-10b for SWNF/SRHA mixtures deviate significantly from CF formation expected through addition of each component. Specifically, the slopes of the two lines and their non-overlapping standard error suggest distinct formation mechanisms in each system. SWNF represents the most hydrophobic form of CNT explored herein. Its hydrophobicity, and lack of charged surface sites, make it most likely to sorb SRHA. This uptake thereby limits SRHA availability in solution, and in turn inhibits CF production.

4.4.6 Environmental implications of bromide, pH, and NOM on DBP formation

The bromide concentrations tested here are representative of natural aquatic matrixes (100 µg/L on average [4, 185]). We showed the role of bromide incorporation (expressed as BIF) into THMs depended on the mass loading, chlorine concentration, and reaction time where generally decreasing any of the three increased the BIF. Oxidized CNTs exhibited the highest BIF of all the CNTs tested here while PABS functionalized, the most reactive CNT towards chlorine, showed characteristics identical to NOM in the presence of bromide with matching BIF.

The value of data in Figure 4-6 is that it allow us to extrapolate to our results to other systems, particularly to identify those conditions in water treatment most likely to favor the formation of more toxic Br-THMs. In fact, to predict BIF in other, related systems, prior studies have used power regression analysis, like that shown in Figure 4-6, to develop an empirical model [64, 203]. We would expect the greatest degree of Br^- THM formation at low CNT solution concentrations, low initial HOCl concentrations, and shorter reaction times. Unfortunately, these conditions imply a high likelihood of Br^-

THM formation in water and wastewater treatment systems, in which CNT loadings will be quite low (sub µg/L at most), free chlorine concentrations will be typically <10 mg/L, and retention times generally <10 h.

The pH effect on SWPABS and SWCOOH as precursors to THMs was similar to what is observed for NOM where an increase in pH increases the THM formation. However, to reach regulatory MCL, polymer functionalized and oxidized CNTs must be present at high loadings (>10 mg/L CNTs, for 200 µg/L of bromide and pH 8). Though these concentrations are unattainable in typical engineered water systems were the expected concentration is in the sub to low ng/L levels [77, 78], their implementation as materials during or post chlorination could yield DBPs at levels of concern, and hence could have negative implications to the quality of the product water. In additions, their reactivity towards chlorine peaked at around pH 8, a typical pH value found during disinfection [55].

NOM is present in environmental waters at varying concentrations (ranging 1–50 mg/L [207]) based on the type and source of the water. Hence, the interaction between CNTs and NOM is important to predict when controlling DBPs. CNT interaction with NOM showed to have additive effect to the reactivity with chlorine and the CF formation potential with the exception of SWNF which showed reductive contribution to the formation of CF. However, knowing that SWNF can oxidize during chlorination (see Chapter 3), its presence in disinfection would be problematic during chlorination where in time its behavior is more representative of carboxylated CNTs. Finally, our work is another illustration of how functionalized CNTs can mimic the reactivity of NOM. Ultimately, with the extensive degree and range of surface groups added via

functionalization, CNTs can be effectively transformed into an analog of natural organic

carbon.

Table 4-1: Concentrations of THMs generated during chlorination of CNTs or SRHA in the presence of bromide. Values are plotted in Figure 4-1.

THM (µg/L)	CF	BDCM	DBCM	BF
CNT	134 µg/L (1.68 µM) Br⁻			
SWCOOH	0.4	0.5	1.9	0.6
SWNF	0.8	0	0	0
SWPABS	27.7	13.3	7.1	0.8
SWPEG	2.3	3.6	4.6	1.3
SRHA	44.9	31.3	11.9	0.6
	67 µg/L (0.84 µM) Br⁻			
SWCOOH	0.5	0.5	1.1	0.2
SWNF	0.5	0	0	0
SWPABS	33.7	8.1	2.5	0.1
SWPEG	4.6	3.7	2.7	0.5
SRHA	49.5	15.4	2.5	0
	0 µg/L (0 µM) Br⁻			
SWCOOH	0.8	0	0	0
SWNF	0.5	0	0	0
SWPABS	32.6	0.2	0	0
SWPEG	7.1	0.2	0	0
SRHA	55.2	0.3	0	0
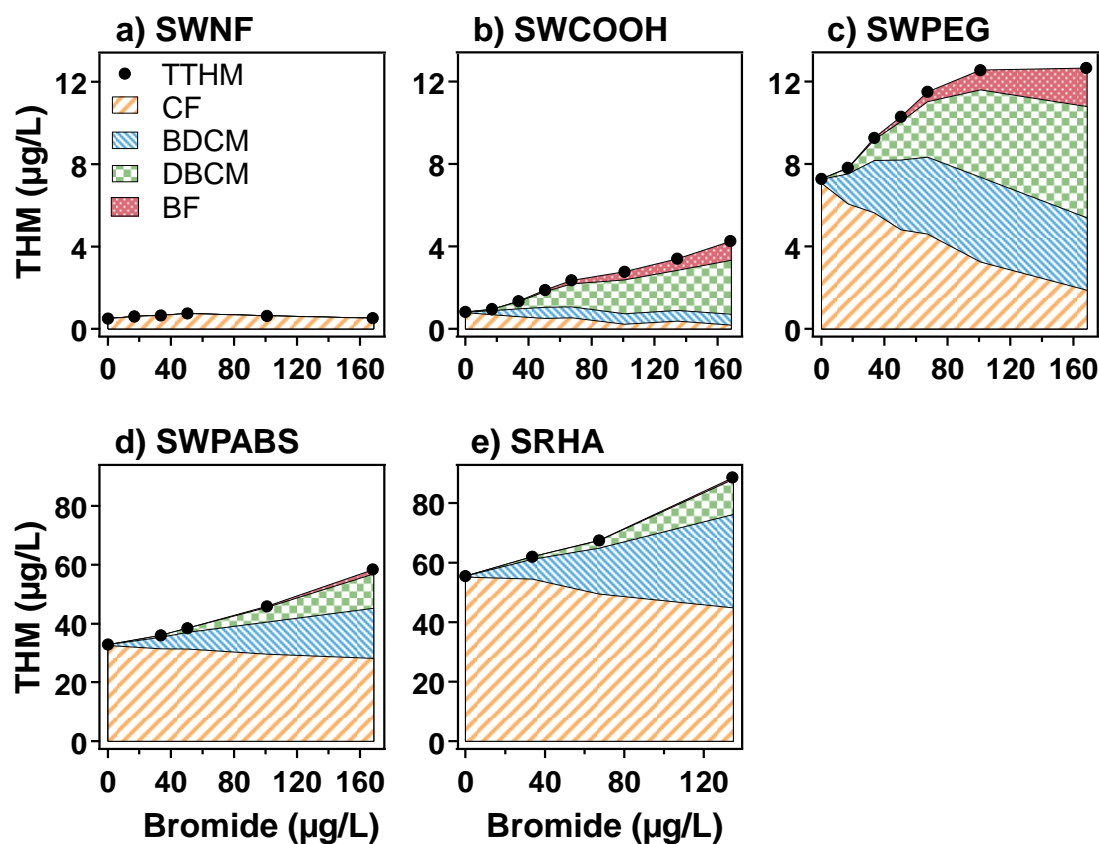
Figure 4-1: Speciation of THM formation during chlorination of (a) SWNF, (b) SWCOOH, (c) SWPEG, (d) SWPABS, and (e) SRHA versus bromide ion concentration. Experimental conditions: 10 mg/L CNT or 2.5 mg/L SRHA, 15 mg-Cl_2/L HOCl, pH 8, 4 h reaction, and 0–168 µg/L bromide. These are representative results from duplicate experiments.
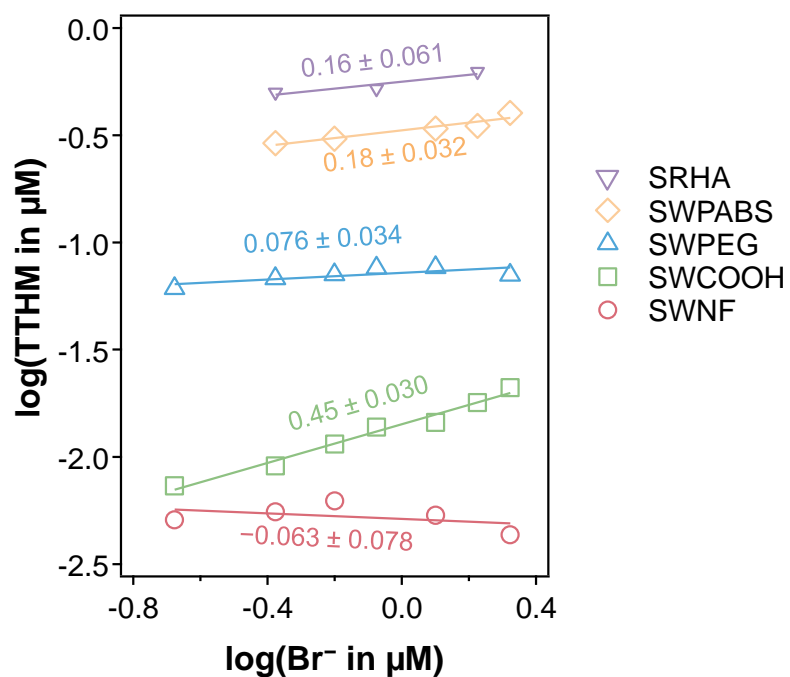
Figure 4-2: Formation of total THMs (TTHM; in μM) as a function of Br⁻ (in μM) on a log-log scale. Experimental conditions: 10 mg/L CNT or 2.5 mg/L SRHA, 15 mg-Cl$_2$/L HOCl, pH 8, 4 h reaction, and 0–168 μg/L Br⁻. Slopes and standard deviations are shown from linear regression analysis.
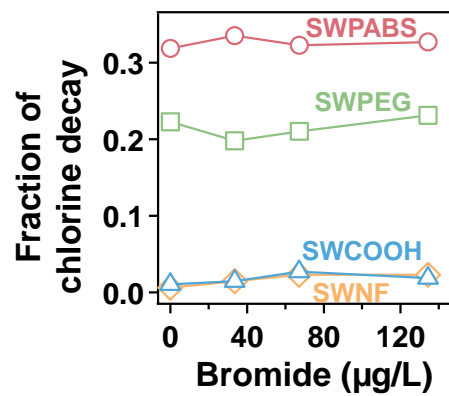
Figure 4-3: Fraction of chlorine loss versus bromide concentration. Experimental conditions: 10 mg/L CNT or 2.5 mg/L SRHA, 15 mg-Cl$_2$/L HOCl, pH 8, 4 h reaction, and 0–168 µg/L bromide. These are representative results from duplicate experiments.
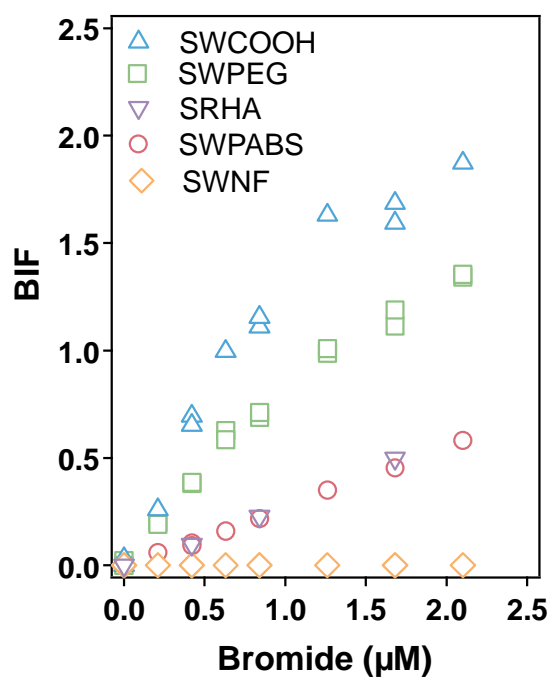
Figure 4-4: Bromine incorporation factor (BIF) versus bromide ion concentration during chlorination of all four types of CNTs and humic acid (SRHA). Experimental conditions: 10 mg/L CNT, 15 mg/L HOCl, pH 8, 4 h reaction, and 0–168 µg/L bromide. BIF describes the distribution of the four THM compounds (see Equation 2) with values ranging from 0 (all chloroform) to 3 (all bromoform).
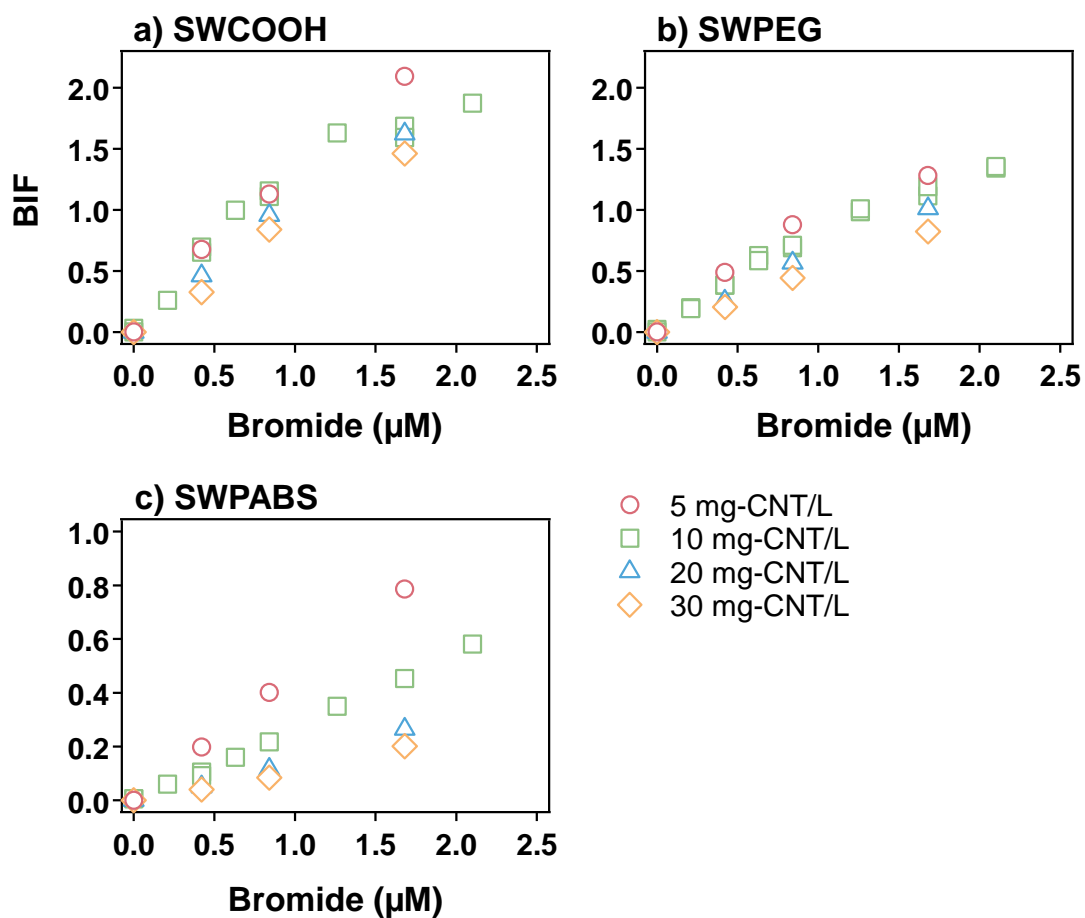
Figure 4-5: CNT loading effect on the BIF versus bromide ion concentration during chlorination of (a) SWCOOH, (b) SWPEG, and (c) SWPABS. Experimental conditions: 5–30 mg/L CNT, 15 mg/L HOCl, pH 8, 4 h reaction, and 0–168 µg/L Br$^-$.
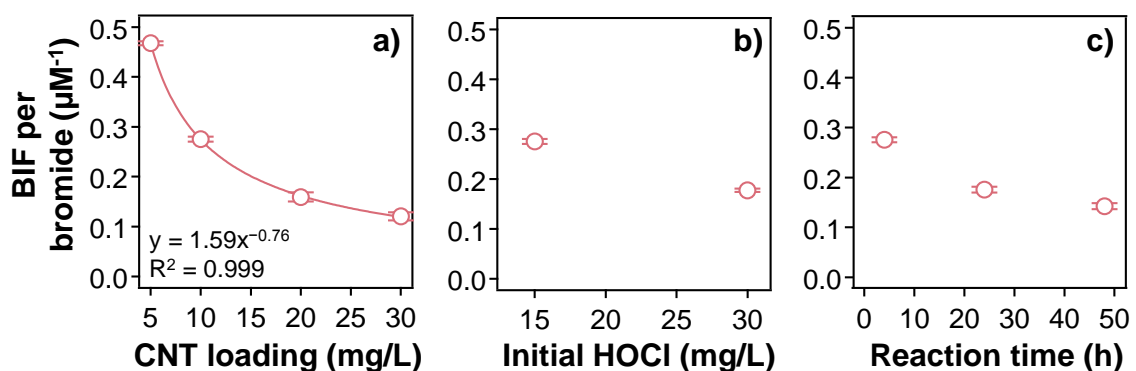
Figure 4-6: BIF per bromide ion concentration (μM^{-1}) of SWPABS versus (a) CNT loading, (b) initial HOCl, and (c) reaction time. Experimental conditions: 10 mg/L SWPABS, 15 or 30 mg-Cl$_2$/L HOCl, pH 8, 4–48 h reaction, and 0–168 µg/L bromide. BIF per bromide was determined by the slope of a linear regression of BIF versus bromide ion concentration relationship (see Figure 4-4 and 4-5). Error bars are standard error from linear regressions of at least 5 observations.
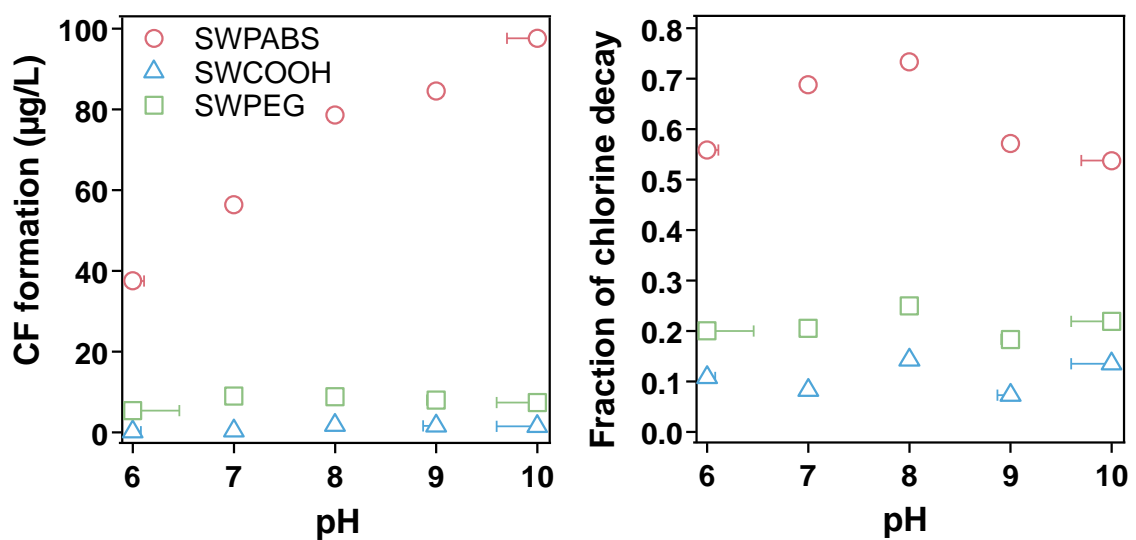
Figure 4-7: Effect of pH on (a) CF formation and (b) fraction of chlorine decay during chlorination of all four types of CNTs. Experimental conditions: 10 mg/L CNT, 15 mg/L HOCl, pH 6–10, and 4 reaction period. Error bars represent pH shift where the end cap was the pH at the end of the experiment.
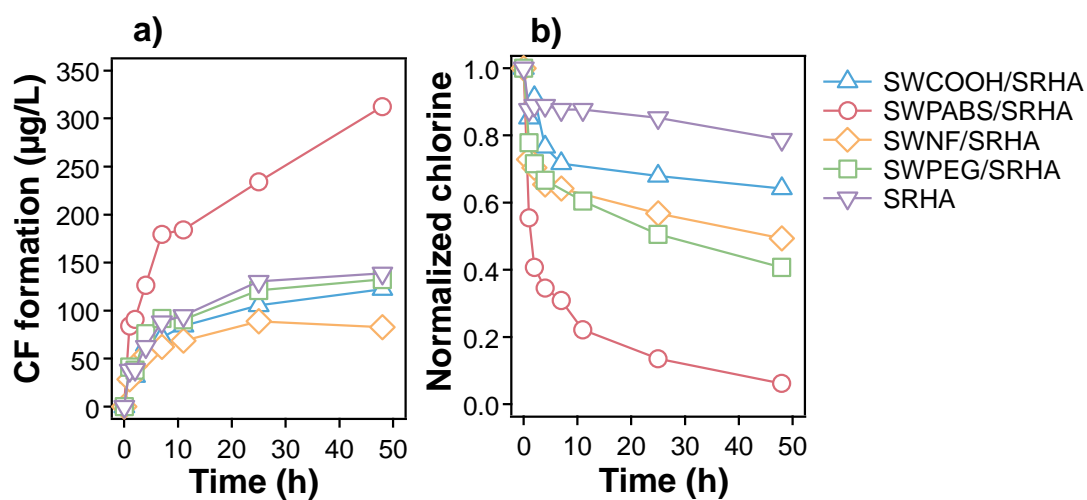
Figure 4-8: Effect of NOM as humic acid from the Suwannee River (SRHA) on (a) CF formation and (b) chlorine decay during chlorination of all four types of CNTs. Experimental conditions: 10 mg/L CNT, 2.5 mg/L SRHA, 15 mg/L initial HOCl, pH 8, 0–48 h reaction period.
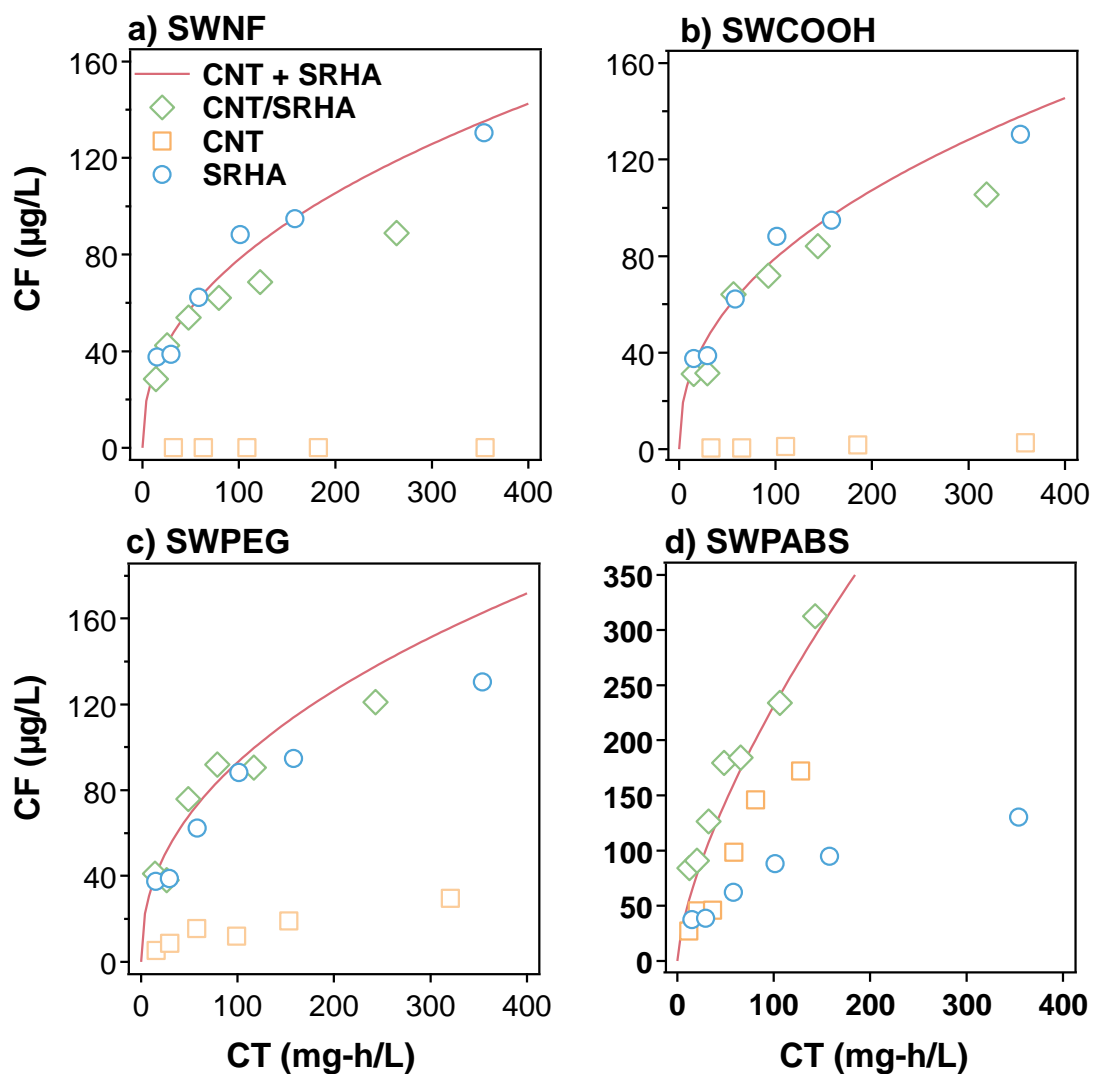
Figure 4-9: CF formation versus CT during chlorination of (a) SWNF, (b) SWCOOH, (c) SWPEG, and (d) SWPABS in the presence of SRHA plotted versus the added CF formation of independent experiments with CNTs or SRHA (CNT + SRHA). Experimental conditions: 10 mg/L CNT, 2.5 mg/L SRHA, 15 mg/L initial HOCl, pH 8, 0–48 h reaction period. Added results were calculated by summing the linear regression on a log-log scale plot of the separate components and interpolating across the experimental range of CT values.
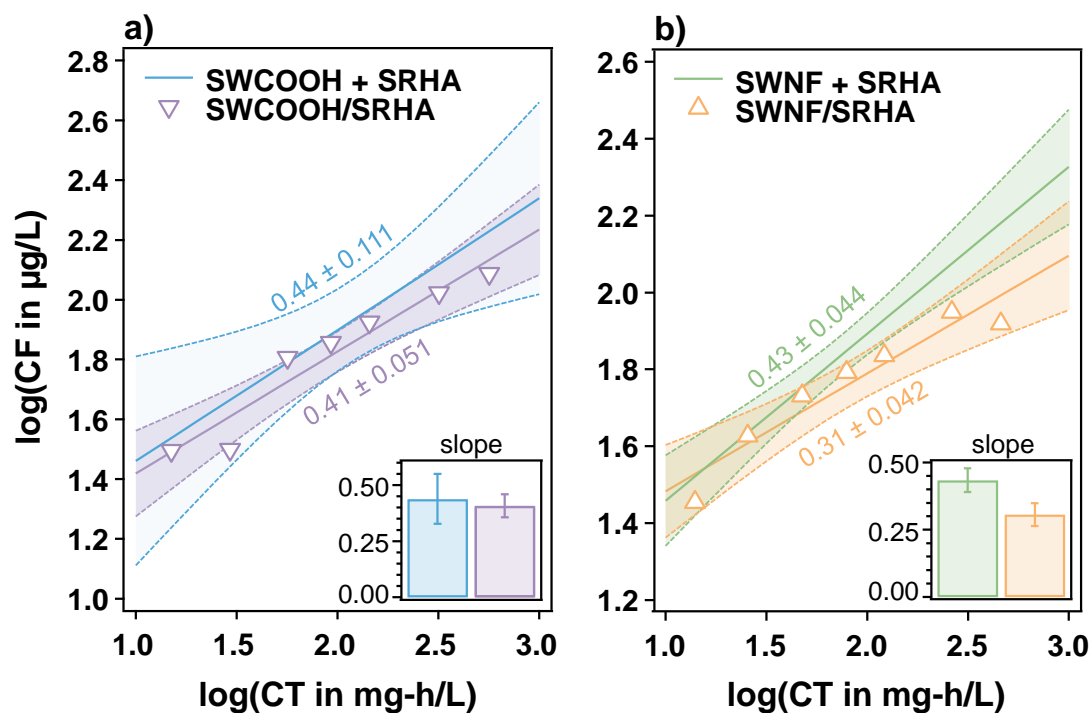
Figure 4-10: Log-log plot of CF formation versus CT during chlorination of (a) SWCOOH and (b) SWNF in the presence of SRHA plotted versus the added CF formation of independent experiments with CNTs or SRHA (CNT + SRHA). Experimental conditions: 10 mg/L CNT, 2.5 mg/L SRHA, 15 mg/L initial HOCl, pH 8, 0–48 h reaction period. Shown are slopes of their linear regressions plus or minus its standard error.

CHAPTER 5: CONCLUSIONS

Undoubtedly, nanotechnology and nanoscience will help advance society, but we must make it a priority to ensure that such development is sustainable. While there has been considerable focus on environmental implications of nanomaterials, work has revolved predominantly around human toxicology (focusing on workplace exposure) [208], environmental transport [209, 210], and ecosystem impact [211]. Little work has yet to be done to consider the implications for reactivity of nanomaterials in engineered water systems. These implications include their ability to produce hazardous byproducts and the reactive transformations that change the physicochemical properties of nanomaterials in ways that alter, and perhaps even magnify, their adverse impacts.

This work was motivated by these gaps, and by the growing realization that several carbonaceous nanomaterials like carbon nanotubes, particularly those with surface functional groups, resemble natural organic matter (NOM). Accordingly, we expect them to exhibit reactivity in natural and engineered systems similar to NOM. Indeed, several studies have shown CNTs functioning, like NOM, as sorbents for organics [100, 116, 117, 212], complexation agents for metals [88, 116, 213], and promoters of reactive oxygen species upon irradiation with sunlight [214-216] or exposure to ozone [81, 217]. This work explored the potential for CNTs to generate hazardous byproducts during chemical disinfection.

Collectively, this work provides a more comprehensive understanding of the environmental implications of engineered nanomaterials. For CNTs, insights are developed regarding their role in disinfection, spanning from their potential role as a

source for known DBPs as a byproduct of their manufacturing to their role as DBP precursors during reactions occurring on CNT surfaces. Answering such questions related to the role of CNTs as potential sources or precursors for DBPs has practical consequences for water treatment systems that use CNTs in next-generation membranes or sensing, or that have to treat water contaminated with CNTs from industrial waste or inadvertent leaching/release.

Each research chapter illustrates a new, previously unrecognized contribution to our understanding of the role of CNTs in disinfection water processes. Briefly, Chapter 2 identifies nitrogen-functionalized CNTs as sources and precursors of N-nitrosodimethyamine. Chapter 3 highlights the ability of CNTs, especially those functionalized with polymers and oxygen containing moieties, to serve as precursors to trihalomethanes (THMs), haloacetic acids (HAAs), and a host of other DBPs. Chapter 4 shows that DBP formation by CNTs is influenced by water quality, most notably generating brominated-DBPs in the presence of bromide, as would be expected from established trends for DBP formation from NOM. In addition, Chapters 1 and 2 showed that CNTs undergo surface chemical alterations due to chemical oxidation that could be linked to changes in environmental mobility and toxicity. A more detailed outline of these findings is shown below.

Outcomes of this work should assist decision-making regarding potential regulations for CNTs as next-generation pollutant classes. Further, results herein should help ensure the safe and sustainable application of CNTs in water treatment, while also helping to better anticipate challenges associated with nanomaterial-containing waste streams. We also develop some insights as to what properties of CNTs are most

responsible for DBP formation, which may help to guide the fabrication of more environmentally responsible nanomaterials for future applications. Of course, as with most research, some results led to additional questions and new hypotheses that merit further consideration, some of which is discussed in greater detail below.

5.1 Release and formation of NDMA from N-CNTs

The unique contribution of Chapter 2 is the release of N-nitrosodimethylamine (NDMA) from suspensions of N-functionalized CNTs (N-CNTs), in addition to their ability to generate NDMA upon reaction with free chlorine and other chemical disinfectants (e.g., chloramines and ozone). Therefore, N-CNTs are not only a precursor, but also a source of NDMA. This work was conducted with a suite of N-CNTs containing amine, amide, and polymeric functional groups. In all cases, the release of NDMA upon their dispersion into bulk water was rapid, although the extent of release varied across different CNT types (i.e., functionalization approaches) and batches from the same vendor. We posit that the NDMA is a byproduct of functionalization routes used to introduce N to the CNT surface, existing on commercial powders as a dry and highly soluble residue (consistent with its instantaneous release). The formation of NDMA during chlorination, chloramination, and ozonation was generally at low levels (ng of NDMA per mg CNT) in all cases. These findings represent the first observation of DBPs generated from the chemical processing of CNTs, and will ultimately help to better predict the adverse implications of N-CNTs in engineered treatment systems.

The key outcomes of Chapter 2 relate to generalizable trends about NDMA formation potential of different types of N-CNTs, results that may help to guide the more sustainable development and application of such nanomaterials. For example, the

formation of NDMA from chlorination or ozonation of amine-functionalized CNTs was significantly higher than that from chlorination or ozonation of amide- or polymer-functionalized CNTs (although we note that this was not the case for chloramination). In fact, the magnitude of the increase of NDMA formation from N-CNTs did not scale with surface N concentration (from XPS), implying that the chemical nature of the functional group was more important than the availability of surface N.

For the release of NDMA from commercial N-CNT powders, the extent of residual NDMA from the synthesis process appears to be strongly dependent on functionalization procedure and whether any subsequent purification (e.g., washing) is conducted prior to commercial distribution. In fact, we showed that 2 ng of NDMA per mg of CNT formed from a functionalization procedure using ethylenediamine and a coupling reagent. However, due to insufficient details in the procedures published by manufacturers, we are unable to determine a solution to controlling the release of NDMA. Hence, additional work is needed to fully understand the factors controlling the extent of NDMA formation during N-CNT manufacturing.

Finally, it must be recognized that in addition to the production of NDMA as a byproduct of N-CNT oxidation, another non-traditional disinfection byproduct is the reacted N-CNT. Reaction with free chlorine not only results in surface oxygen, but also decreases the amount of surface N available while resulting in oxidized forms of surface chlorine (presumably a species analogous to a surface chloramine). This transformation generally results in greater environment mobility of N-CNTs after chemical disinfection. Despite the presence of surface chlorine, it does not appear that chlorination enhances the acute toxicity N-CNTs based upon the results of a standard *E. coli* bioassay.

From the work in Chapter 2, it is evident that N-CNTs can generate nitrogenous disinfection byproducts such as nitrosamines (e.g., NDMA), as well as other species that were not specifically explored. Given that all forms of N-containing surface groups generated NDMA, even when their solution phase analogs were not viable precursors, it is likely that most commercially available N-CNTs should be viewed as a probable NDMA precursor. More practically, empirical relationships presented in Chapter 2 that relate NDMA yields to oxidant type and initial oxidant concentration, CNT loading, surface functionality, N content of N-CNT, and N-CNT type will be useful in helping predict the ability of N-CNTs to release and produce NDMA in water treatment. Lastly, the work in Chapter 2 serves as a reminder of how environmental processing of nanomaterials can alter their fate and effects. For other engineered nanomaterials, a priority should be placed on examining transformations and changes in surface chemistry resulting from the relatively extreme oxidizing environment of chemical disinfection systems.

5.2 Halogenated DBP formation from chlorination of CNTs

A limitation with the work in Chapter 2 is that it only focused on NDMA production during N-CNT reaction with chemical disinfectants. It remained unclear whether other DBPs could be generated during chlorination not only of N-CNTs, but also of other forms of commercially available CNTs. To fill these voids, Chapter 3 examined the formation of trihalomethanes (THMs) and haloacetic acids (HAAs), as well as some emerging halogenated DBPs, during chlorination of various CNTs with a spectrum of surface chemistry.

Results in Chapter 3 demonstrated that non-functionalized CNTs generally do not produce DBPs. Rather, the chlorine demand they exhibit results primarily in the oxidation of the CNT surface. This is evidenced by the increase in surface oxygen (from XPS) on these CNTs after chlorination. Unlike work in Chapter 2, there was no evidence of surface chlorine after the reaction of these non-functionalized CNTs, and we presume the prominent soluble byproduct is chloride. Thus, non-functionalized CNTs do not pose a concern as a DBP precursor, although they are not a form of CNT widely utilized in commercial products.

In contrast, the presence of surface oxides results in the formation of DBPs during CNT chlorination. Most prominent is the formation of haloacetic acids, which we presume form readily from the surface carboxyl groups most commonly present on the surface of CNTs oxidized via reaction with strong acid. We also found that the method used to oxidize CNTs can influence DBP formation. In particular, extensive chlorination or ozonation leads to oxidized CNTs that produce greater THM and HAA yields, even relative to CNTs oxidized via other methods (e.g., nitric acid) that have the same concentration of surface oxygen. This observation has implications for CNT manufacturing, as some have suggested extended ozonation as an alternative to acid functionalization for bulk scale CNT production. It also helps to better anticipate the fate of CNTs used in water treatment applications (e.g., CNT-enabled membranes), which may become more prone to DBP formation over extended exposure to certain chemical disinfectants used upstream or in tandem with the application. Therefore, findings in Chapter 3 provide guidance as to how CNTs should be deployed during treatment,

suggesting that they should be applied at a point in the treatment train where exposure to chemical disinfectants is minimized.

Findings in Chapter 3, taken together with results from Chapter 2, suggest that polymer-coated CNTs present the biggest risk as a DBP precursor. CNTs coated with PABS and PEG, which are gaining popularity in various applications, generate chloroform (CF), dichloroacetic acid (DCAA), and trichloroacetic acid (TCAA) at levels of concern under chlorine contact times (CT value) representative of water treatment processes. A noteworthy result is that PEGylated CNTs represent effective DBP precursors (generating 2.5 µg/mg of CF and total HAAs per mg) even though several forms of commercially available PEG, in the absence of the CNT support, are unable to generate DBPs. This result highlights the unique reactivity of polymer-functionalized CNTs, suggesting they pose as surface sites suitable for DBP formation that are distinct from those available in either PEG or CNTs alone. PEGylated CNTs, therefore, represent a case where the whole is indeed greater than the sum of its parts.

A final outcome from Chapter 3 was the discovery of other forms of emerging DBPs generated during CNT chlorination. Evidence of several other DBPs is noticeable in the ECD chromatograms of pentane extracts taken from chlorine reaction samples. Though not all DBPs were identified and quantified, their detection by GC-ECD implies the presence of volatile halogenated (chlorinated) compounds. Several lines of evidence (including matching retention times with an analytical standard) strongly suggest that one of these products is chloropicrin (trichloronitromethane), a lung damaging agent. The identification of chloropicrin was somewhat unexpected, particularly for oxidized CNTs

(forming ~23 μg/mg-CNT of chloropicrin), because it is a halonitroalkane. We propose that oxidation of CNTs with nitric acid must leave behind some residual N-containing groups on the oxidized CNT surface that contribute to the formation of nitrogenous DBPs (N-DBPs). Alternatively, we cannot rule out that a source of N in these oxidized CNT systems is N_2 from the atmosphere, as has been proposed in previous studies about nitrogenous DBP formation on activated carbon. More work is certainly needed to explore this phenomenon, and to identify other DBP classes that may be generated during CNT chlorination. Thus, Chapter 3 should be viewed as only the beginning of what could be a plethora of byproducts generated from CNTs during chemical disinfection processes.

5.3 Influence of natural aquatic variables on the formation of DBPs from CNT precursors

The major take away from results in Chapter 4 is that functionalized CNTs are, in most ways, analogous to NOM with respect to DBP formation. Specifically, Chapter 4 explored how natural aquatic variables including pH and bromide concentration, which are known to affect DBP formation in natural waters, influence DBP formation in functionalized CNT suspensions. In addition, it explored how the interplay of suspended CNTs and soluble organic matter, in the form of humic acid, impacts DBP production. Thus, relative to work in the previous Chapters, this work explicitly explored DBP formation potential of CNT precursors under *environmentally relevant* water matrices.

Work in Chapter 4 convincingly shows that DBP formation observed in relatively simple water matrices will be amplified by more relevant natural aquatic conditions. Our results showed that DBP production trends as a function of pH and bromide concentration matched expectations from trends observed for NOM and model precursors

for NOM. For example, the magnitude of THM formation increased in the presence of bromide. Additionally, CF formation increased with increasing pH, whereas DCAA and TCAA formation exhibited the opposite trend with increasing pH. We note that general trends in CNT reactivity in Chapter 4 are consistent with those developed in Chapters 2 and 3. Once again, polymer functionalized CNTs are most reactive in these more complex aquatic systems, followed by oxidized and N-containing CNTs.

The value of these observations is two-fold. First, it suggests that the reactivity of CNTs during chlorination can be anticipated from the well-established behavior of NOM during chlorination. Second, we conclude that fundamental insights regarding CNT reactivity developed in Chapters 2 and 3 can be reasonably extended to these more complex, environmentally relevant conditions. For THMs, as an example, results imply that their greatest extent of formation will occur at circumneutral pH values and at levels of bromide typically encountered in surface waters, and thus we anticipate that the results herein are directly relevant to conditions associated with water treatment.

Results from Chapter 4 also showed that the extent of interaction (i.e., sorption) between CNTs and NOM (e.g., humic substances) influences net DBP production. For oxidized and polymer functionalized CNTs, DBP formation in the presence of Suwannee River Humic Acid (SRHA) is simply additive. We attribute this additive nature of the CNT and SRHA mixture to the limited degree of interaction (e.g., sorption) between SRHA and the relatively polar CNT surface (we note that oxidized and polymer functionalized CNTs are quite stable in suspension). Meanwhile, CF formation during chlorination of humic acid in the presence of non-functionalized CNTs is less than expected from such additive behavior. Because non-functionalized CNTs produce little to

no CF, this suggests their inhibitory effect on the DBP formation potential of SRHA. We attribute this result to uptake of SRHA on the hydrophobic, non-functionalized CNT surface, where such interactions reduce the freely dissolved SRHA available to react with chlorine.

5.4 Future research

This work introduces a new paradigm regarding how we should think about the fate of CNTs in water systems. It demonstrates that CNTs are reactive towards common chemical disinfectants including free chlorine, chloramines and ozone, and that their surface chemistry (i.e., functionalization) ultimately dictates their DBP formation capacity. Further, as a result of reactions with chemical disinfectants, the CNT surface chemistry changes, which not only increases CNT suspension stability and thus mobility in natural aquatic systems but also results in an oxidized surface with greater DBP formation potential. Outcomes of this work should, therefore, lead to closer scrutiny regarding the release of CNTs into aquatic systems and their utilization in water treatment applications. There are also several, potentially fruitful avenues of future research on related topics stemming from knowledge gained in this work.

5.4.1 Comprehensive byproduct identification and quantification

From more than 30 years of research, more than 600 DBPs have been identified from drinking water [8]. However, despite much research, about 50% of the halogenated DBPs in chlorinated drinking water remain unaccounted for, and much less are accounted for when using ozone, chloramines, or chlorine dioxide for disinfection [218]. Also, more water treatment plants in the U.S. are changing from chlorine to alternative disinfectants

to meet requirements of new regulations. For these reason, it is important to investigate the types of DBPs formed when exposing CNTs to alternative disinfectants.

Like NOM, CNTs are complex precursors especially when functionalized. The work herein has demonstrated the ability for CNTs to dechlorinate water while undergoing surface modification and producing traditional DBPs including CF and HAAs. However, in the experiments herein, the chlorine mass balance does not close with the DBPs we observed and quantified (i.e., THMs and HAAs). Therefore, it is not unreasonable to expect a more diverse distribution of chlorinated byproducts than those reported here. A necessary next step motivated by this work is broadening analytical methods to be more inclusive and target more than NDMA, THMs, and HAAs, including several so-called emerging DBPs classes that are not yet regulated (e.g., halonitromethanes, haloacetonitriles, iodomethanes, and other nitrosamines).

We note that such an endeavor will likely require additional method development. Because DBPs are typically formed at low levels (ng/L-µg/L), samples in this work were concentrated to allow for THM and HAA detection. However, there are other concentration methods that are commonly used that can extract various other DBPs of interest. These include solid phase extraction (SPE), solid phase microextraction (SPME), liquid-liquid extraction, and XAD resin extraction (polymeric adsorbent), the extracts of which can be analyzed in a multitude of ways. Below is a brief overview of additional or alternative analytical instrumentation that could help in identifying additional DBPs.

Gas chromatography-mass spectroscopy (GC-MS) is an important tool for measuring and identifying new DBPs. Mass spectral libraries (NIST and Wiley

databases) have been used to facilitate identification through mass spectrum matching. Additionally, high-resolution MS, chemical ionization-MS, and sometimes GC-infrared spectroscopy (IR) are more specialized options that have been used with GC-MS to determine the structures of product compounds. GC-MS-MS is another popular alternative for quantifying DPBs. Selected ion monitoring (SIM) or multiple reaction monitoring (MRM) mode are used with GC-MS and GC-MS-MS, respectively, to maximize the sensitivity and provide low detection limits.

Liquid chromatography-mass spectrometry (LC-MS) is increasingly being used to identify and quantify polar DBPs and probe high-molecular weight DBPs [219]. It has been used to identify haloquinone DBPs in drinking water [220], as well as other nitrosamines [221]. Ion chromatography-inductively coupled plasma-mass spectrometry (IC-ICP-MS) can be used to separate and quantify bromate, iodate, and HAAs [222]. IC with conductivity detectors can also be used to measure bromate as well as chlorite and chlorate [223].

Finally, total organic halides (TOX) analysis is an approach that can be used to estimate the total organic bound halogen in a water sample. Analysis of TOX uses carbon adsorption with a microcoulometric-titration detector to detect all organic halides containing chlorine, bromine, and iodine that are adsorbed on granular activated carbon. TOX measurements can prove useful in attempting to close the chlorine mass balance, allowing comparison to observations of chlorine demand as well as the identification and quantification of specific, targeted DBPs. Advances in this method have allowed for speciation of TOX into total organic chlorine (TOCl), total organic bromine (TOBr), and total organic iodine (TOI) [218]. This modern method can help to better assess the

toxicological risks of treated water samples by distinguishing the more toxic brominated and iodinated DBPs.

5.4.2 Mechanistic investigations and model approach

A reaction mechanism would describe the sequence of elementary reactions by which overall formation of products form. A complete mechanism would account for the chlorine loss, any catalytic reactions, as well as all the products formed (potential and observed). It would also describe the relative rates of the reaction steps and the rate equation of the overall reaction. A mechanistic model for the formation kinetics of THMs and HAAs that is consistent with the current understanding of DBP formation has been developed in the past [27, 224].

This project demonstrated complex kinetic rates of chlorine decay and DBP formation indicative of multistep surface reactions. Since mechanistic modeling can provide insights into the chemical nature of reactions and has the potential to reduce the amount of site-specific testing that would be required to model DBP formation under new conditions, it is preferred over statistical modeling in most cases. Modeling of DBP formation as a function of CNT contact can provide complementary information to classical kinetic modeling. In particular, effort should be devoted to further elucidation of the effects of pH, temperature, and halogen content on the rate constants, and to enhancing the conceptual basis of the model so that it can explain both kinetic and CNT chemistry observations. The integration of our data with the mechanistic model for a representative range of water qualities and reaction conditions could constitute an

important advance in the evolution of drinking water chemistry and its engineering applications.

One important first step is to try to identify the reaction intermediates, which are often unstable and short lived species. Reaction intermediates are often free radicals or ions. Therefore, their measurement could be difficult, but useful for determining the reaction rate limitations and overall mechanism. Another experimental method that can be used to determine the mechanism is measurement of the effect of temperature which allows for the calculation of activation energy. More advanced methods include identifying the stereochemistry of products and conducting isotopic substitution reactions.

5.4.3 Other carbon precursors

The suite of CNTs available commercially or fabricated for research purposes has not been exhausted. There are many types of other CNT functionalities ranging from halogens (Cl and Br) to metals (i.e., iron and silver) that can facilitate reactivity with oxidants and generate even more types of DBPs and at higher yields. Hence, more research could be done to expand our knowledge of DBP precursors from CNTs.

CNTs with amorphous carbon introduced as a byproduct of its synthesis or from experiencing extreme redox conditions can have altering effects to total potential formation of DBPs. Current CNT synthesis methods suffer from the production of impurities. The main impurities produced together with carbon nanotubes are multishell carbon nanocapsules, both empty and filled with the metal catalyst, amorphous carbon nanoparticles, and fullerenes [225]. Purity of CNTs vary from vendor to vendor, where

cheaper production methods typically yield lower purity products and hence more impurities. In this regard, we can correlate the reactivity of chlorine and DPB formation to synthesis route.

To test for the influence of impurities associated with the synthesis of CNTs, one can implement a separation process that releases and captures amorphous carbon impurities. One way to do this is mechanically separating the CNT from its impurities through sonication, then filtering with a polymeric membrane with pores smaller than the length of the CNT or alternatively using centrifugation to separate the fractions by weight.

Other C nanomaterials like graphene, C60, and C70, which are byproducts of CNT synthesis and are commercially available, could be recognized as precursors to DBPs. Other nanomaterials with potential for reactivity are nanomaterials (e.g., Au nanoparticles) stabilized with carbon based stabilizing agents (e.g., surfactants). Their behavior as precursors could contribute greatly to our knowledge on DBPs, and raise awareness to their popularity and ubiquity in research and industry.

5.4.4 Toxicity of chlorinated CNTs

The toxicity of chlorinated CNTs could be different from that of their unreacted form since we found that CNTs reacted with chlorine contained trace levels of chlorine on their surface. In Chapter 2 we found that there was no difference in acute toxicity between both unreacted and chlorinated CNTs. However, nothing has been shown regarding the adverse effects as a result of long term exposure to these chlorinated CNTs. Various toxicity tests can be performed on an organism's lifespan to assess the chronic

toxicity of chlorinated CNTs. Perhaps the best way to carry out this assessment is to expose an organism to the environmentally representative concentration of chlorinated CNTs (sub µg/L level) and combined with the mixture of produced byproducts.

5.4.5 CNT membranes exposed to chlorination

The exposure of disinfectants to CNTs before use for water remediation as sorbents or incorporations into membranes must be assessed. Work presented in this thesis showed CNTs are capable of producing DBPs in suspensions; however, their activity when immobilized is not completely understood. In Chapter 2, we showed that filtrate of a CNT solutions exposed to ozone did not form CF when reacted with chlorine and hence believe that the majority of the reactivity occurs on the CNT surface. Because of this, it would be valuable to observe the reactivity of immobilized CNTs, where the reaction would occur much more quickly, to better represent CNTs in next generation water purification processes.

To research this question, one can implement a separate reactor design utilizing permeable CNT mats immobilized on a polymer filter through which chlorine-containing solutions would be pumped. CNT mats have been fabricated by pulling a well-dispersed CNT suspension in water (e.g., carboxylated CNT suspension via vacuum through the porous support) [226, 227]. This system provides clear separation of the CNTs from the aqueous phase. This will facilitate post-reaction handling and analysis of CNTs and labile precursors. It can be operated continuously by filtering chlorinated water (e.g., from the tap) or use a recirculated water source to give a concentrated sample.

LITERATURE CITED

1.	Mitch, W.A., et al., *N-Nitrosodimethylamine (NDMA) as a drinking water contaminant: A review.* Environ. Eng. Sci., 2003. **20**(5): p. 389-404.
2.	Moran, J.E., S.D. Oktay, and P.H. Santschi, *Sources of iodine and iodine 129 in rivers.* Water Resour. Res., 2002. **38**(8): p. 24-1-24-10.
3.	Krasner, S.W., et al., *Occurrence of a new generation of disinfection byproducts.* Environ. Sci. Technol., 2006. **40**(23): p. 7175-7185.
4.	Sohn, J., G. Amy, and Y. Yoon, *Bromide ion incorporation into brominated disinfection by-products.* Water Air Soil Poll., 2006. **174**(1-4): p. 265-277.
5.	Hua, G., D.A. Reckhow, and J. Kim, *Effect of bromide and iodide ions on the formation and speciation of disinfection byproducts during chlorination.* Environ. Sci. Tech., 2006. **40**(9): p. 3050-3056.
6.	von Gunten, U., et al., *Kinetics and mechanisms of N-nitrosodimethylamine formation upon ozonation of N,N-dimethylsulfamide-containing waters: Bromide catalysis.* Environ. Eng. Sci., 2010. **44**(15): p. 5762-5768.
7.	USEPA, *Comprehensive Disinfectants and Disinfection Byproducts Rules (Stage 1 and Stage 2): Quick Reference Guide*. 2010: http://www.epa.gov/ogwdw/mdbp/qrg_st1.pdf.
8.	Richardson, S.D., et al., *Occurrence, genotoxicity, and carcinogenicity of regulated and emerging disinfection by-products in drinking water: A review and roadmap for research.* Mutat. Res., Rev. Mutat. Res., 2007. **636**(1–3): p. 178-242.
9.	Rook, J.J., *Formation of haloforms during chlorination of natural waters.* Water Treat. Exam., 1974. **23**: p. 234-243.
10.	Keith, L.H., *Identification & analysis of organic pollutants in water*. 1976: Ann Arbor Science Publishers.
11.	Page, N.P., N.C. Institute, and U. Saffiotti, *Report on carcinogenesis bioassay of chloroform*. 1976: U.S.Dept. of Health, Education, and Welfare, Public Health Service, National Institutes of Health],National Cancer Institute, Division of Cancer Cause and Prevention, Carcinogenesis Program, Carcinogen Bioassay and Program Resources Branch.

12. USEPA, *EPA protocol for the review of existing national primary drinking water regulations*, USEPA, Editor. 2003: http://www.epa.gov/ogwdw/standard/review/pdfs/support_6yr_protocal_final.pdf.

13. Hebert, A., et al., *Innovative method for prioritizing emerging disinfection by-products (DBPs) in drinking water on the basis of their potential impact on public health.* Water Res., 2010. **44**(10): p. 3147-3165.

14. Krasner, S.W., *The formation and control of emerging disinfection by-products of health concern.* Phil. Trans. R. Soc. A, 2009. **367**(1904): p. 4077-4095.

15. Plewa, M.J., et al., *Mammalian cell cytotoxicity and genotoxicity analysis of drinking water disinfection by-products.* Environ. Mol. Mutagen., 2002. **40**(2): p. 134-142.

16. Yahya, K., et al., *A New Assessment of the Cytotoxicity and Genotoxicity of Drinking Water Disinfection By-Products*, in *Natural Organic Matter and Disinfection By-Products*. 2000, American Chemical Society. p. 16-27.

17. Plewa, M.J., et al., *Mammalian cell cytotoxicity and genotoxicity of the haloacetic acids, a major class of drinking water disinfection by-products.* Environ. Mol. Mutagen., 2010. **51**(8-9): p. 871-878.

18. Michael, J.P., et al., *Comparative mammalian cell toxicity of N-DBPs and C-DBPs*, in *Disinfection By-Products in Drinking Water*. 2008, American Chemical Society. p. 36-50.

19. Plewa, M.J., et al., *Halonitromethane drinking water disinfection byproducts: Chemical characterization and mammalian cell cytotoxicity and genotoxicity.* Environ. Sci. Technol., 2004. **38**(1): p. 62-68.

20. USEPA, *Technical Fact Sheet – N-Nitroso-dimethylamine (NDMA)*. 2012: http://www2.epa.gov/fedfac/technical-fact-sheet-n-nitroso-dimethylamine-ndma.

21. Plewa, M.J., et al., *Chemical and biological characterization of newly discovered iodoacid drinking water disinfection byproducts.* Environ. Sci. Technol., 2004. **38**(18): p. 4713-4722.

22. USEPA, *Fact Sheet: Final Third Drinking Water Contaminant Candidate List (CCL 3)* USEPA, Editor. 2009: http://www2.epa.gov/sites/production/files/2014-09/documents/fact_sheet_final_third_ccl.pdf.

23. USEPA, *Unregulated Contaminant Monitoring Regulation (UCMR) for Public Water Systems Revisions*, USEPA, Editor. 2007: https://federalregister.gov/a/E6-22123.

24. Glaze, W.H. and J.E. Henderson. *Analysis of new chlorinated organic compounds formed by chlorination of municipal wastewater*. in *Conference on the Environmental Impact of Water Chlorination*. 1975. Oak Ridge National Laboratory, Oak Ridge, TN.

25. Bond, T., et al., *Occurrence and control of nitrogenous disinfection by-products in drinking water – A review.* Water Res., 2011. **45**(15): p. 4341-4354.

26. Rook, J.J., *Chlorination reactions of fulvic acids in natural waters.* Environ. Sci. Technol., 1977. **11**(5): p. 478-482.

27. Bond, T., et al., *A critical review of trihalomethane and haloacetic acid formation from natural organic matter surrogates.* Environ. Sci. Technol., 2012. **1**(1): p. 93-113.

28. Richardson, S.D., *Disinfection by-products: Formation and occurrence in drinking water*, in *Encyclopedia of Environmental Health*, J.O. Nriagu, Editor. 2011, Elsevier: Burlington. p. 110-136.

29. Aiken, G.R., *Humic Substances in Soil, Sediment, and Water: Geochemistry, Isolation, and Characterization*. 1985: John Wiley and Sons.

30. Suffet, I.H. and M. Patrick, *Aquatic Humic Substances*. Advances in Chemistry. Vol. 219. 1988: American Chemical Society. 900.

31. Gu, B., et al., *Adsorption and desorption of different organic matter fractions on iron oxide.* Geochimica et Cosmochimica Acta, 1995. **59**(2): p. 219-229.

32. Chowdhury, S., P. Champagne, and P.J. McLellan, *Models for predicting disinfection byproduct (DBP) formation in drinking waters: A chronological review.* Sci. Total Environ., 2009. **407**(14): p. 4189-4206.

33. Bond, T., et al., *Disinfection byproduct formation and fractionation behavior of natural organic matter surrogates.* Environ. Sci. Technol., 2009. **43**(15): p. 5982-5989.

34. Hua, G. and D.A. Reckhow, *Characterization of disinfection byproduct precursors based on hydrophobicity and molecular size.* Environ. Sci. Technol., 2007. **41**(9): p. 3309-3315.

35. Choi, J. and R.L. Valentine, *Formation of N-nitrosodimethylamine (NDMA) from reaction of monochloramine: a new disinfection by-product.* Water Res., 2002. **36**(4): p. 817-824.

36.   Choi, J., S.E. Duirk, and R.L. Valentine, *Mechanistic studies of N-nitrosodimethylamine (NDMA) formation in chlorinated drinking water.* J. Environ. Monitor., 2002. **4**(2): p. 249-252.

37.   Shah, A.D. and W.A. Mitch, *Halonitroalkanes, halonitriles, haloamides, and N-nitrosamines: A critical review of nitrogenous disinfection byproduct formation pathways.* Environ. Sci. Technol., 2012. **46**(1): p. 119-131.

38.   von Gunten, U., *Ozonation of drinking water: Part I. Oxidation kinetics and product formation.* Water Res., 2003. **37**(7): p. 1443-1467.

39.   Shah, A.D., et al., *Impact of UV disinfection combined with chlorination/chloramination on the formation of halonitromethanes and haloacetonitriles in drinking water.* Environ. Sci. Technol., 2011. **45**(8): p. 3657-3664.

40.   Reckhow, D.A., et al., *Effect of UV treatment on DBP formation.* J. Am. Water. Works. Ass., 2010. **102**(6): p. 100-113.

41.   Richardson, S.D., et al., *Identification of new drinking water disinfection byproducts formed in the presence of bromide.* Environ. Sci. Technol., 1999. **33**(19): p. 3378-3383.

42.   Krasner, S.W., et al., *The occurrence of disinfection by-products in US drinking water.* J. Am. Water. Works. Ass., 1989. **81**(8): p. 41-53.

43.   Heller-Grossman, L., et al., *Formation and distribution of haloacetic acids, THM and tox in chlorination of bromide-rich lake water.* Water Res., 1993. **27**(8): p. 1323-1331.

44.   Pourmoghaddas, H., et al., *Effect of bromide ion on formation of HAAs during chlorination.* J. Am. Water. Works. Ass., 1993. **85**(1): p. 82-87.

45.   Pourmoghaddas, H. and A.A. Stevens, *Relationship between trihalomethanes and haloacetic acids with total organic halogen during chlorination.* Water Res., 1995. **29**(9): p. 2059-2062.

46.   Deborde, M. and U. von Gunten, *Reactions of chlorine with inorganic and organic compounds during water treatment - Kinetics and mechanisms: A critical review.* Water Res., 2008. **42**(1-2): p. 13-51.

47.   Nawrocki, J. and P. Andrzejewski, *Nitrosamines and water.* J. Hazard. Mater., 2011. **189**(1–2): p. 1-18.

48.   Arnold, W.A., et al., *Evaluation of functional groups responsible for chloroform formation during water chlorination using compound specific isotope analysis.* Environ. Sci. Technol., 2008. **42**(21): p. 7778-7785.

49.   Shen, R. and S.A. Andrews, *NDMA formation kinetics from three pharmaceuticals in four water matrices.* Water Res., 2011. **45**(17): p. 5687-5694.

50.   Mitch, W.A. and D.L. Sedlak, *Characterization and fate of N-nitrosodimethylamine precursors in municipal wastewater treatment plants.* Environ. Sci. Technol., 2004. **38**: p. 1445-1454.

51.   Chang, E.E., et al., *Relationship between chlorine consumption and chlorination by-products formation for model compounds.* Chemosphere, 2006. **64**(7): p. 1196-1203.

52.   Chang, E.E., et al., *Modeling the formation and assessing the risk of disinfection by-products in water distribution systems.* J. Environ. Sci. Heal. A, 2010. **45**(10): p. 1185-1194.

53.   Zhao, Q., et al., *Formation of halogenated organic byproducts during medium-pressure UV and chlorine coexposure of model compounds, NOM and bromide.* Water Res., 2011. **45**(19): p. 6545-6554.

54.   Navalon, S., M. Alvaro, and H. Garcia, *Carbohydrates as trihalomethanes precursors. Influence of pH and the presence of Cl− and Br− on trihalomethane formation potential.* Water Res., 2008. **42**(14): p. 3990-4000.

55.   Eddy, M., et al., *Wastewater Engineering: Treatment and Reuse*. 4 ed. 2003, New York: McGraw Hill.

56.   Snoeyink, V.L. and W.J. Weber, *The surface chemistry of active carbon; a discussion of structure and surface functional groups.* Environ. Sci. Technol., 1967. **1**(3): p. 228-234.

57.   Pan, D. and M. Jaroniec, *Adsorption and thermogravimetric studies of unmodified and oxidized active carbons.* Langmuir, 1996. **12**(15): p. 3657-3665.

58.   Karanfil, T. and J.E. Kilduff, *Role of granular activated carbon surface chemistry on the adsorption of organic compounds. 1. Priority pollutants.* Environ. Eng. Sci., 1999. **33**(18): p. 3217-3224.

59.   Biniak, S., et al., *The characterization of activated carbons with oxygen and nitrogen surface groups.* Carbon, 1997. **35**(12): p. 1799-1810.

60.   Metcalf & Eddy, I. and Aecom, *Water Reuse*. 2007, New York: McGraw-Hill.

61.   Voudrias, E.A., R.A. Larson, and V.L. Snoeyink, *Effects of activated carbon on the reactions of combined chlorine with phenols.* Water Res., 1985. **19**(7): p. 909-915.

62. Voudrias, E.A., R.A. Larson, and V.L. Snoeyink, *Effects of activated carbon on the reactions of free chlorine with phenols.* Environ. Sci. Technol., 1985. **19**(5): p. 441-449.

63. Hwang, S.C., R.A. Larson, and V.L. Snoeyink, *Reactions of free chlorine with substituted anilines in aqueous-solution and on granular activated carbon.* Water Res., 1990. **24**(4): p. 427-432.

64. Padhye, L., et al., *Unexpected role of activated carbon in promoting transformation of secondary amines to N-nitrosamines.* Environ. Sci. Technol., 2010. **44**(11): p. 4161-4168.

65. Padhye, L.P., et al., *N-Nitrosamines formation from secondary amines by nitrogen fixation on the surface of activated carbon.* Environ. Sci. Technol., 2011. **45**(19): p. 8368-8376.

66. Dresselhaus, M.S., G. Dresselhaus, and A. Jorio, *Unusual properties and structure of carbon nanotubes.* Ann. Rev. Mater. Res., 2004. **34**(1): p. 247-278.

67. De Volder, M.F.L., et al., *Carbon nanotubes: Present and future commercial applications.* Science, 2013. **339**(6119): p. 535-539.

68. Mauter, M.S. and M. Elimelech, *Environmental applications of carbon-based nanomaterials.* Environ. Sci. Technol., 2008. **42**(16): p. 5843-5859.

69. Hirsch, A. and O. Vostrowsky, *Functionalization of Carbon Nanotubes*, in *Functional Molecular Nanostructures*, A.D. Schlüter, Editor. 2005, Springer Berlin Heidelberg. p. 193-237.

70. Tasis, D., et al., *Chemistry of carbon nanotubes.* Chemical Rev., 2006. **106**(3): p. 1105-1136.

71. Dresselhaus, M. and M. Endo, *Relation of Carbon Nanotubes to Other Carbon Materials*, in *Carbon Nanotubes*, M. Dresselhaus, G. Dresselhaus, and P. Avouris, Editors. 2001, Springer Berlin Heidelberg. p. 11-28.

72. Niyogi, S., et al., *Chemistry of single-walled carbon nanotubes.* Accounts Chem. Res., 2002. **35**(12): p. 1105-1113.

73. Choi, H.C., et al., *Spontaneous reduction of metal ions on the sidewalls of carbon nanotubes.* J. Am. Chem. Soc., 2002. **124**(31): p. 9058-9059.

74. Zheng, M. and B.A. Diner, *Solution redox chemistry of carbon nanotubes.* J. Am. Chem. Soc., 2004. **126**(47): p. 15490-15494.

75. Mattison, N.T., et al., *Impact of porous media grain size on the transport of multi-walled carbon nanotubes.* Environ. Sci. Technol., 2011. **45**(22): p. 9765-9775.

76. Chowdhury, I., et al., *Impact of synthesis methods on the transport of single walled carbon nanotubes in the aquatic environment.* Environ. Sci. Technol., 2012. **46**(21): p. 11752-11760.

77. Mueller, N.C. and B. Nowack, *Exposure modeling of engineered nanoparticles in the environment.* Environ. Sci. Technol., 2008. **42**(12): p. 4447-4453.

78. Gottschalk, F., et al., *Modeled environmental concentrations of engineered nanomaterials (TiO$_2$, ZnO, Ag, CNT, fullerenes) for different regions.* Environ. Sci. Technol., 2009. **43**(24): p. 9216-9222.

79. Rahaman, M.S., C.D. Vecitis, and M. Elimelech, *Electrochemical carbon-nanotube filter performance toward virus removal and inactivation in the presence of natural organic matter.* Environ. Sci. Technol., 2012. **46**(3): p. 1556-1564.

80. Gao, G. and C.D. Vecitis, *Electrochemical carbon nanotube filter oxidative performance as a function of surface chemistry.* Environ. Sci. Technol., 2011. **45**(22): p. 9726-9734.

81. Oulton, R., et al., *Hydroxyl radical formation during ozonation of multiwalled carbon nanotubes: Performance optimization and demonstration of a reactive CNT filter.* Environ. Sci. Technol., 2015. **49**(6): p. 3687-3697.

82. Lu, C., Y.-L. Chung, and K.-F. Chang, *Adsorption thermodynamic and kinetic studies of trihalomethanes on multiwalled carbon nanotubes.* J. Hazard. Mater., 2006. **138**(2): p. 304-310.

83. Lu, C., Y.-L. Chung, and K.-F. Chang, *Adsorption of trihalomethanes from water with carbon nanotubes.* Water Res., 2005. **39**(6): p. 1183-1189.

84. Li, Y.-H., et al., *Adsorption of fluoride from water by amorphous alumina supported on carbon nanotubes.* Chem. Phys. Lett., 2001. **350**(5–6): p. 412-416.

85. Yang, S., et al., *Adsorption of Ni(II) on oxidized multi-walled carbon nanotubes: Effect of contact time, pH, foreign ions and PAA.* J. Hazard. Mater., 2009. **166**(1): p. 109-116.

86. Chen, C., et al., *Adsorption behavior of multiwall carbon nanotube/iron oxide magnetic composites for Ni(II) and Sr(II).* J. Hazard. Mater., 2009. **164**(2–3): p. 923-928.

87. Li, Y.-H., et al., *Lead adsorption on carbon nanotubes.* Chem. Phys. Lett., 2002. **357**(3–4): p. 263-266.

88. Li, Y.-H., et al., *Competitive adsorption of Pb^{2+}, Cu^{2+} and Cd^{2+} ions from aqueous solutions by multiwalled carbon nanotubes.* Carbon, 2003. **41**(14): p. 2787-2792.

89. Sheng, G., et al., *Adsorption of copper(II) on multiwalled carbon nanotubes in the absence and presence of humic or fulvic acids.* J. Hazard. Mater., 2010. **178**(1–3): p. 333-340.

90. Di, Z.-C., et al., *Chromium adsorption by aligned carbon nanotubes supported ceria nanoparticles.* Chemosphere, 2006. **62**(5): p. 861-865.

91. Gupta, V.K., S. Agarwal, and T.A. Saleh, *Chromium removal by combining the magnetic properties of iron oxide with adsorption properties of carbon nanotubes.* Water Res., 2011. **45**(6): p. 2207-2212.

92. Wang, X., et al., *Sorption of 243Am(III) to multiwall carbon nanotubes.* Environ. Sci. Technol., 2005. **39**(8): p. 2856-2860.

93. Peng, X., et al., *Ceria nanoparticles supported on carbon nanotubes for the removal of arsenate from water.* Mater. Lett., 2005. **59**(4): p. 399-403.

94. Lin, Y., X. Cui, and J. Bontha, *Electrically controlled anion exchange based on polypyrrole and carbon nanotubes nanocomposite for perchlorate removal.* Environ. Sci. Technol., 2006. **40**(12): p. 4004-4009.

95. Ji, L., et al., *Mechanisms for strong adsorption of tetracycline to carbon nanotubes: A comparative study using activated carbon and graphite as adsorbents.* Environ. Sci. Technol., 2009. **43**(7): p. 2322-2327.

96. Yan, H., et al., *Adsorption of microcystins by carbon nanotubes.* Chemosphere, 2006. **62**(1): p. 142-148.

97. Lin, D. and B. Xing, *Adsorption of phenolic compounds by carbon nanotubes: Role of aromaticity and substitution of hydroxyl group.* Environ. Sci. Technol., 2008. **42**(19): p. 7254-7259.

98. Yang, K., et al., *Aqueous adsorption of aniline, phenol, and their substitutes by multi-walled carbon nanotubes.* Environ. Sci. Technol., 2008. **42**(21): p. 7931-7936.

99. Cho, H.-H., et al., *Influence of surface oxides on the adsorption of naphthalene onto multiwalled carbon nanotubes.* Environ. Sci. Technol., 2008. **42**(8): p. 2899-2905.

100. Hyung, H. and J.-H. Kim, *Natural organic matter (NOM) adsorption to multi-walled carbon nanotubes: Effect of NOM characteristics and water quality parameters.* Environ. Sci. Technol., 2008. **42**(12): p. 4416-4421.

101. Holt, J.K., et al., *Fast mass transport through sub-2-nanometer carbon nanotubes.* Science, 2006. **312**(5776): p. 1034-1037.

102. Das, R., et al., *Carbon nanotube membranes for water purification: A bright future in water desalination.* Desalination, 2014. **336**(0): p. 97-109.

103. Wang, Y.-Q., et al., *Generation of anti-biofouling ultrafiltration membrane surface by blending novel branched amphiphilic polymers with polyethersulfone.* J. Membrane Sci., 2006. **286**(1–2): p. 228-236.

104. Dudchenko, A.V., et al., *Organic fouling inhibition on electrically conducting carbon nanotube–polyvinyl alcohol composite ultrafiltration membranes.* J. Membrane Sci., 2014. **468**(0): p. 1-10.

105. Gunawan, P., et al., *Hollow fiber membrane decorated with Ag/MWNTs: Toward effective water disinfection and biofouling control.* ACS Nano, 2011. **5**(12): p. 10033-10040.

106. Lee, J.-F., et al., *Behavior of organic polymers in drinking water purification.* Chemosphere, 1998. **37**(6): p. 1045-1061.

107. Park, S.H., et al., *N-nitrosodimethylamine (NDMA) formation potential of amine-based water treatment polymers: Effects of in situ chloramination, breakpoint chlorination, and pre-oxidation.* J. Hazard. Mater., 2015. **282**(0): p. 133-140.

108. Unger, E., et al., *Electrochemical functionalization of multi-walled carbon nanotubes for solvation and purification.* Curr. Appl. Phys., 2002. **2**(2): p. 107-111.

109. Ray, S.C., et al., *Electronic structures and bonding properties of chlorine-treated nitrogenated carbon nanotubes: X-ray absorption and scanning photoelectron microscopy studies.* Appl. Phys. Lett., 2007. **90**(19): p. 192107.

110. Ray, S.C., et al., *Enhancement of electron field emission of nitrogenated carbon nanotubes on chlorination.* Diam. Relat. Mater., 2009. **18**(2–3): p. 457-460.

111. Yuan, J.-M., et al., *An easy method for purifying multi-walled carbon nanotubes by chlorine oxidation.* Carbon, 2008. **46**(9): p. 1266-1269.

112. Gohier, A., et al., *Optimized network of multi-walled carbon nanotubes for chemical sensing.* Nanotechnology, 2011. **22**: p. 105501 (8 pp).

113. Saito, R., et al., *Electronic structure of chiral graphene tubules.* Appl. Phys. Lett., 1992. **60**(18): p. 2204-2206.

114. Chiang, I.W., et al., *Purification and characterization of single-wall carbon nanotubes.* J. Phys. Chem. B, 2001. **105**(6): p. 1157-1161.

115. Wepasnick, K.A., et al., *Surface and structural characterization of multi-walled carbon nanotubes following different oxidative treatments.* Carbon, 2011. **49**(1): p. 24-36.

116. Ren, X., et al., *Carbon nanotubes as adsorbents in environmental pollution management: A review.* Chem. Eng. J., 2011. **170**(2–3): p. 395-410.

117. Yang, K. and B. Xing, *Adsorption of fulvic acid by carbon nanotubes from water.* Environ. Pollut., 2009. **157**(4): p. 1095-1100.

118. Zhang, S., et al., *Adsorption of synthetic organic chemicals by carbon nanotubes: Effects of background solution chemistry.* Water Res., 2010. **44**(6): p. 2067-2074.

119. He, X., et al., *Preparation of a carbon nanotube/carbon fiber multi-scale reinforcement by grafting multi-walled carbon nanotubes onto the fibers.* Carbon, 2007. **45**(13): p. 2559-2563.

120. Zhang, S., et al., *Adsorption of aromatic compounds by carbonaceous adsorbents: A comparative study on granular activated carbon, activated carbon fiber, and carbon nanotubes.* Environ. Sci. Technol., 2010. **44**(16): p. 6377-6383.

121. Hassan, K., K. Bower, and C. Miller, *Iron oxide enhanced chlorine decay and disinfection by-product formation.* J. Environ. Eng. ASCE, 2006. **132**(12): p. 1609-1616.

122. Stevenson, F.J., *Humus Chemistry: Genesis, Composition, Reactions.* 1994: Wiley.

123. Richardson, S.D., et al., *Results of a nationwide DBP occurence study: Indentification of new DBPs of potential health concern.* Epidemiology, 2002. **13**(4): p. S109-S110.

124. Komaki, Y., et al., *Nanowire-based electrochemical biosensorscomparative DNA damage and repair kinetics study in mammalian cells by chloro-, bromo-, and iodoacetic acid.* Environ. Mol. Mutagen., 2009. **50**(7): p. 566-566.

125. Sharma, V.K., *Kinetics and mechanism of formation and destruction of N-nitrosodimethylamine in water – A review.* Sep. Purif. Technol., 2012. **88**(0): p. 1-10.

126. Wanekaya, A.K., et al., *Nanowire-based electrochemical biosensors.* Electroanalysis, 2006. **18**(6): p. 533-550.

127. Wenrong, Y., et al., *Carbon nanotubes for biological and biomedical applications.* Nanotechnology, 2007. **18**(41): p. 412001.

128. Yoon, S. and H. Tanaka, *Formation of N-nitrosamines by chloramination or ozonation of amines listed in pollutant release and transfer registers (PRTRs).* Chemosphere, 2014. **95**(0): p. 88-95.

129. Chen, W.-H. and T.M. Young, *NDMA formation during chlorination and chloramination of aqueous diuron solutions.* Environ. Sci. Technol., 2008. **42**(4): p. 1072-1077.

130. Mitch, W.A. and D.L. Sedlak, *Formation of N-nitrosodimethylamine (NDMA) from dimethylamine during chlorination.* Environ. Sci. Technol., 2002. **36**: p. 588-595.

131. Lee, C., et al., *Oxidation of N-nitrosodimethylamine (NDMA) precursors with ozone and chlorine dioxide: Kinetics and effect on NDMA formation potential.* Environ. Sci. Technol., 2007. **41**(6): p. 2056-2063.

132. Pan, B. and B. Xing, *Adsorption mechanisms of organic chemicals on carbon nanotubes.* Environ. Sci. Technol., 2008. **42**(24): p. 9005-9013.

133. Herrero Latorre, C., et al., *Carbon nanotubes as solid-phase extraction sorbents prior to atomic spectrometric determination of metal species: A review.* Anal. Chim. Acta, 2012. **749**(0): p. 16-35.

134. Smith, B., et al., *Colloidal properties of aqueous suspensions of acid-treated, multi-walled carbon nanotubes.* Environ. Sci. Technol., 2008. **43**(3): p. 819-825.

135. Chen, C.-Y. and C.T. Jafvert, *Photoreactivity of carboxylated single-walled carbon nanotubes in sunlight: Reactive oxygen species production in water.* Environ. Sci. Technol., 2010. **44**(17): p. 6674-6679.

136. Bekyarova, E., et al., *Chemically engineered single-walled carbon nanotube materials for the electronic detection of hydrogen chloride.* Adv. Mater., 2010. **22**(7): p. 848-852.

137. Worsley, K.A., et al., *Functionalization and dissolution of nitric acid treated single-walled carbon nanotubes.* J. Am. Chem. Soc., 2009. **131**(50): p. 18153-18158.

138. *Carbon Solutions, Inc.* 2015 [cited 2015 May 21]; Available from: http://www.carbonsolution.com/.

139. *NanoLab Inc.* 2014 [cited 2015 May 21]; Available from: http://www.nano-lab.com/.

140. Zhao, B., H. Hu, and R.C. Haddon, *Synthesis and properties of a water-soluble single-walled carbon nanotube–poly(m-aminobenzene sulfonic acid) graft copolymer.* Adv. Funct. Mater., 2004. **14**(1): p. 71-76.

141. Ramanathan, T., et al., *Amino-functionalized carbon nanotubes for binding to polymers and biological systems.* Chem. Mater., 2005. **17**(6): p. 1290-1295.

142. Lee, C., J. Yoon, and U. Von Gunten, *Oxidative degradation of N-nitrosodimethylamine by conventional ozonation and the advanced oxidation process ozone/hydrogen peroxide.* Water Res., 2007. **41**(3): p. 581-590.

143. Bader, H. and J. Hoigne, *Determination of ozone in water by the indigo method.* Water Res., 1981. **15**(4): p. 449-456.

144. Baltrusaitis, J., C.R. Usher, and V.H. Grassian, *Reactions of sulfur dioxide on calcium carbonate single crystal and particle surfaces at the adsorbed water carbonate interface.* Phys. Chem. Chem. Phys., 2007. **9**(23): p. 3011-3024.

145. Fairley, N., *CasaXPS.* 1999-2012: www.casaxps.com.

146. Kang, S., et al., *Single-walled carbon nanotubes exhibit strong antimicrobial activity.* Langmuir, 2007. **23**: p. 8670-8673.

147. Pasquini, L.M., et al., *Realizing comparable oxidative and cytotoxic potential of single- and multiwalled carbon nanotubes through annealing.* Environ. Sci. Technol., 2013. **47**(15): p. 8775-8783.

148. Clesceri, L.S., et al., *Standard Methods for the Examination of Water and Wastewater.* 1998: American Public Health Association.

149. Flowers, R.C. and P.C. Singer, *Anion exchange resins as a source of nitrosamines and nitrosamine precursors.* Environ. Sci. Technol., 2013. **47**(13): p. 7365-7372.

150. Park, S.-H., et al., *Degradation of amine-based water treatment polymers during chloramination as N-nitrosodimethylamine (NDMA) precursors.* Environ. Sci. Technol., 2009. **43**(5): p. 1360-1366.

151. Mitch, W.A. and I.M. Schreiber, *Degradation of tertiary alkylamines during chlorination/chloramination: Implications for formation of aldehydes, nitriles, halonitroalkanes, and nitrosamines.* Environ. Sci. Technol., 2008. **42**(13): p. 4811-4817.

152. Selbes, M., et al., *The roles of tertiary amine structure, background organic matter and chloramine species on NDMA formation.* Water Res., 2013. **47**(2): p. 945-953.

153. Kemper, J.M., S.S. Walse, and W.A. Mitch, *Quaternary amines as nitrosamine precursors: A role for consumer products?* Environ. Sci. Technol., 2010. **44**(4): p. 1224-1231.

154. Chen, Z. and R.L. Valentine, *Modeling the formation of N-nitrosodimethylamine (NDMA) from the reaction of natural organic matter (NOM) with monochloramine.* Environ. Sci. Technol., 2006. **40**(23): p. 7290-7297.

155. Buffle, M.-O. and U. von Gunten, *Phenols and amine induced HO• generation during the initial phase of natural water ozonation.* Environ. Sci. Technol., 2006. **40**(9): p. 3057-3063.

156. Debiemme-Chouvy, C., S. Haskouri, and H. Cachet, *Study by XPS of the chlorination of proteins aggregated onto tin dioxide during electrochemical production of hypochlorous acid.* Appl. Surf. Sci., 2007. **253**(12): p. 5506-5510.

157. Do, V.T., et al., *Effects of chlorine exposure conditions on physiochemical properties and performance of a polyamide membrane: Mechanisms and implications.* Environ. Sci. Technol., 2012. **46**(24): p. 13184-13192.

158. Beverly, S., S. Seal, and S. Hong, *Identification of surface chemical functional groups correlated to failure of reverse osmosis polymeric membranes.* J. Vac. Sci. Technol., A, 2000. **18**(4): p. 1107-1113.

159. Liu, S., et al., *Sharper and faster "nano darts" kill more bacteria: A study of antibacterial activity of individually dispersed pristine single-walled carbon nanotube.* ACS Nano, 2009. **3**(12): p. 3891-3902.

160. U.S. Agency for Toxic Substances and Disease Registry (ATSDR). *Toxicological Profile for N-Nitrosodimethylamine.* U.S. Government Printing Office, December 1989.

161. Pelech, I., et al., *Chlorination of carbon nanotubes obtained on the different metal catalysts.* J. Nanomater., 2013. **2013**: p. 9.

162. Simmons, J.M., et al., *Effect of ozone oxidation on single-walled carbon nanotubes.* J. Phys. Chem. B, 2006. **110**(14): p. 7113-7118.

163. Naeimi, H., et al., *Efficient and facile one pot carboxylation of multiwalled carbon nanotubes by using oxidation with ozone under mild conditions.* Appl. Surf. Sci., 2009. **256**(3): p. 631-635.

164. Singer, P.C., *Humic substances as precursors for potentially harmful disinfection by-products.* Water Sci. Technol., 1999. **40**(9): p. 25-30.

165. Bekyarova, E., et al., *Chemically functionalized single-walled carbon nanotubes as ammonia sensors.* J. Phys. Chem. B, 2004. **108**(51): p. 19717-19720.

166. Hu, H., et al., *Chemically functionalized carbon nanotubes as substrates for neuronal growth.* Nano Lett., 2004. **4**(3): p. 507-511.
167. Avouris, P., et al., *Carbon nanotube electronics.* P. IEEE, 2003. **91**(11): p. 1772-1784.
168. Fam, D.W.H., et al., *A review on technological aspects influencing commercialization of carbon nanotube sensors.* Sensor. Actuat. B: Chem., 2011. **157**(1): p. 1-7.
169. Wang, Y. and J.T.W. Yeow, *A review of carbon nanotubes-based gas sensors.* J. Sensors, 2009. **2009**: p. 24.
170. Qian, H., et al., *Carbon nanotube-based hierarchical composites: A review.* J. Mater. Chem., 2010. **20**(23): p. 4751-4762.
171. Gogotsi, Y. and P. Simon, *True performance metrics in electrochemical energy storage.* Science, 2011. **334**(6058): p. 917-918.
172. Rosca, I.D., et al., *Oxidation of multiwalled carbon nanotubes by nitric acid.* Carbon, 2005. **43**(15): p. 3124-3131.
173. Esumi, K., et al., *Chemical treatment of carbon nanotubes.* Carbon, 1996. **34**(2): p. 279-281.
174. Smith, B., et al., *Influence of surface oxides on the colloidal stability of multi-walled carbon nanotubes: A structure−property relationship.* Langmuir, 2009. **25**(17): p. 9767-9776.
175. Hiura, H., T.W. Ebbesen, and K. Tanigaki, *Opening and purification of carbon nanotubes in high yields.* Adv. Mater., 1995. **7**(3): p. 275-276.
176. Roy, B.C., et al., *Studies on water soluble conducting polymer: Aniline initiated polymerization of m-aminobenzene sulfonic acid.* Synth. Met., 1999. **100**(2): p. 233-236.
177. Hong, H.C., M.H. Wong, and Y. Liang, *Amino acids as precursors of trihalomethane and haloacetic acid formation during chlorination.* Arch. Environ. Contam. Toxicol., 2009. **56**(4): p. 638-645.
178. Liang, L. and P.C. Singer, *Factors influencing the formation and relative distribution of haloacetic acids and trihalomethanes in drinking water.* Environ. Sci. Technol., 2003. **37**(13): p. 2920-2928.
179. Morales-Lara, F., et al., *Functionalization of multiwall carbon nanotubes by ozone at basic pH. Comparison with oxygen plasma and ozone in gas phase.* J. Phys. Chem. C, 2013. **117**(22): p. 11647-11655.
180. Vennerberg, D.C., et al., *Oxidation behavior of multiwalled carbon nanotubes fluidized with ozone.* ACS Appl. Mater. Interfaces, 2014. **6**(3): p. 1835-1842.

181. Gallard, H. and U. von Gunten, *Chlorination of natural organic matter: Kinetics of chlorination and of THM formation.* Water Res., 2002. **36**(1): p. 65-74.

182. Prütz, W.A., *Reactions of hypochlorous acid with biological substrates are activated catalytically by tertiary amines.* Arch. Biochem. Biophys., 1998. **357**(2): p. 265-273.

183. Thibaud, H., et al., *Formation de chloropicrine en milieu aqueux: Influence des nitrites sur la formation de precurseurs par oxydation de composes organiques.* Water Res., 1987. **21**(7): p. 813-821.

184. Jansen, R.J.J. and H. van Bekkum, *XPS of nitrogen-containing functional groups on activated carbon.* Carbon, 1995. **33**(8): p. 1021-1027.

185. Symons, J.M., et al., *Measurement of THM and precursor concentrations revisited: The effect of bromide ion.* J. Am. Water. Works. Ass., 1993. **85**(1): p. 51-62.

186. Luong, T.V., C.J. Peters, and R. Perry, *Influence of bromide and ammonia upon the formation of trihalomethanes under water-treatment conditions.* Environ. Sci. Technol., 1982. **16**(8): p. 473-479.

187. Cowman, G.A. and P.C. Singer, *Effect of bromide ion on haloacetic acid speciation resulting from chlorination and chloramination of aquatic humic substances.* Environ. Sci. Technol., 1996. **30**(1): p. 16-24.

188. Acero, J.L., P. Piriou, and U. von Gunten, *Kinetics and mechanisms of formation of bromophenols during drinking water chlorination: Assessment of taste and odor development.* Water Res., 2005. **39**(13): p. 2979-2993.

189. Morris, J.C., *The acid ionization constant of HOCl from 5 to 35°.* J. Phys. Chem., 1966. **70**(12): p. 3798-3805.

190. Hansen, K.M.S., et al., *Effect of pH on the formation of disinfection byproducts in swimming pool water – Is less THM better?* Water Res., 2012. **46**(19): p. 6399-6409.

191. Cynthia, M.M.B., et al., *Parameters Affecting Haloacetic Acid and Trihalomethane Concentrations in Treated UK Drinking Waters*, in *Disinfection By-Products in Drinking Water*. 2008, American Chemical Society. p. 95-108.

192. Boyce, S.D. and J.F. Hornig, *Reaction pathways of trihalomethane formation from the halogenation of dihydroxyaromatic model compounds for humic acid.* Environ. Sci. Technol., 1983. **17**(4): p. 202-211.

193. Mazov, I., et al., *Direct vapor-phase bromination of multiwall carbon nanotubes.* J. Nanotechno., 2012. **2012**: p. 5.

194. Ritchie, J.D. and E.M. Perdue, *Proton-binding study of standard and reference fulvic acids, humic acids, and natural organic matter.* Geochim. Cosmochim. Acta, 2003. **67**(1): p. 85-96.

195. *International Humic Substances Society.* 2015 [cited 2015 June 5]; Available from: http://www.humicsubstances.org/.

196. Chellam, S. and S.W. Krasner, *Disinfection byproduct relationships and speciation in chlorinated nanofiltered waters.* Environ. Sci. Technol., 2001. **35**(19): p. 3988-3999.

197. Wang, H., et al., *Factors influencing the formation of chlorination brominated trihalomethanes in drinking water.* Journal of Zhejiang University SCIENCE A, 2010. **11**(2): p. 143-150.

198. Heeb, M.B., et al., *Oxidative treatment of bromide-containing waters: Formation of bromine and its reactions with inorganic and organic compounds — A critical review.* Water Res., 2014. **48**(0): p. 15-42.

199. Sweetman, J.A. and M.S. Simmons, *The production of bromophenols resulting from the chlorination of waters containing bromide ion and phenol.* Water Res., 1980. **14**(3): p. 287-290.

200. Junwen, L., et al., *Chlorination of water containing bromide and formation of the bromide-substituted trihalomethanes.* J. Environ. Sci., 1995. **7**(4): p. 443-448.

201. Sivey, J.D., M.A. Bickley, and D.A. Victor, *Contributions of BrCl, Br2, BrOCl, Br2O, and HOBr to regiospecific bromination rates of anisole and bromoanisoles in aqueous solution.* Environ. Sci. Technol., 2015. **49**(8): p. 4937-4945.

202. Gould, J.P., L.E. Fitchhorn, and E. Urheim. *Formation of brominated trihalomethanes: Extent and kinetics.* in *Proceedings of the 4th Conference on Water Chlorination.* 1981. Ann Arbor, MI: Ann Arbor Science Publishers.

203. Rathbun, R.E., *Bromine incorporation factors for trihalomethane formation for the Mississippi, Missouri, and Ohio Rivers.* Sci. Total Environ., 1996. **192**(1): p. 111-118.

204. Zhao, W., C. Song, and P.E. Pehrsson, *Water-soluble and optically pH-sensitive single-walled carbon nanotubes from surface modification.* J. Am. Chem. Soc., 2002. **124**(42): p. 12418-12419.

205. Shieh, Y.-T., et al., *Effects of polarity and pH on the solubility of acid-treated carbon nanotubes in different media.* Carbon, 2007. **45**(9): p. 1880-1890.

206. ChemAxon, *Marvin Suite*. 2015: www.chemaxon.com.

207. Thurman, E.M., *Amount of organic carbon in natural waters*, in *Org. Geochem. Nat. Waters*. 1985, Springer Netherlands. p. 7-65.

208. Singh, S. and H.S. Nalwa, *Nanotechnology and health safety – Toxicity and risk assessments of nanostructured materials on human health.* J. Nanosci. Nanotechno., 2007. **7**(9): p. 3048-3070.

209. Lin, D., et al., *Fate and transport of engineered nanomaterials in the environment.* J. Environ. Qual., 2010. **39**(6): p. 1896-1908.

210. Soni, D., et al., *Release, Transport and Toxicity of Engineered Nanoparticles*, in *Reviews of Environmental Contamination and Toxicology*, D.M. Whitacre, Editor. 2015, Springer International Publishing. p. 1-47.

211. Dunphy Guzmán, K.A., M.R. Taylor, and J.F. Banfield, *Environmental risks of nanotechnology: National nanotechnology initiative funding, 2000−2004.* Environ. Sci. Technol., 2006. **40**(5): p. 1401-1407.

212. Delle Site, A., *Factors affecting sorption of organic compounds in natural sorbent/water systems and sorption coefficients for selected pollutants. A review.* J. Phys. Chem. Ref. Data, 2001. **30**(1): p. 187-439.

213. Baken, S., et al., *Metal complexation properties of freshwater dissolved organic matter are explained by its aromaticity and by anthropogenic ligands.* Environ. Sci. Technol., 2011. **45**(7): p. 2584-2590.

214. Bitter, J.L., et al., *Transformations of oxidized multiwalled carbon nanotubes exposed to UVC (254 nm) irradiation.* Environ. Sci. Nano, 2014. **1**(4): p. 324-337.

215. Paul, A., et al., *Photogeneration of singlet oxygen by humic substances: Comparison of humic substances of aquatic and terrestrial origin.* Photoch. Photobio. Sci., 2004. **3**(3): p. 273-280.

216. Latch, D.E. and K. McNeill, *Microheterogeneity of singlet oxygen distributions in irradiated humic acid solutions.* Science, 2006. **311**(5768): p. 1743-1747.

217. Glaze, W.H., *Reaction products of ozone: A review.* Environ. Health Perspect., 1986. **69**: p. 151-157.

218. Shinya, E., et al., *Differentiation of Total Organic Brominated and Chlorinated Compounds in Total Organic Halide Measurement: A New Approach with an Ion-Chromatographic Technique*, in *Natural Organic Matter and Disinfection By-Products*. 2000, American Chemical Society. p. 330-342.

219. Zwiener, C. and S.D. Richardson, *Analysis of disinfection by-products in drinking water by LC–MS and related MS techniques.* TrAC, Trends Anal. Chem., 2005. **24**(7): p. 613-621.

220. Qin, F., et al., *A toxic disinfection by-product, 2,6-dichloro-1,4-benzoquinone, identified in drinking water.* Angew. Chem. Int. Ed., 2010. **49**(4): p. 790-792.

221. Zhao, Y.-Y., et al., *Characterization of new nitrosamines in drinking water using liquid chromatography tandem mass spectrometry.* Environ. Sci. Technol., 2006. **40**(24): p. 7636-7641.

222. Shi, H. and C. Adams, *Rapid IC–ICP/MS method for simultaneous analysis of iodoacetic acids, bromoacetic acids, bromate, and other related halogenated compounds in water.* Talanta, 2009. **79**(2): p. 523-527.

223. Pfaff, J.D., D.P. Hautman, and D.J. Munch, *Method 300.1 Determination of Inorganic Anions in Drinking Water by Ion Chromatography*, USEPA, Editor. 1997: Cincinnati, OH.

224. Hutton, P. and F. Chung, *Simulating THM formation potential in the Sacramento Delta. Part II.* J. Water. Res. Pl. ASCE, 1992. **118**(5): p. 530-542.

225. Shelimov, K.B., et al., *Purification of single-wall carbon nanotubes by ultrasonically assisted filtration.* Chem. Phys. Lett., 1998. **282**(5–6): p. 429-434.

226. Brady-Estévez, A.S., et al., *SWNT−MWNT Hybrid Filter Attains High Viral Removal and Bacterial Inactivation.* Langmuir, 2010. **26**(24): p. 19153-19158.

227. Brady-Estévez, A.S., S. Kang, and M. Elimelech, *A single-walled-carbon-nanotube filter for removal of viral and bacterial pathogens.* Small, 2008. **4**(4): p. 481-484.